NASA-CR-202124

AN EXPERIMENTAL STUDY OF ATMOSPHERIC HOMOGENEOUS NUCLEATION; CLUSTER GROWTH AND GAS-PARTICLE REACTIONS OF H_2SO_4

NASA Grant No. NAGW-3767
Georgia Tech Project No. A-9603

Final Project Report covering the period June 1, 1993 - May 31, 1996

Submitted to:

NASA Headquarters
Washington, DC 20546
Attn: Dr. Jack A. Kaye

Submitted by:

Electro-Optics and Environmental Materials Laboratory
Georgia Tech Research Institute
Georgia Institute of Technology
Atlanta, GA 30332

Principal Investigator: Dr. F. L. Eisele

August 2, 1996

AN EXPERIMENTAL STUDY OF ATMOSPHERIC HOMOGENEOUS NUCLEATION; CLUSTER GROWTH AND GAS-PARTICLE REACTIONS OF H_2SO_4

Final Technical Report

The work proposed on this project included both field and laboratory studies. The laboratory studies were to consist of measurements of H_2SO_4 uptake and evaporation from aerosols of varying chemical composition, while the field component would include measurements of H_2SO_4 and other compounds which would be conducted as part of a large field campaign. The exact field campaign in which we would participate could not be identified at the time the proposal was written, but it was hoped that participation in a larger campaign would provide additional knowledge of the chemical and physical environment in which the H_2SO_4/aerosol interactions under study were taking place. All studies proposed would also be conducted jointly with Dr. Peter McMurry's aerosol group. By chance, the opportunity to conduct such an H_2SO_4/aerosol/ultrafine particle study in conjunction with an OH intercomparison/photochemistry study became available very early in this project (September 1993). This study was conducted at Caribou, Colorado in conjunction with several other groups from NCAR, NOAA and a number of universities. Our group measured OH, H_2SO_4, SO_2, and H_2O, while Dr. McMurry's group measured ultrafine particles, and total particle number and size distribution. In addition measurements of HO_2/RO_2, O_3, NO, NO_2, NO_y, CO, hydrocarbons, CH_2O, and other chemical compounds and meteorological parameters were performed by the other participants and a new laser oblation/mass spectrometry technique was also employed by the NOAA Aeronomy Laboratory to study aerosol composition. The study of aerosol production and growth in conjunction with photochemical measurements is highly advantageous because particle growth precursors such as H_2SO_4 or MSA are formed by OH initiated sulfur oxidation. The large number of hydrocarbon measurements included in this study were also important in understanding particle growth as discussed in Appendix A.

Participation in this study produced a wealth of new understanding in a variety of aerosol growth related areas, each of which is summarized below:

Balancing the production and loss of H_2SO

The major sources and sinks for gas phase H_2SO_4 in a remote measurement site are shown below:

$$SO_2 + OH \xrightarrow[\text{step}]{\text{multi}} H_2SO_4 \quad (1)$$

$$DMS + OH \xrightarrow[\text{step}]{\text{multi}} H_2SO_4 \quad (2)$$

$$\xrightarrow[\text{step}]{\text{multi}} \text{other products}$$

$$H_2SO_4 + \text{particles} \xrightarrow[\text{step}]{\text{multi}} \text{particle growth} \quad (3)$$

$$H_2SO_4 + ? \xrightarrow[\text{nucleation}]{\text{particle}} \text{new particle} \quad (4)$$

Reaction sequence one is reasonably well understood and the SO_2 + OH reaction is the rate limiting step. Reaction three is not well understood, but its net result is at least quantifiable in terms of an accommodation coefficient and a particle distribution. Reaction sequence two and four, however, are particularly poorly characterized. Thus, an attempt to balance all sources and sinks of H_2SO_4 would prove most difficult. At a remote continental site, however, the concentration of SO_2 is typically much larger than that of DMS and therefore reaction sequence two is expected to make only a minor contribution. Continental air masses are also typically expected to have aerosol concentrations sufficiently high to make H_2SO_4 loss through reaction sequence three much larger than through four. As will be shown in the following section, particle nucleation can occur in continental air masses, but the ultrafine particles formed have much lower concentrations and surface areas than the residual particles. Thus, in a remote continental site, the production of H_2SO_4 through reaction sequence one should be approximately equal to its loss onto existing particles (3). The production of H_2SO_4 can then be equated with the loss rate for steady state conditions:

$$[OH][SO_2]k_1 = [H_2SO_4]k_3$$

where k_1 is the reaction rate coefficient of SO_2 + OH and k_3 is the rate of loss onto particles. The ability to simultaneously measure all of the above parameters i.e., OH, SO_2, H_2SO_4 and particle number and size distribution has made a test of our understanding of H_2SO_4 production and loss possible. Also, fortuitously OH and H_2SO_4 concentrations are found on the opposite side of the above equation. These two compounds are measured using the same instrument and reaction scheme, therefore, the relative uncertainties introduced into the above equality by these two measurements is quite small.[1] Unfortunately, however, the SO_2 concentration and the aerosol number density and size distribution measurements probably still introduce about a factor of 2 uncertainty into this calculation, particularly at low SO_2 concentrations (a commercial Thermal Electron 43S Instrument with a detection limit of 100 pptv was used to measure SO_2 and particle size and number density was measured with a University of Minnesota DMA). Within a factor of 2, however, the following tests provided the first real indication of our understanding of H_2SO_4 production and loss.

Figure 1a shows a comparison between measured H_2SO_4 concentrations and those calculated using measured OH and SO_2 concentrations, aerosol size and number distribution, and which assume an accommodation coefficient of 1.0. These same measurements were also performed at Mauna Loa Observatory in Hawaii in 1992; these results are plotted in figure 1b in the same format used in figure 1a. In both cases, agreement is often seen to be better than a factor of 2. These measurements are described in more detail in Appendix B.

The relatively good overall agreement both in the variability and absolute value of calculated H_2SO_4 production and loss provides hope that this same approach might be applicable in estimating H_2SO_4 production from DMS (if SO_2 sources can be accounted for using the above method). Data from the recently completed ACE-I campaign presently provide an ideal

opportunity to test these ideas, offering far more sensitive SO_2 and DMS measurements, multiple particle number and size distribution measurements, and more sensitive OH and H_2SO_4 measurements.

Particle Nucleation

While the previous discussion of H_2SO_4 uptake by particles tends to support classical understanding of particle growth, recent nucleation studies are suggesting mechanisms quite different from classic bimolecular nucleation theory. By making simultaneous measurements of gas phase H_2SO_4 and ultrafine particles, it was quickly determined that, as expected, these two parameters were closely correlated. The concentration of ultrafine particles, however, depends both on production (as shown by reaction sequence four) and loss onto existing particle surfaces. Therefore it is not the concentration of ultrafine particles but rather only their rate of production that should depend on H_2SO_4 concentration directly.

Figures 2a and b show the calculated flux (j) of ultrafine particles passing through the 3 to 4 nm diameter size range as a function of the H_2SO_4 concentration at the Mauna Loa and Colorado measurement sites respectively. Both plots show a compilation of all relevant data obtained during the campaigns, and j was calculated from the measured particle distribution function and by assuming an H_2SO_4 accommodation coefficient of 1.0 for ultrafine growth. Since 3-4 nm is the smallest size range of particles that can be measured, the flux through this size range presently provides the best estimate of nucleation rate. Also, however, because nucleating particles can be lost onto varying concentrations of larger particles prior to being detected in the 3-4 nm range, it is assumed that the highest calculated fluxes best characterize the actual nucleation rate (see Appendix C). If a line is drawn approximately through these high flux points in both figures 2a and b, its slope in both cases appears to be about 2. This suggests a nucleation rate which varies approximately as the square of the H_2SO_4 concentration. This is in

sharp contrast to the far more vertical lines showing classical nucleation theory predictions. Present results suggest a far weaker functional dependence on H_2SO_4 and also that nucleation can occur at much lower absolute concentration of H_2SO_4 than predicted by classical theory. If an accommodation coefficient of 0.5 were assumed in the calculation of j, the slope of the maximum flux lines would remain the same (2) and the j values would only drop by a factor of two. These calculations are discussed in more detail in Appendix C.

The large disparity between classical bimolecular nucleation theory and the present results requires a re-evaluation of the use of this theory for describing nucleation in the troposphere or at least the lower troposphere where the present measurements were performed. To pose this issue in a different way: why, in hindsight would molecular clusters of H_2SO_4 and H_2O not be expected to react with basic compounds such as NH_3? NH_3 is typically more abundant than gas phase H_2SO_4, it is highly soluble, and is commonly found along with H_2SO_4 in larger particles. If NH_3 were to react with a molecular cluster containing nucleation precursors such as H_2SO_4 and H_2O, it could form ammonium bisulfate or even ammonium sulfate. This might well reduce the vapor pressure or the loss rate of H_2SO_4 from these clusters. If this were to occur, the ammonia could have a significant effect on the nucleation process such as that shown in figure 2. This possibility is discussed in more detail in the laboratory results section.

Ultrafine Growth Rates

Small particles (particle diameter << mean free path) are typically assumed to grow at a constant diameter growth rate, independent of their size; i.e., they incorporate molecules at a rate which is proportional to their surface area. The most conspicuous growth thus occurs when aerosols are the smallest. If nucleation is assumed to begin with a cluster of just a few H_2SO_4,

H_2O, and maybe some NH_3 molecules, then the initial size of this nucleating particle is ~ 1 nm. It need then only grow an additional 2 nm in diameter before it can be detected as a particle. Small ultrafine particles therefore offer a unique opportunity to study early stages of growth. Since the nucleation process requires the presence of relatively high H_2SO_4 concentrations, it is expected to have at least as strong a diurnal variation as H_2SO_4 and probably stronger ($[H_2SO_4]^2$). Thus, the time between sunrise and the appearance of the first ultrafines provides a measure of the approximate time required for growth into the 3-4 nm range or ~ 2 nm of growth, under the ambient conditions for which the observations were made. Figure 3a shows a compilation of all the H_2SO_4 data and the average clear sky solar fluxes plotted as a function of time of day for the previously discussed 1993 Colorado measurements. Note the close correspondence between the rise of solar flux and H_2SO_4 concentration. Unfortunately, afternoon and evening were often cloudy and/or rainy and therefore H_2SO_4 values did not decrease with clear sky solar flux. Figure 3b shows a similar plot for ultrafine particles. These do not begin to rise at sunrise with H_2SO_4. Rather, they change little until one or two hours after H_2SO_4 has risen. Using this rise time, a 1-2 nm diameter/hour growth rate is estimated for ultrafine particles at this site. Maybe a slightly better estimate of growth rate would be obtained by assuming that on average the nucleation process begins when the average H_2SO_4 concentrations shown in figure 2a were reached. This would suggest growth rates closer to 2 nm/hour. Interestingly, this rapid growth rate can not be obtained by the incorporation of H_2SO_4, H_2O or even NH_3 alone. This observed growth rate is about an order of magnitude larger than can be explained by H_2SO_4 incorporation, even with an accommodation coefficient of one. Though the data were more scattered at the MLOPEX II study and probably more dominated by transport, this large disparity between observed and calculated H_2SO_4 induced

growth did not arise. At present, the most likely explanation for this very rapid observed growth rate is that other low volatility compounds are contributing to the growth process. Since this disparity appears very large only in continental air masses, very large or highly polar hydrocarbons would seem likely candidates to account for this rapid growth. This possibility is discussed in more detail in Appendix A.

In November and December of 1995 the ACE-I (Aerosol Characterization Experiment) was conducted in a remote southern hemisphere marine environment with many goals in common with the present project. After our past success it was decided that participation in this study could be even more productive than the past study particularly since it also provide an opportunity to contrast continental vs marine environments. Our instrument made measurement of OH, H_2SO_4, and MSA for nearly 300 hours on the NCAR C-130 as part of this field campaign. While our measurements were highly successful much of the data from other investigators is not yet available. Therefore, most of the data interpretation is not yet possible. Figure 4a, b, and c, however, show some typical measurement results for OH, H_2SO_4, and MSA respectively.

Laboratory studies in support of and sometime even helping to guide field measurement strategies (such as the inclusion of NH_3 measurements in ACE-I) have also been highly successful. One of the major questions raised by the 1993 campaign and explored by ACE-I, is the possible role of NH_3 in particle nucleation. To investigate this possibility, joint laboratory studies were conducted to measure the vapor pressure of H_2SO_4 above aerosols containing various mixtures of H_2SO_4 and NH_3. Figure 5 shows the results of these studies for several different ratios of NH_3 to H_2SO_4 from 0-2. In each case, the H_2SO_4 vapor pressure is plotted as a function of relative humidity. For pure H_2SO_4 the vapor pressure is compared to that calculated by Ayer et al.,[2] and agreement is seen to be reasonably good. As the ammonium

content of the particles is increased to 13, 15 or 33%, the vapor pressure of H_2SO_4 appears to drop slightly. However, when ammonia concentration reaches 80% of H_2SO_4, the drop becomes very pronounced. When the average composition of ammonium bisulfate is reached, the vapor pressure of H_2SO_4 is reduced by two-three orders of magnitude, depending on relative humidity. To a crude approximation, this dependence on ammonia content suggests that each ammonia molecule dramatically reduces the ability of one sulfuric acid molecule to leave the particle with the excess acid molecules loss largely unimpeded. At still higher ammonium/sulfate ratios (2) the H_2SO_4 vapor pressure drops so low that it is difficult to measure. While the H_2SO_4 vapor pressure above ammonium sulfate is very low, the vapor pressure of ammonia is probably quite high.[3] It is therefore less likely that ambient NH_3 concentrations will be sufficiently high such that ammonium sulfate molecular clusters will play an important role in atmospheric nucleation (though little quantitative can be said about ammonia vapor pressures until additional measurements are made). The two to three order of magnitude reduction in H_2SO_4 vapor pressures for the ratio of 1:1 shown in figure 5 is, however, already sufficient to dramatically alter calculated nucleation rates if this same vapor pressure dependence applies to molecular clusters/ultrafine particles.

In attempting to understand how NH_3 stabilized molecular clusters might grow into particles, one must also briefly examine the role that statistics might play in this process. For the large particles shown in figure 3 (10^2 nm diameter) ammonium content is listed in fractional concentrations. However, for small molecular clusters with only a few H_2SO_4 molecules, there is presumably a probability distribution for having 1, 2, 3, --- ammonia molecules associated with each cluster. If the molecular cluster of interest has no ammonia molecules or perhaps only one ammonia molecule compared to 2 or 3 sulfuric acid molecules, then from the predictions of

classical theory shown in figure 2, it probably has essentially no possibility of growth for the H_2SO_4 concentrations typically measured. However, even if the average NH_3/H_2SO_4 concentration ratio is well below one there will still be some significant fraction of molecular clusters containing, for example, two H_2SO_4 molecules and two NH_3 molecules. If the results shown in figure 5 can be applied to molecular cluster growth, a reduction in H_2SO_4 loss by several orders of magnitude might well make the further growth of the latter cluster probable. While highly speculative, a scenario such as this could explain the present results, which suggest a kinetically controlled process depending on $[H_2SO_4]^2$ and, at the same time, predict a nucleation rate which is many orders of magnitude slower than that calculated for H_2SO_4, uptake by the clusters at the collision rate. It is also interesting to note that the calculated j values in figure 2b are somewhat higher than in figure 2a, and the ammonia concentrations are also expected to be much higher over the continent than at Mauna Loa.[4,5] These measurements are discussed in more detail in Appendix D.

Most recently, measurements of the uptake of H_2SO_4 on sodium chloride and ammonium sulfate particles have been conducted. The preliminary results of these studies suggest an accommodation coefficient in the 0.5-1.0 range which is in good agreement with the previous field study results for balancing the production and loss of H_2SO_4 (see Appendix B). Analysis of these data are still underway but the results will be written up and published once the analysis is completed.

Conclusions

Recently developed instrumentation is opening up exciting new avenues for investigating particle nucleation and growth. In the absence of significant DMS and particle nucleation, H_2SO_4 production and loss can be reasonably well-characterized and balanced. This offers

hope that the production rate of H_2SO_4 from DMS might also be quantifiable in the near future. The application of classical nucleation theory in the troposphere has been questioned, and a more kinetically controlled process possibly involving NH_3 is posed as a possible alternative. The results of ACE-I which included NH_3 measurements along with those of H_2SO_4, H_2O and ultrafines are expected to substantially improve present understanding in this area. If the results shown in figure 2 represent tropospheric nucleation in general, then nucleation events may be far more prevalent and important than present models would suggest. Finally, the measurement of small, size selected, ultrafine particles now opens up the possibility of studying particle growth processes on a time scale which is short compared to a day. This is extremely important, because particle growth precursors and dynamics both vary substantially over the time period of a day. Thus, attempting to understand an already highly complex process with multiple varying parameters is particularly difficult. The ability to determine growth over the period of an hour or two under relatively stable chemical and dynamic conditions, however, offers far more hope of obtaining a detailed understanding of this process over the next decade.

A great deal of new insight into particle nucleation and growth has been gained by this group and others over the past half decade and far more progress is anticipated in the near future. Some of the areas in which this progress is desired and anticipated are: understanding DMS oxidation and the subsequent yield of H_2SO_4 and MSA; quantifying the role of NH_3 in particle nucleation; being able to accurately predict nucleation events from precursors or even source gas measurements; and understanding and quantifying the role of hydrocarbons in aerosol growth.

New Particle Formation at a Remote Continental Site: Assessing the Contributions of SO_2 and Organic Precursors

James J. Marti[+], Rodney J. Weber[++], and Peter H. McMurry[*]

Department of Mechanical Engineering

University of Minnesota, Minneapolis, Minnesota

Fred Eisele, David Tanner and Anne Jefferson

Atmospheric Chemistry Division

National Center for Atmospheric Research, Boulder, Colorado

Submitted to Journal of Geophysical Research-Atmospheres July, 1995.

(1993 Idaho Hill Tropospheric OH Experiment Special Issue).

Revised June 1996

PTL Publication No. 949

* To whom correspondence should be addressed.

Current Affiliations:

+ Computational Physics Inc., Fairfax, VA

++ Brookhaven National Laboratory, Upton, NY

Abstract. Ultrafine aerosols, with diameters below 10 nm, nucleate from gas phase species. The composition of newly formed ultrafine atmospheric aerosols is not known with certainty; new particles have variously been conjectured to be sulfates, organic compounds, and sulfate/organic mixtures. The 1993 Tropospheric OH Photochemistry Experiment at Idaho Hill, Colorado provided an opportunity to examine the question of which class of compounds--sulfates or organics--make the major contribution to new particle formation in the unpolluted troposphere. This study compared the production rates of sulfuric acid (from the oxidation of sulfur dioxide) and oxidized organic compounds to gauge their relative contributions to the formation of ultrafine particles. Potential organic precursor species examined in this study were the naturally occurring terpenes α– and β pinene, and the anthropogenic hydrocarbons toluene, m-xylene, ethyl benzene, 1,2,4 trimethyl benzene and methylcyclohexane. The calculated production of oxidized organics appeared well correlated with total particle surface area and volume, suggesting that at least some of the organic compounds formed in gas phase reactions condensed upon the preexisting aerosol. New particle formation was found to be more highly associated with elevated production of gas phase sulfuric acid (via the SO_2-OH reaction) than with production of oxidized organic products, although data from one day, during which sulfuric acid production and total aerosol surface area were both lower than usual, provided evidence for the involvement of terpene species in new particle formation. The results suggest that for this continental site, sulfuric acid was probably responsible for most of the observed new ultrafine particle formation. Low volatility organic compounds may have caused particle formation under the right conditions, but were more likely to condense upon pre-existing particles.

Introduction

Atmospheric aerosols play a significant role in shaping the Earth's climate, both by the direct scattering of solar energy [Charlson et al., 1992] and through their role as cloud condensation nuclei [Twomey et al., 1984]. Since atmospheric particles are continually subject to coagulation, scavenging by larger particles, and removal by precipitation, a source of new aerosols is evidently required to maintain observed particle size distributions in the background troposphere. These newly formed particles comprise the ultrafine aerosol. With diameters less than 10 nm, ultrafine particles lie at the small size extreme of the atmospheric aerosol. They are formed from gas phase precursors, having grown past the critical cluster size to attain stability as particles. Since ultrafine particles are quickly lost by diffusion to the surfaces of larger particles, their presence in regions far from primary emissions is evidence that nucleation from gas phase precursor species is taking place.

The sources and composition of the ultrafine aerosol have been subject to much debate. The question attracted attention early in the history of aerosol science. In the mid nineteenth century, John Tyndall passed intense light through a vessel of organic vapors and observed the formation of a light blue cloud, which gradually turned whitish over time [Tyndall, 1868]. He was observing the formation of small particles which scattered strongly in the short wavelengths, followed by particle growth to the Mie scattering regime. This arcane experiment became known to millions living in the Los Angeles basin when Haagen-Smit and Fox [1956] established the mechanisms for the various smog reactions, driven by the photochemistry of oxides of nitrogen and reactive hydrocarbons. The production of small particles in mixtures of organic vapors and oxidizing agents has been repeated in the laboratory many times in the last four decades. Went [1960] proposed that the same reactions may produce sub-micrometer aerosols by oxidation of terpenes, naturally occurring hydrocarbons emitted by many species of vegetation. He and others [Rasmussen and Went, 1965; Went, 1966; Lopez et al., 1985] have argued that these reactions are the cause of the small particles comprising the "blue haze", common over forested areas.

Laboratory studies of hydrocarbon reactions with the hydroxyl radical (OH) and/or ozone (O_3) have observed the production of condensable species and aerosols. Naturally occurring monoterpenes ($C_{10}H_{16}$) and sesquiterpenes ($C_{15}H_{24}$) may be oxidized by OH or O_3 to form a large number of terpenoid products [Graedel, 1979; Yokouchi and Ambe, 1985; Hatakeyama et al., 1991; Pandis et al., 1991; Palen et al., 1992; Grosjean et al., 1992; Shu and Atkinson, 1995]. In addition, OH and ozone reactions with many anthropogenic hydrocarbons have been observed to form aerosols [Stern et al, 1987; Wang et al, 1992]. The products of these organic reactions possess a wide range of vapor pressures, making it difficult to specify the condensing compound. Two probable reaction products of α–pinene and OH , pinonic acid and pinonaldehyde, have been identified in atmospheric aerosols [Wilson et al., 1972; Hatakeyama et al., 1989].

In the 1970s attention within the aerosol community generally shifted from terpenes to the sulfate aerosol. New ultrafine particles in the background atmosphere were postulated to nucleate from vapor phase water and sulfuric acid (H_2SO_4), the latter formed by the oxidation of sulfur dioxide (SO_2) by OH [Doyle, 1961; Mirabel and Katz, 1974; Jaecker-Voirol, 1989]. Subsequent reaction with gas phase ammonia results in a partially to totally neutralized particle, the latter usually as ammonium sulfate, $(NH_4)_2SO_4$. Most recent modeling studies of new particle formation in the atmosphere have used modifications of classical binary nucleation theory involving water and sulfuric acid [Kreidenweis et al., 1991; Raes and Van Dingenen, 1992; Easter and Peters, 1994; Raes, 1995].

No direct composition information exists for ultrafine particles. Composition measurements of particles down to the lower practical size limit (about 0.05 μm to date) suggest that submicron particles have mixed compositions, with organic/sulfate ratios that may vary according to particle size and sampling location. Weiss and co-workers [1977] examined aerosols from three rural locations in the southern and midwestern United States. Their method focused on particles between 0.1 and 1.0 μm in diameter, which includes the bulk of the optically important haze producing aerosol. The authors found that sulfate dominated the sub-micrometer aerosol under all wind and meteorological conditions, consistent with an earlier study [Charlson et al.,

1974]. On the other hand, size resolved particle composition measurements in the western United States (the Los Angeles area and near the Grand Canyon) by Zhang and coworkers [1993] found that carbon comprises a significant fraction of the aerosol mass in the diameter range 0.05 to 1.0 μm. Earlier studies [Hoffman and Duce, 1974; Ketseridis and Eichmann, 1978] also showed considerable organic material in particles smaller than 1 μm. Particle composition was measured in a number of U.S. national parks and wilderness areas by Malm et al [1994]; the authors found the largest single component of aerosols under 2.5 μm in diameter to be sulfates in the eastern United States and organic compounds in the west. Recent measurements [Novakov and Penner, 1993; Rivera-Carpio et al, 1994] suggest that organic carbon may be a major constituent of cloud condensation nuclei.

While composition data on particles large enough to be measured may yield insight about particle growth, they tell us little about the nucleation phenomena that form new particles from the gas phase. In the absence of such data for nanometer-sized particles, inferences about the composition of newly formed particles may be made through simultaneous measurements of ultrafine particles and possible gas phase precursors. The opportunity for such a study arose during the 1993 Tropospheric OH Photochemistry Experiment at Idaho Hill, Colorado. For most of the month of September 1993, concurrent measurements were made of ultrafine particles, fine particles (with diameters between 15 and 500 nm), gas phase SO_2 and H_2SO_4, ozone, OH, and a number of nonmethane hydrocarbons. Wind, temperature and other meteorological data were also collected. This paper analyzes the Idaho Hill data set to gain insights into the contributions of possible precursor gas reactions to new particle formation at this relatively clean continental site.

Correlations between particle formation rates and steady state sulfuric acid concentrations at Idaho Hill were the subject of an extensive analysis by Weber et al [1996]. The study found that new particle formation was well correlated with the concentration of vapor phase sulfuric acid. However, the study also found 1) particle nucleation occurred at H_2SO_4 concentrations much lower than predicted by classical binary nucleation theory for the H_2SO_4 -H_2O system; 2) particle nucleation rate appeared to depend on the square of H_2SO_4 concentrations, rather than the higher

power indicated by theory; and 3) particle growth after nucleation was eight to thirteen times faster than could be explained by condensation of H_2SO_4 and its associated water. The authors concluded that new particles at Idaho Hill formed from sulfates, possibly with the involvement of other species, such as atmospheric ammonia. It was hypothesized that condensation of organics might contribute to the observed high growth rates of ultrafine particles, although organic species were not explicitly considered in the analysis. The present work extends the analysis of Weber et al, examining the contributions of sulfate and organic precursor species to new particle formation at Idaho Hill.

Apparatus and Techniques

The site. The measurements were made during September 1993 on a forested ridge in the Rocky Mountains about 25 km west of Boulder, Colorado at a pressure elevation of about 700 mb (3070m above mean sea level). Detailed descriptions of the physical and meteorological conditions at the site are found in Mount and Williams [this issue] and Olson et al [this issue].

The local topography tended to force ground level winds into either an easterly (upslope) or a westerly (downslope) direction. Areas to the west of the site were sparsely populated, so the westerly downslope winds brought clean, nearly background continental air to the site. The easterly upslope winds were associated with anthropogenic influences from the Denver metro area and from agricultural land within Boulder County. The arrival of upslope winds shows clearly in the aerosol record as an increase in the concentration of anthropogenic hydrocarbons and particles with diameters greater than 50 nm.

Aerosol apparatus. The concentration of ultrafine (hereafter UF) aerosols was measured with an ultrafine condensation nucleus counter (UFCNC), a modified commercial CNC (Model 3020, TSI, St. Paul, MN) which had a lower detection limit of about 2.7 nm (50% detection threshold of 3 nm) [Stolzenburg and McMurry, 1991]. Samples were collected with a 2.5 cm inlet about 5 m above ground level. The aerosol sample flow was taken from the centerline of the inlet flow to minimize the effects of diffusional losses to tubing walls. Measurements were made

continuously with time resolution of about 2.5 minutes. The UFCNC was capable of detecting UF particles (3 to 4 nm diameter) at a concentration as low as about 0.1 cm^{-3}.

Like all CNCs, the UFCNC gives a count of total particles greater than a threshold size by condensing a working fluid (butyl alcohol in this case) on these particles; the resulting droplets are sensed optically. While CNCs allow optical detection of particles much smaller than the wavelength of light, they do so at the expense of size information on the original aerosol. The UFCNC partially overcomes this limitation of conventional CNCs by modifying the aerosol flow through the instrument's condenser region, confining all particles to the condenser centerline. This ensures that all particles are exposed to about the same peak saturation ratio and have similar transport times through the condenser. Along the centerline, input particles encounter a rising supersaturation that peaks about 2/3 of the length of the condenser. Smaller input particles, which require higher supersaturations to nucleate droplets, nucleate later than larger particles. This results in a final droplet size that reflects the size of the original input particle, allowing a method of UF aerosol size discrimination [Brockmann, 1981; Stolzenburg, 1988; Ahn and Liu, 1990]. In practice, particles with diameters larger than about 12 nm all grow to about the same final droplet size, but the sizes of particles smaller than this may be measured with the UFCNC by analyzing the height of the pulse produced at the optical detector [Saros et al, 1996; Weber et al., 1995a]. The optical output from the UFCNC was coupled to a multichannel analyzer (EG&G model 916A) for pulse height analysis.

The response of the UFCNC to particles of sub-15 nm diameter was determined using monodisperse test aerosols. The concentration of newly formed aerosol was calculated from the count rate in the portion of the pulse height spectrum corresponding to particles between about 3 and 4 nm diameter. While this size is much larger than that of the critical molecular cluster which would truly represent a new nucleated particle, it is the nearest to the newly formed particle size range we can observe with our instrument. Throughout this study, measured concentrations of 3 to 4 nm diameter particles are taken to be the concentration of newly formed aerosol (the time delay between actual nucleation and attainment of detectable size is addressed in Results and Discussion,

below). Experimental uncertainty increased with decreasing particle concentration; the relative uncertainty for a concentration of 0.1 cm^{-3} was about 15% .

Measurements of fine particle size distributions were made with a scanning electrical mobility spectrometer (SEMS), consisting of a differential mobility analyzer (DMA) and a CNC (TSI 3760). In the SEMS, the DMA is continuously scanned through its voltage range as the CNC detects particle concentrations in each of several discrete size ranges [Wang and Flagan, 1990]. A full scan through the DMA voltage range (up and down) took about 2.5 minutes. For most of the experiment, the SEMS measured particles in the diameter range between 0.015 and 0.5 μm; on occasion, high particle loading required altered instrument flows which set the upper limit of the detected size range at 0.26 μm. SEMS data were inverted by the method of Hagan and Alofs [1983] to yield the fine particle size distributions. This inversion technique accounts for both multiple charging and aerosol transport losses in the DMA. From these distributions were calculated the total aerosol surface area and total volume. Both these quantities were dominated by particles above 0.1 μm in diameter, even though smaller particles (0.05 to 0.1 μm) were much more numerous throughout the experiment. Measurements of fine particles, including those over 1 μm in size, are treated in more detail elsewhere [Murphy, this issue].

Gas Phase Sulfuric Acid, Sulfur Dioxide, OH and Ozone. The gas phase concentrations of H_2SO_4 and OH were measured every five minutes with a chemical ionization mass spectrometer (CIMS). Detection thresholds for both species were about 10^5 molecules cm^{-3}. More details on the operation of the CIMS can be found in Tanner et al [this issue] and [Eisele, 1993]. Uncertainties in gas phase concentration measurements were a maximum of +/- 35%. Additional OH concentration data was available from the long path measurements [Mount et al, this issue]. Sulfur dioxide was measured with a commercial pulsed fluorescence instrument (Thermo Environmental Instruments Model 43S) at about ten minute intervals. Uncertainties were usually under 20%, but at times ranged over 100% due to problems with instrument zero drift. Ozone concentrations were measured both by long path differential absorption spectroscopy and a

commercial instrument. The results of the two methods agreed to within about 2% [Harder et al, this issue].

Nonmethane Hydrocarbons (NMHCs). The concentrations of a number of NMHCs were measured hourly by gas chromatography with cryogenic trapping; details of the hydrocarbon sampling are found in [Goldan and Kuster, this issue]. Of particular interest among the measured organic species are the monoterpenes, α– and β pinene. These two compounds are often invoked as candidates for precursors of particle nucleation (other potential terpene precursors, such as *d*-limonene and the sesquiterpenes, were not measured at Idaho Hill). Also examined were the aromatics trimethyl benzene, ethyl benzene, toluene, and m-xylene and the alkane methylcyclohexane. These (presumably) anthropogenic NMHCs have all been observed to react with OH or other oxidants to yield measurable aerosol mass. During the early part of the experiment, data were collected only during the hours 10 a.m. to 3 p.m.; sampling was expanded to 24 hour during the latter half of the field campaign.

Analysis. Theoretical and laboratory studies of particle nucleation in chemically reacting systems [McMurry and Friedlander, 1979; McMurry, 1980; McMurry, 1983; Kreidenweis et al., 1991; Wang et al., 1992] have shown that the maximum concentration of new particles formed in such systems (N_{max}) depends on 1) the vapor pressure of the condensable compound(s) formed by gas phase reactions, 2) the rate of formation of these compounds, and 3) the total surface area of any preexisting aerosol. In the present work, we examine the Idaho Hill data set to determine whether or not the daily N_{max} of UF particles exhibit dependence on the formation rate of the nucleating species and total aerosol surface area. The aim of this investigation is to compare the relative importance to new particle formation of gas phase SO_2-OH reactions, which ultimately form sulfate particles, versus the oxidation reactions involving natural and anthropogenic NMHCs, a subset of which may form new particles.

The peak value of UF particle concentration N_{max} was determined for each of the 17 days for which complete data existed. Reaction rates R were calculated separately for each potential precursor-oxidant combination

$$R_{PRECURSOR} = k\,[precursor]\,[oxidant]$$

using literature values for the rate coefficients k. Thus the $R_{SO2\text{-}OH}$ is given as

$$R_{SO2\text{-}OH} = k_1[SO_2][OH] \qquad (1)$$

where k_1 is that given by [Seinfeld, 1986]. Sulfur dioxide-ozone reactions were not considered in this study.

Unlike the sulfate system, reactions of the NMHCs do not yield a single condensable product. To facilitate comparison between reacting systems, reaction rates were summed for the terpenes and the anthropogenic hydrocarbons. An aggregate formation rate for terpenoid products, R_{TERP}, is defined as

$$R_{TERP} = \sum_{t,i} n_t O_i k_{ti} f_{ti} \qquad (2)$$

where n_t are the gas phase concentrations of the monoterpenes (α– or β-pinene), O_i the concentrations of OH or ozone, and k_{ti} the appropriate rate constant for each reaction. The terms f_{ti} are fractional aerosol coefficients (FACs), introduced as weighting factors to account for the varying tendency of these reactions to form aerosol products. Experimental values of FACs for the pinenes are those of Grosjean and Seinfeld [1989], Hatakeyama et al [1989], Arey et al [1990], and Grosjean et al [1992]. Similarly, an aggregate rate for the formation of condensable species from the anthropogenic hydrocarbons is defined as

$$R_{ANTHRO} = \sum_{a,i} n_a O_i k_{ai} f_{ai} \qquad (3)$$

where the n_a are concentrations of toluene, m-xylene, ethyl benzene, methylcyclohexane and 1,2,4 trimethyl benzene. Rate constants and FACs are from Wang et al [1992], Stern et al [1987], and

the above references. The rate constant and aerosol fraction for 1,2,4 trimethyl benzene were approximated using laboratory data for its 1,3,5 isomer.

Mean values of the concentration of total aerosol surface area (in $cm^2\ cm^{-3}$) and volume (in $cm^3 cm^{-3}$) were also determined for each day of the experiment. When and if condensable species are produced in the gas phase, they may form new particles or condense upon preexisting particle surfaces. The latter is energetically favored, so new particle formation should be observed more often during periods of low total particle surface area, and the dependence of N_{max} on R should be most pronounced under these conditions. Accordingly, the N_{max} data for each reacting system (i.e., SO_2-OH, terpenes, and anthropogenic hydrocarbons) were stratified according to the total surface area present during the measurement. Evidence of R dependence was taken to be an indication that the reacting species was involved in new particle formation. In this way, the relative roles played by organic and sulfate species in new particle formation may be directly compared.

Results and Discussion

A representative plot of UF particle concentration versus time of day is shown in Figure 1a. The Figure includes periods of downslope winds (Sept. 21, 24-25) and upslope wind conditions (Sept. 22-23). A diurnal variation is apparent in the UF data for the downslope days. Ultrafine particles typically appeared shortly after sunrise, increased to a peak between 8 and 10 a.m. local time, then decreased sharply after noon, usually vanishing by about 3 p.m. Such variation was observed on 80% of all experiment days; the portion rises to 85% if only downslope wind conditions are considered (9 of the total 17 days analyzed). Diurnal variations similar in shape, although delayed in time, have been observed with Aitkin nuclei in continental boundary layer air [Hogan, 1968; Marti, 1990]. The particle counter used in the present work is capable of detecting aerosols much smaller and at lower concentrations than those used in previous studies, which may explain the earlier daily onset and disappearance of measured UF particles. Ultrafine particle concentrations varied widely during upslope wind conditions, with the size distributions typically dominated by larger particles (diameter > 50 nm).

The data were examined for temporal relationships between UF concentrations and the R for each reacting system. Diurnal patterns in R_{SO2}, R_{TERP}, and R_{ANTHRO} would be expected due to the photochemical creation of OH and the diurnal changes in terpene emissions. If a given precursor is contributing to UF particle production, a time lag should be observed between increases in R and the first detection of UF particles, i.e., the time required for a newly nucleated particle to grow to the 3 nm lower detection limit. This growth time is a function of monomer size and gas phase concentration of the condensable species. For example, growth time for H_2SO_4 aerosols under conditions observed at Idaho Hill is estimated to be at least two to four hours, using the assumptions of collision controlled nucleation (for a discussion of collision controlled nucleation, the reader is referred to McMurry [1983] and Weber et al [1996]). In Figure 1a the daily variation of $R_{SO2\text{-}OH}$ is coplotted with UF concentrations for the period of September 21-26. The SO_2-OH reaction rates show a diurnal pattern. On seven of the 17 days analyzed, daily increases in $R_{SO2\text{-}OH}$ preceded those of UF particles, with a mean lead time of 1.9 hours. Figure 1b shows daily variation in UF particles and R_{TERP}. Daily increases in R_{TERP} preceded those of UF particle concentration on five of 17 sample days (by an average of 2.1 hours) and lagged UF concentration increases on 8 days. Figure 1c compares the time variation of R_{ANTHRO} and UF concentrations for the same period. Increases in the former preceded the latter on only one day during the experiment. On the basis of the data in figures 1a-c, terpenes appear to be the more likely than the anthropogenic NMHCs to be associated with new particle and growth.

As noted in the previous section, we are looking for a positive dependence of N_{max} on R for the possible condensing species. In Figure 2a, N_{max} is plotted against the daily mean value of R_{TERP}. Data collected under both upslope and downslope wind conditions are included in the Figure. The data have been segregated into two groups according to the total aerosol surface area, low (below about 5.0×10^{-7} cm^2cm^{-3}) and high (greater than 6.0×10^{-7} cm^2cm^{-3}). If terpene-OH/ozone reactions were associated with the production of new UF particles, a dependence of N_{max} on R should show up most clearly in the low surface area data. The data in Figure 2a do not seem to show such dependence; the data collected under low aerosol surface area conditions span a

wide range of N_{max} for a given R_{TERP}. A linear fit of N_{max} yielded near zero or negative dependence on R_{TERP}.

Similar treatments of R_{ANTHRO} and $R_{SO2\text{-}OH}$ are presented in Figures 2b and 2c, respectively. As in Figure 2a, the data have been segregated into low and high values of total surface area. The data in Figure 2b exhibit little evident dependence of N_{max} on R_{ANTHRO}. On the other hand, Figure 2c appears to show a slight N_{max} dependence on $R_{SO2\text{-}OH}$ among the low area subset of the data. Although the data is sparse, a linear fit of N_{max} to $R_{SO2\text{-}OH}$ for the low surface area data reveals a positive dependence, while the $R_{SO2\text{-}OH}$ dependence for the high surface area N_{max} data is near zero. The scatter and scarcity of the SO_2 data do not permit rigorous statistical analysis; nevertheless this difference in R dependence distinguishes the SO_2-OH data from that of the organic systems.

Unlike with the organic systems, measurements of the SO_2-OH system included data on its condensable product, H_2SO_4. To extend the examination of the role played by sulfate in new particle formation, the daily mean measured concentration of gas phase H_2SO_4 at Idaho Hill is plotted against N_{max} in Figure 3. Only data collected on days with low surface area conditions are included. A positive correlation of N_{max} with $[H_2SO_4]$ is evident from the Figure.

Figures 2 and 3 suggest that the new particle nucleation observed at Idaho Hill may have been more likely caused by SO_2-OH reactions (that ultimately formed H_2SO_4) than by reactions involving the terpenes or the anthropogenic hydrocarbons. This is consistent with the analysis of Idaho Hill data by Weber et al [1996], where the authors found a correlation between measured concentrations of H_2SO_4 and UF particle concentration.

If the organic compounds are reacting with ozone and/or OH to form a vapor species of low volatility, the latter may be condensing upon pre-existing particles, adding to the total aerosol surface area and volume. To check this, reaction rates R were compared with daily mean values of total particle surface area and volume for each day during which downslope (clean) wind conditions prevailed. All quantities were averaged from 6 a.m. to the peak daily value of R. Figure 4a shows both total surface area and total volume plotted against R_{TERP}. The Figure

shows that under clean air conditions, increased terpenoid production rates were associated with increases in particle surface area and volume. A similar plot of R_{ANTHRO} is shown in Figure 4b. Note the low values of R_{ANTHRO} present in this downslope data (compare Figure 2b). Since the anthropogenic compounds included in R_{ANTHRO} may be considered markers for upslope (polluted) air, this downslope data set considers only the low end of the R_{ANTHRO} data range. Within this range, R_{ANTHRO} also appears correlated with particle surface area and volume. Figure 4c shows that increasing $R_{SO2\text{-}OH}$ is associated with increasing total aerosol volume, albeit weakly; little association with surface area can be seen in the Figure. Figures 4a-c suggest that as organic products were created, they may have preferentially condensed on pre-existing particles, adding to total surface area and volume, rather than nucleating new particles. This view is consistent with the lack of positive R dependence by N_{max} found for the organic reactions in Figures 2a and b. It also fits with the time lag between observations of new particles and increases in R_{TERP} seen on about half of the sample days: as the products from pinene-OH/ozone reactions condensed on preexisting particles and increased the total particle surface area, new particle nucleation was increasingly inhibited; thus as R_{TERP} peaked, UF particle concentration was typically dropping. An alternate explanation for the observations shown in Figure 4 is that organic compounds may have been advected into the area along with larger particles, which dominate the aerosol area and volume distributions. Most of this effect, however, has been screened out of the data in Figure 4 by removing days with upslope wind conditions, which typically brought sharp increases in larger particles and anthropogenic hydrocarbons.

While in general, oxidized organic products appeared not to play a primary role in new particle formation, there were possible exceptions. September 26 was a day of clean downslope wind conditions with low total particle surface area, about 2×10^{-7} cm^2cm^{-3} (the mean value for downslope wind conditions during the experiment was about 5×10^{-7} cm^2cm^{-3}). Sulfuric acid concentration was near the lowest seen during the experiment, averaging about 6×10^5 cm^{-3} over the daylight hours. Figure 5 shows that the peak UF particle concentration was relatively low (70 cm^{-3}) but non zero; $R_{SO2\text{-}OH}$ remained below its mean value for downslope wind days, and its

variations did not appear to precede or coincide with those of UF particle concentration. The R_{TERP} values on this day were comparable to those of surrounding days. Unlike on most other days however, changes in R_{TERP} on Sept. 26 led rather than lagged the appearance of UF particles, as shown in Figure 5. This correspondence, along with the lack of such correspondence with $R_{SO2\text{-}OH}$ and the low concentration of H_2SO_4 during this time, suggests that pinene reactions may have contributed to new particle formation seen on September 26. Increases in R_{TERP} were observed to lead changes in UF particles on four other days (September 20, 21, 25, and 28). However, $R_{SO2\text{-}OH}$ and/or H_2SO_4 concentrations were well correlated with UF particle concentration on these days as well, leaving open the question of which species may have played the major role in particle formation and growth on the days in question. On all other days with downslope winds, changes in $R_{SO2\text{-}OH}$ and H_2SO_4 concentrations more closely corresponded to changes in new particle concentration than those of R_{TERP}.

Conclusion

If organic particle formation is an important source of new particles in the troposphere, a forested site in the western U.S. such as Idaho Hill may have been an ideal place to measure it. Organic aerosols found in marine environments are thought to be largely of continental origin [Cachier et al, 1986]. The eastern U.S. has many anthropogenic sources of SO_2 which presumably cause sulfates to dominate new UF particle formation. Locations with significant vegetation and well removed from marine and anthropogenic sulfur emissions should offer the best setting to assess the role in new particle formation played by organic compounds in the undisturbed troposphere. The data from Idaho Hill do not provide strong evidence that this contribution is a major one.

The sample size in the present study is admittedly small, and the data show a high degree of scatter, which limit the ability to make definitive statements about the ultimate source of new particles at Idaho Hill. However, while subject to caveats, the above analysis offers a fairly consistent picture of new particle formation. This study, and related work by Weber et al, suggest

that in general sulfates probably dominated the observed new particle formation at Idaho Hill, while organic compounds appeared to be predominately involved with particle growth. Terpenoid compounds may have shown evidence of contributing to new particle formation on one day when sulfate particle production was suppressed. However, the condensable species formed when α– and β pinene were oxidized appeared more likely to condense upon preexisting particle surfaces, adding to particle volume and surface area. These findings suggest a mechanism for the mixed sulfate-organic particles observed by several researchers over the past two decades, and provide insight into a process not at present directly observable.

Acknowledgments. We express our gratitude to all the researchers who took part in the Idaho Hill campaign and freely shared their data. Special thanks are due to Paul Goldan for helpful discussions. This work was supported by NASA grant No. NAGW-3767.

References

Ahn, K. and B. Liu, Particle activation and droplet growth processes in condensation nucleus counters-1. Theoretical background, Journal of Aerosol Science, 21, 249-261, 1990.

Brockmann, J. E., Coagulation and Deposition of Ultrafine Aerosols in Turbulent Pipe Flow, Ph.D. Thesis, University of Minnesota, Minneapolis, MN, 1981.

Cachier, H., P. Buat-Menard, M. Fontugne, and R. Chesselet, Long range transport of continentally derived particulate carbon in the marine atmosphere, Tellus 38B, 161-177, 1986.

Charlson, R. J., S. E. Schwartz, J. M. Hales, R. D. Cess, J.A. Coakley, J.E.Hansen and D. J. Hofmann, Climate forcing by anthropogenic aerosols, Science, 255, 423-430, 1992.

Charlson, R. J., A. H. Vanderpol, D. S. Covert, A. P. Waggoner and N. C. Ahlquist, $H_2SO_4/(NH_4)_2SO_4$ Background Aerosol: Optical Detection in St. Louis region, Atmospheric Environment, 8, 1257-1267, 1974.

Doyle, G. J., Self nucleation in the sulfuric acid water system, Journal of Chemical Physics, 35, 765-799, 1961.

Easter, R. C. and L. K. Peters, Binary homogeneous nucleation: temperature and relative humidity fluctuations, nonlinearity, and aspects of new particle production, Journal of Applied Meteorology, 33, 775-790, 1994.

Eisele, F. L., D. J. Tanner, Measurement of the gas phase concentrations of H2SO4 and Methane Sulfonic acid and estimates of H2SO4 production and loss in the atmosphere, Journal of Geophysical Research, 98, 9001-9010, 1993.

Graedel, T. E., Terpenoids in the atmosphere, Reviews of Geophysics and Space Physics, 17, 937-947, 1979a.

Grosjean, D., E. L. Williams and J. H. Seinfeld, Atmospheric oxidation products of selected terpenes and related carbonyls, Environmental Science and Technology, 26, 1526-1533, 1992b.

Haagen-Smit, A. J. and M. M. Fox, Ozone formation in photochemical oxidation of organic substances, Industrial Engineering and Chemistry, 48, 1484-1487, 1956.

Hagan, D. E. and D. J. Alofs, Linear inversion method to obtain aerosol size distributions from measurements with a differential mobility analyzer, Aerosol Science and Technology, 2, 465-475, 1983.

Hatakeyama, S., K. Izumi and T. Fukuyama, Reactions of ozone with alpha pinene and beta pinene in air, Journal of Geophysical Research, 94, 13013-13024, 1989.

Hatakeyama, S., K. Izumi, T. Fukuyama, H. Akimoto and N. Washida, Reactions of OH with alpha pinene and beta pinene in air, Journal of Geophysical Research, 96, 947-958, 1991.

Hoffman, E. J. and R. A. Duce, The organic carbon of marine aerosols collected on Bermuda, Journal of Geophysical Research, 79, 4474-4477, 1974.

Hogan, A. W., An experiment illustrating that gas to particle conversion by solar radiaion is a major influence in the diurnal variation of Aitkin nucleus concentration, Atmospheric Environment, 2, 599-601, 1968.

Jaecker-Voirol, A., P. Mirabel, Heteromolecular nucleation in the sulfuric acid-water system, Atmospheric Environment, 23, 2053-2057, 1989.

Ketseridis, G. and R. Eichmann, Organic compounds in the atmospheric aerosol, Pure appl. Geophysics, 116, 274-282, 1978.

Kreidenweis, S. M., F. Yin, S.-C. Wang, D. Grosjean, R. C. Flagan and J. H. Seinfeld, Aerosol formation during photooxidation of organosulfur species, Atmospheric Environment, 25A, 2491-2500, 1991a.

Lopez, A., J. Fontan and M. O. Barthomeuf, Study of the formation of particles from natural hydrocarbons released by vegetation, J. Rech. Atmos., 19, 295-307, 1985.

Malm, W.C., J.F. Sisler, D. Huffman, R.A. Eldred, and T.A. Cahill, Spatial and seasonal trends in particle concentration and optical extinction in the United States, Journal of Geophysical Research 99(D1), 1347-1370, 1994.

Marti, J. J., Diurnal variation in the undisturbed continental aerosol, Atmospheric Research, 25, 351-362, 1990.

McMurry, P., New particle formation in the presence of an aerosol: Rates, time scales, and sub-0.01 um size distributions, Journal of Colloid and Interface Science, 95, 72-80, 1983.

McMurry, P. H., Photochemical Aerosol Formation from SO2, Journal of Colloid and Interfacial Science, 78, 513-527, 1980.

McMurry, P. H. and S. K. Friedlander, New Particle Formation in the presence of an aerosol, Atmospheric Environment, 13, 1635-1651, 1979.

Mirabel, P. and J. Katz, Binary homogeneous nucleation as a mechanisim for the formation of aerosol, Journal Of Chemical Physics, 60, 1138-1144, 1974.

Novakov, T. and J. E. Penner, Large contribution of organic aerosols to cloud-condensation-nucleus concentrations, Nature, 365, 823-826, 1993.

Palen, E. J., D. T. Allen, S. N. Pandos, S. E. Paulson, J. H. Seinfels and R. C. Flagan, Fourier transform infrared analysis of aerosol formed in the photoxidation of isoprene and beta pinene, Atmospheric Environment, 26A, 1239-1251, 1992.

Pandis, S. N., S. E. Paulson, R. C. Flagan and J. H. Seinfeld, Aerosol Formation in the photooxidation of isoprene and beta pinene, Atmospheric Environment, 25A, 997-1008, 1991.

Raes, F., Entrainment of free tropospheric aerosols as a regulating mechanism for cloud condensation nuclei in the remote marine boundary layer, Journal of Geophysical Research, 100, 2893-2903, 1995.

Raes, F. and R. v. Dingenen, Simulations of condensation and cloud condensation nuclei from biogenic SO2 in the remote marine boundary layer, Journal of Geophysical Research, 99, 20989-21003, 1992.

Rasmussen, R. and F. W. Went, Volatile organic material of plant origin in the atmosphere, Proceedings of the National Academy of Sciences, 53, 215-220, 1965.

Rivera-Carpio, C.A., C.E. Corrigan, T. Novakov, J.E. Penner, C.F.Rogers, and J.C.Chow, Derivation of contributions of sulfate and carbonaceous aerosols to cloud condensation nuclei from mass size distributions, submitted to Journal of Geophysical Research, October 1994.

Saros, M.T., R.J. Weber, J.J. Marti, and P. H. McMurry, Ultrafine aerosol measurements using a condensation nucleus counter with pulse height analysis. *Aerosol Science and Technology.* (in press), 1996.

Seinfeld, J. H. (1986). Atmospheric Chemistry and Physics of Air Pollution. New York, John Wiley and Sons.

Shu, Y. and R. Atkinson, Atmospheroc lifetimes and fates of a series of sesquiterpenes, Journal of Geophysical Research 100(D4), 7275-7281, 1995.

Stern, J.E., R.C. Flagan, D. Grosjean, and J.H. Seinfeld, Aerosol formation and growth in atmospheric aromatic hydrocarbon photooxidation, Environ. Sci. Technol. 21(12), 1224-1234, 1987.

Stolzenburg, M. R., An UF aerosol size distribution measuring system, Ph.D. Thesis, University of Minnesota, Minneapolis, MN, 1988.

Stolzenburg, M. R. and P. H. McMurry, An UF aerosol condensation nucleus counter, Aerosol Science and Technology, 14, 48-65, 1991.

Twomey, S. A., M. Piepgrass and T. L. Wolfe, An assessment of the impact of pollution on global cloud albedo, Tellus, 36B, 356-366, 1984.

Tyndall, J., On a new series of chemical reactions produced by light, Proceedings of the Royal Society of London, 17, 92-102, 1868.

Wang, S.-C., S. E. Paulson, D. Grosjean, R. C. Flagan and J. H. Seinfeld, Aerosol formation and growth in atmospheric organic/NO_x systems-I. Outdoor smog chamber studies of C_7 and C_8 hydrocarbons, Atmospheric Environment, 26A, 403-420, 1992a.

Wang, S. C. and R. C. Flagan, Scanning Electrical Mobility Spectrometer, Aerosol Science and Technology, 13, 230-240, 1990.

Weber, R. J., J. J. Marti, P. H. McMurry, F. L. Eisele, D. J. Tanner and A. Jefferson, Measurements of new particle formation at a clean continental Site, submitted to Journal of Geophysical Research, , 1996.

Weber, R. J., J. J. Marti, P. H. McMurry, F. L. Eisele, D.J.Tanner and A. Jefferson, Measured atmospheric new particle formation rates: Implications for nucleation mechanisms, Submitted to : Chemical Engineering Communications, , 1995b.

Weber, R. J., P. H. McMurry, F. L. Eisele and D.J.Tanner, Measurement of expected nucleation precursor species and 3 to 500 nm particles at Mauna Loa Observatory, Hawaii, Journal of the Atmospheric Sciences, 52, 2242-2257, 1995a.

Weiss, R. E., A. P. Waggoner, R. J. Charlson and N. C. Ahlquist, Sulfate Aerosol: Its Geographical Extent in the Midwestern and Southern United States, Science, 195, 979-981, 1977.

Went, F. W., Blue hazes in the atmosphere, Nature, 187, 641-643, 1960.

Went, F. W., On the nature of Aitkin condensation nuclei, Tellus, 18, 549-555, 1966.

Wilson, W. E. J., W. E. Schwartz and G. W. Kinzer,. Haze formation--its nature and origin. Report #CRC-APRAC-CAPA-6-68-3. Battelle Columbus Laboratories, Columbus, Ohio, 1972.

Yokouchi, Y. and Y. Ambe, Aerosols formed from the chemical reaction of monoterpenes and ozone, Atmospheric Environment, 19, 1271-1276, 1985.

Zhang, X. Q., P. H. McMurry, S. V. Hering and G. S. Casuccio, Mixing characteristics and water content of submicron aerosols measured in Los Angeles and at the Grand Canyon, Atmospheric Environment, 27A, 1593-1607, 1993.

Figure Captions

Figure 1. Representative sample of UF particle concentration, plotted with reaction rates R from sulfate and NMHC systems (see text for definition of R). The diurnal variation in particle concentration was observed on most days.

a. UF particle concentration and sulfate reaction rate, $R_{SO2\text{-}OH}$.

b. UF particle concentration and terpene reaction rate, R_{TERP}.

c. UF particle concentration and reaction rate for anthropogenic hydrocarbons, R_{ANTHRO}.

Figure 2. The peak measured concentration of UF particles for each day (N_{max}) of the Idaho Hill field study, plotted against daily mean values of R for each reacting system. The data are split into subsets according to the value of total aerosol surface area (see text).

a. N_{max} versus R_{TERP}.

b. N_{max} versus R_{ANTHRO}.

c. N_{max} versus $R_{SO2\text{-}OH}$.

Figure 3. The peak measured concentration of UF particles for each day (N_{max}) plotted against daily mean values of gas phase H_2SO_4 concentration. Only data collected during days of low particle surface area are included.

Figure 4. Mean daily values of total particle surface area and total particle volume, plotted against the mean reaction rates of each reacting system.

a. Area and volume versus terpene reaction rate, R_{TERP}.

b. Area and volume versus anthropogenic hydrocarbon reaction rate, R_{ANTHRO}.

c. Area and volume versus sulfate reaction rate, $R_{SO2\text{-}OH}$..

Figure 5. Concentration of UF particles as a function of time on September 26. The calculated reaction rates R_{TERP} and R_{SO2-OH} for that day are also shown.

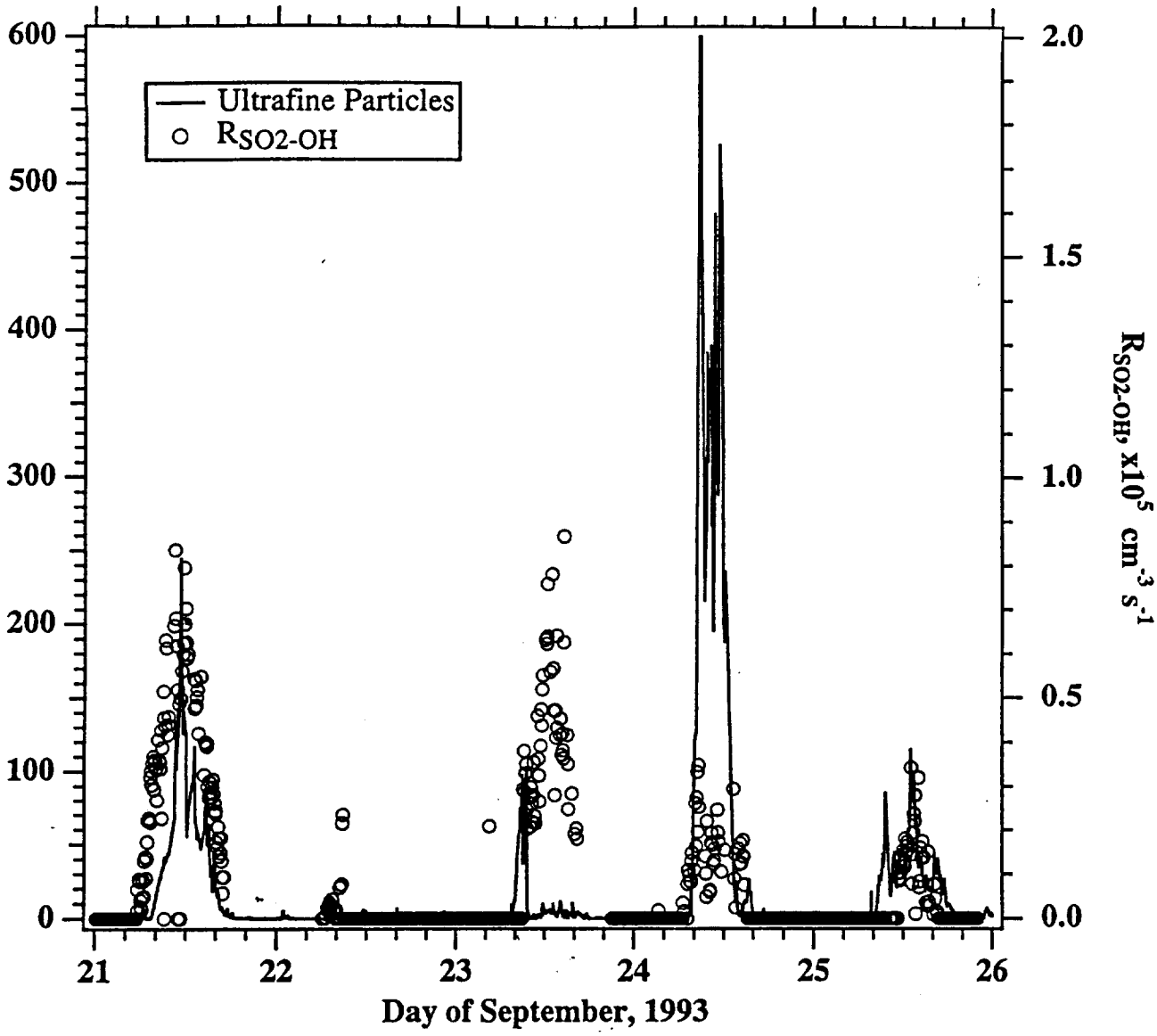
Ultrafine Particles
R_{SO2-OH}
600
500
400
300
200
100
0
2.0
1.5
1.0
0.5
0.0
21
22
23
24
25
26
Day of September, 1993
R_{SO2-OH}, x10^5 cm^{-3} s^{-1}

FIGURE 1a.

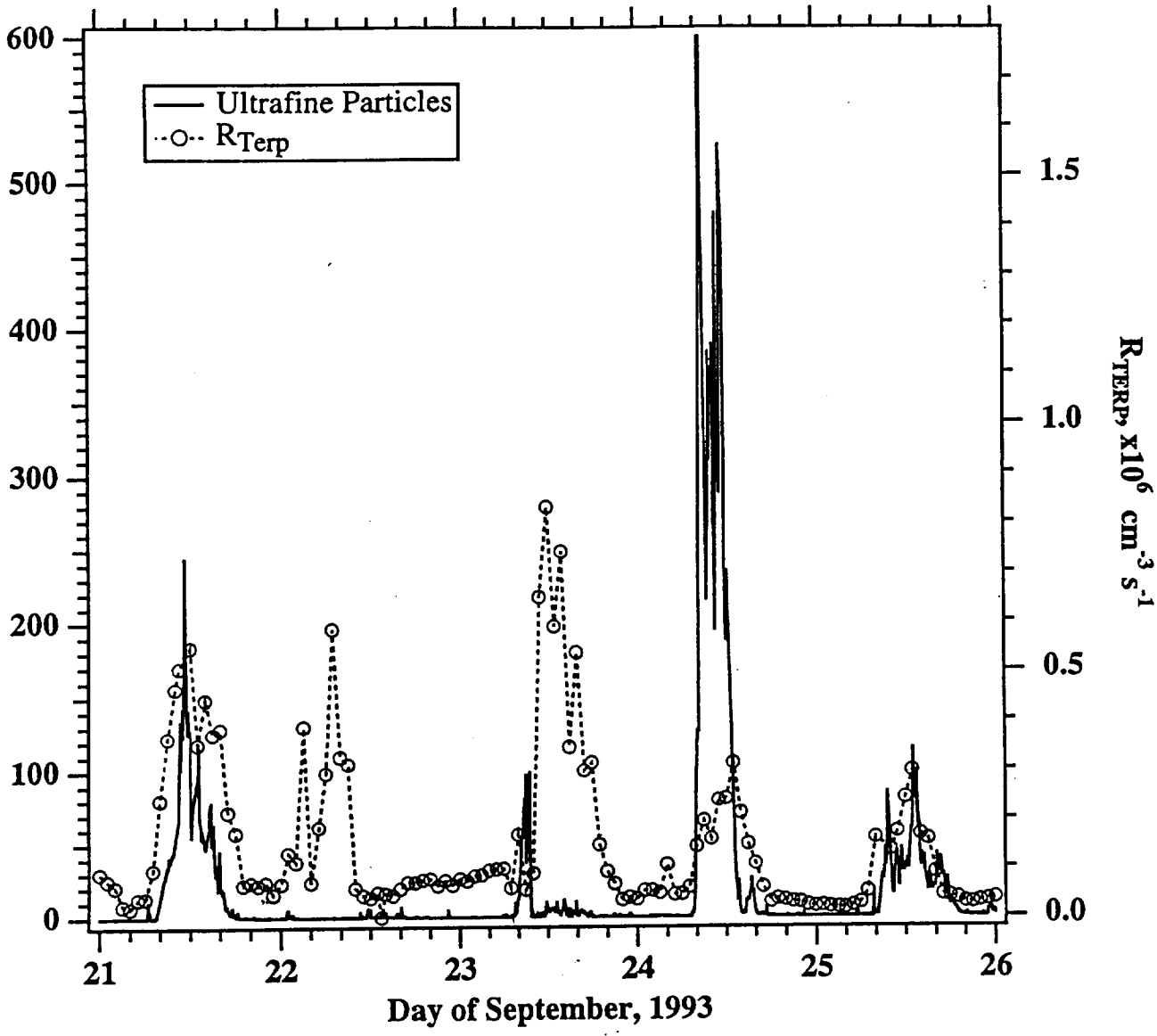
Ultrafine Particles
R_Terp
600
500
400
300
200
100
0
1.5
1.0
0.5
0.0
21
22
23
24
25
26
Day of September, 1993
R_TERP, x10^6 cm^-3 s^-1

FIGURE 1b.

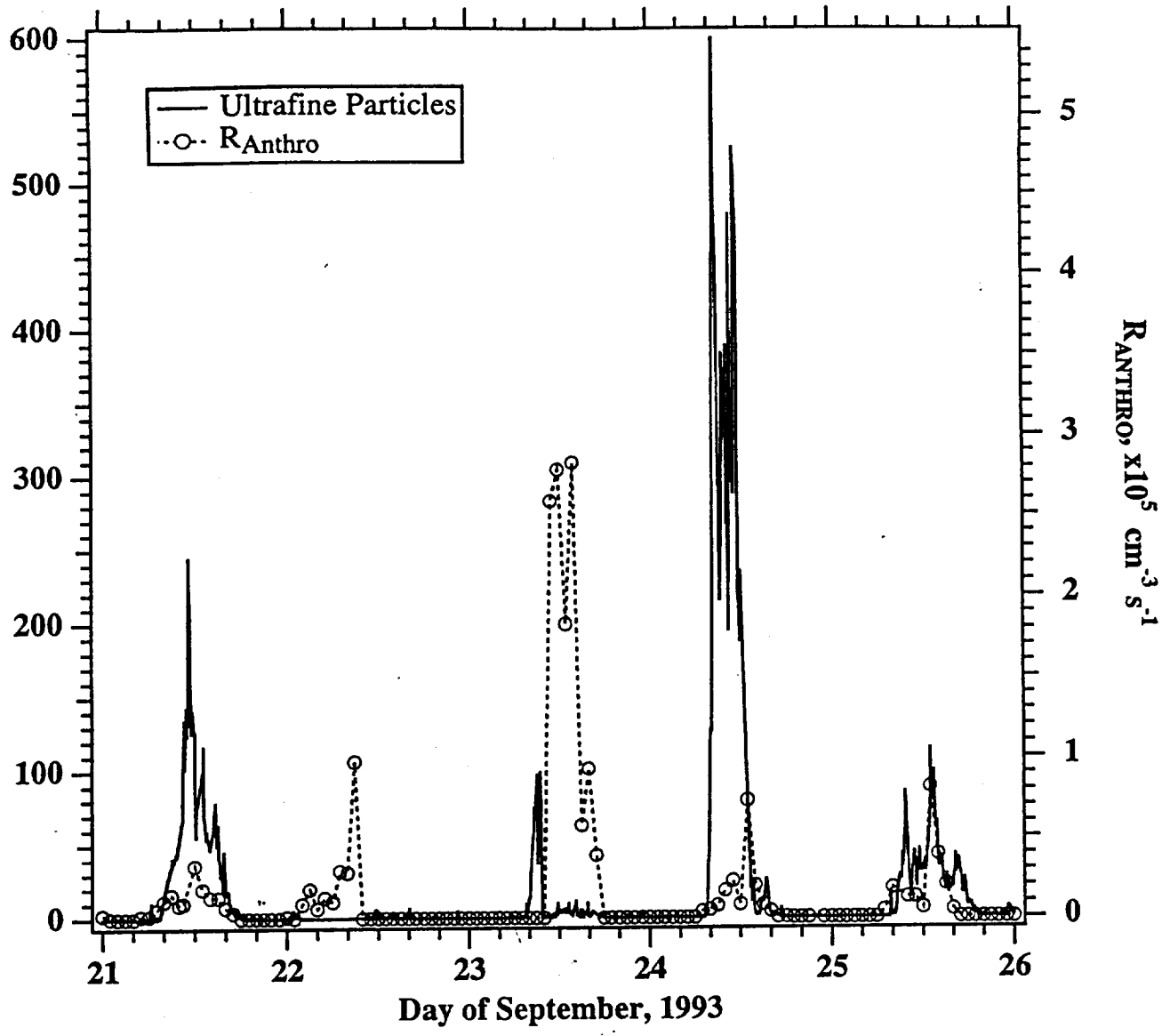
Ultrafine Particles
R_Anthro
600
500
400
300
200
100
0
5
4
3
2
1
0
21
22
23
24
25
26
Day of September, 1993
R_ANTHRO, x10^5 cm^-3 s^-1

FIGURE 1c.

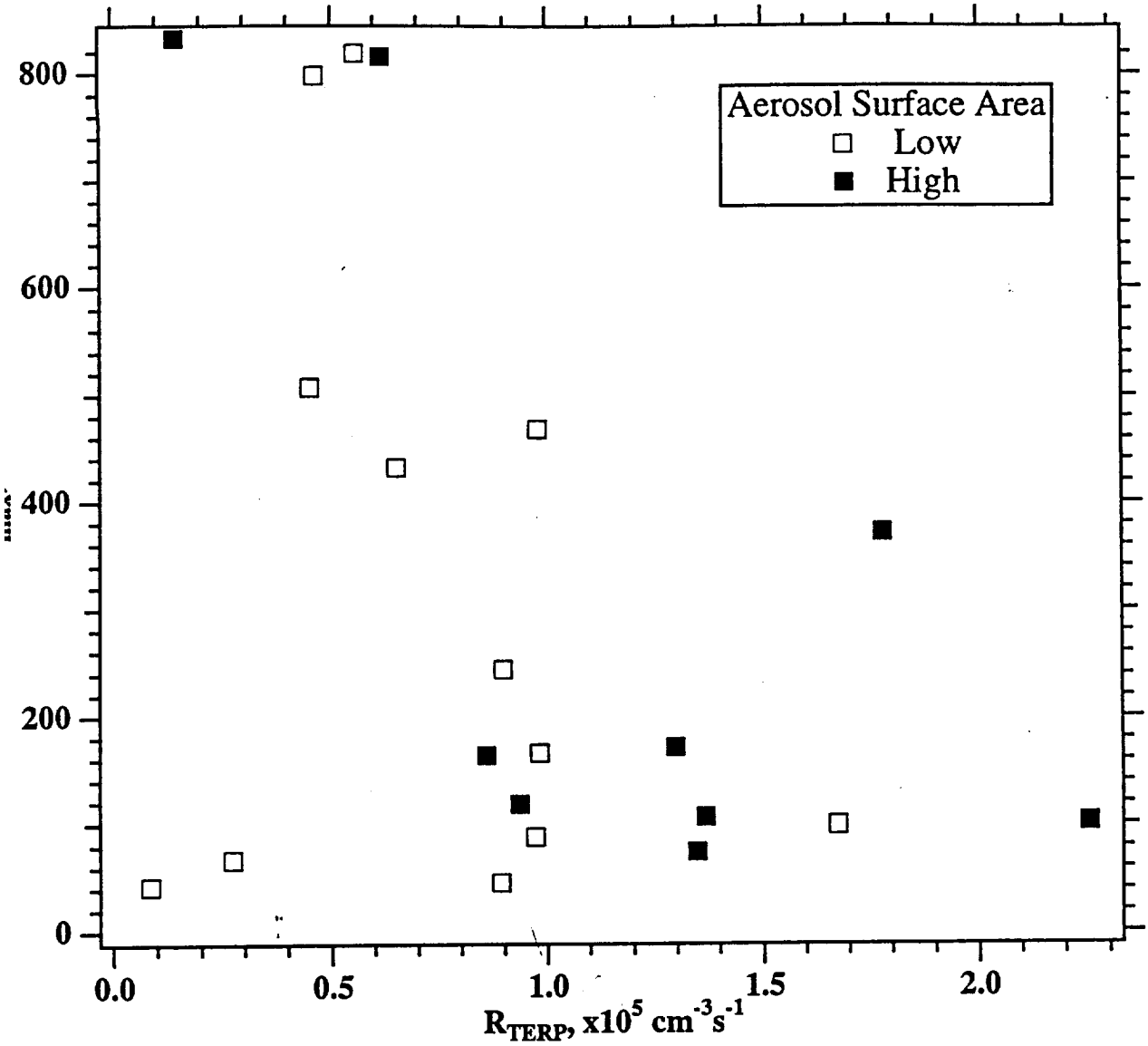
Aerosol Surface Area
Low
High
800
600
400
200
0
0.0
0.5
1.0
1.5
2.0
R_TERP, x10^5 cm^-3 s^-1

FIGURE 2a.

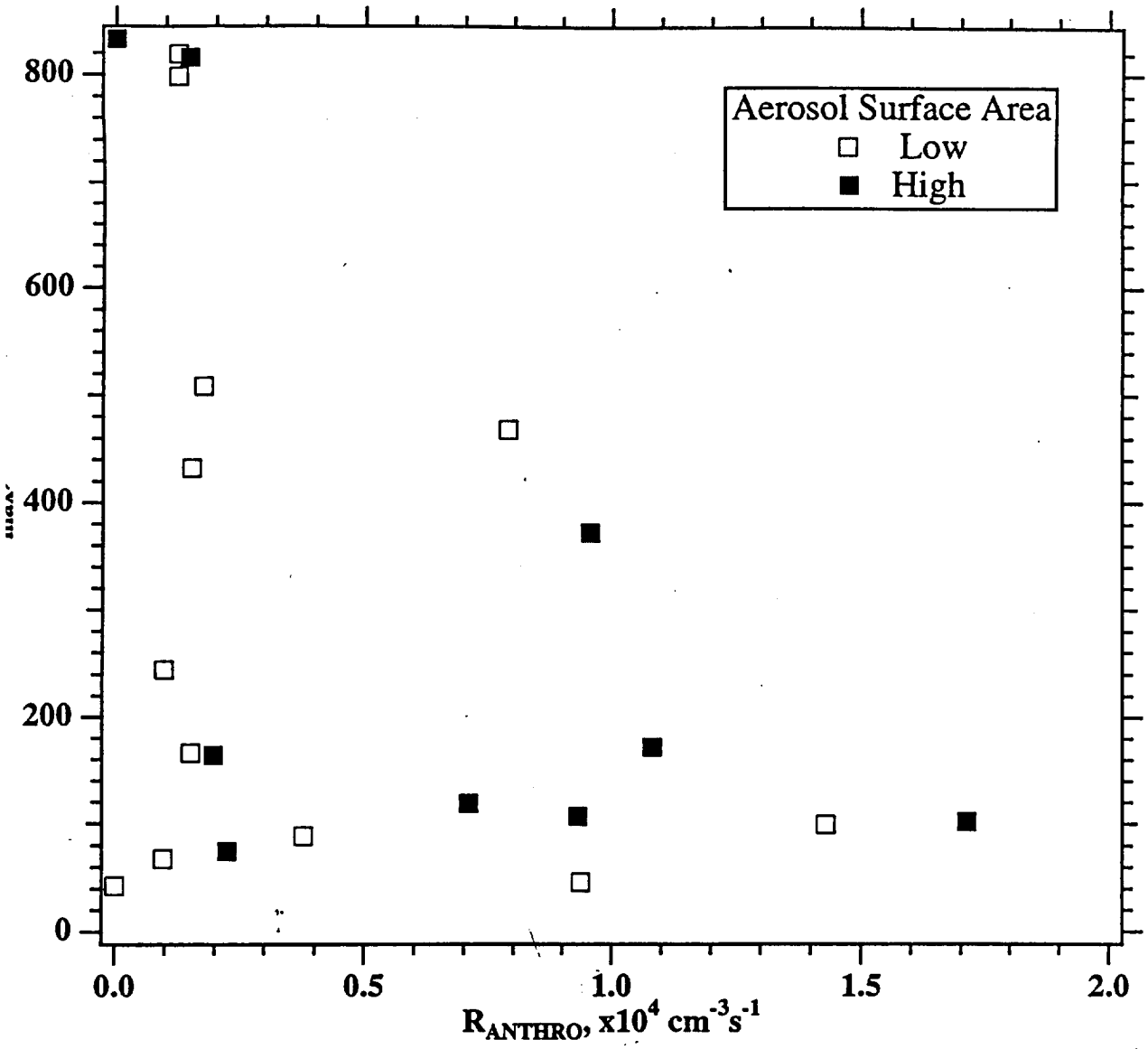
Aerosol Surface Area
Low
High
800
600
400
200
0
0.0
0.5
1.0
1.5
2.0
R_{ANTHRO}, x10^4 cm^{-3}s^{-1}

FIGURE 2b.

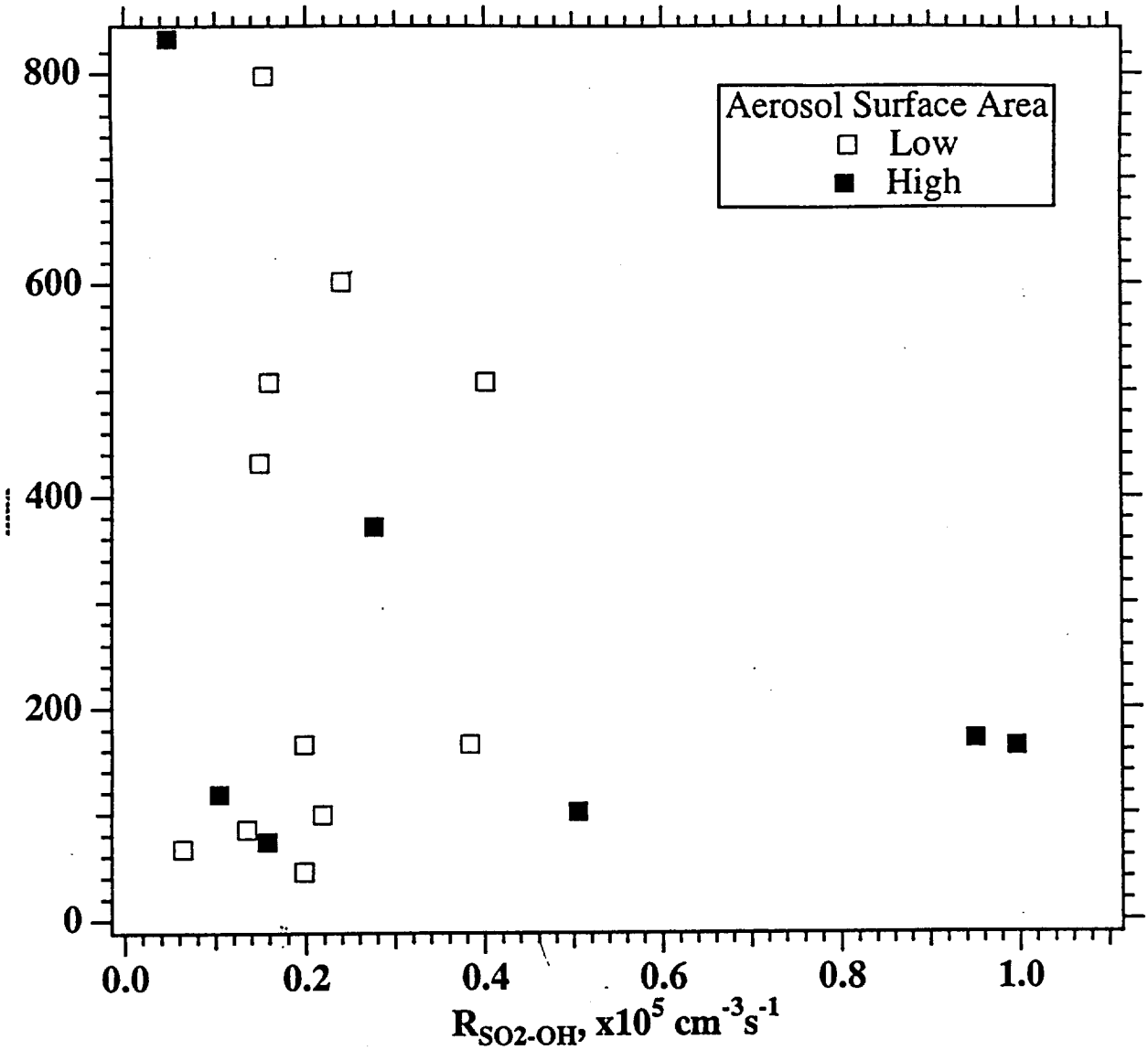
Aerosol Surface Area
Low
High
800
600
400
200
0
0.0
0.2
0.4
0.6
0.8
1.0
R_{SO2-OH}, x10^5 cm^{-3}s^{-1}

FIGURE 2c.

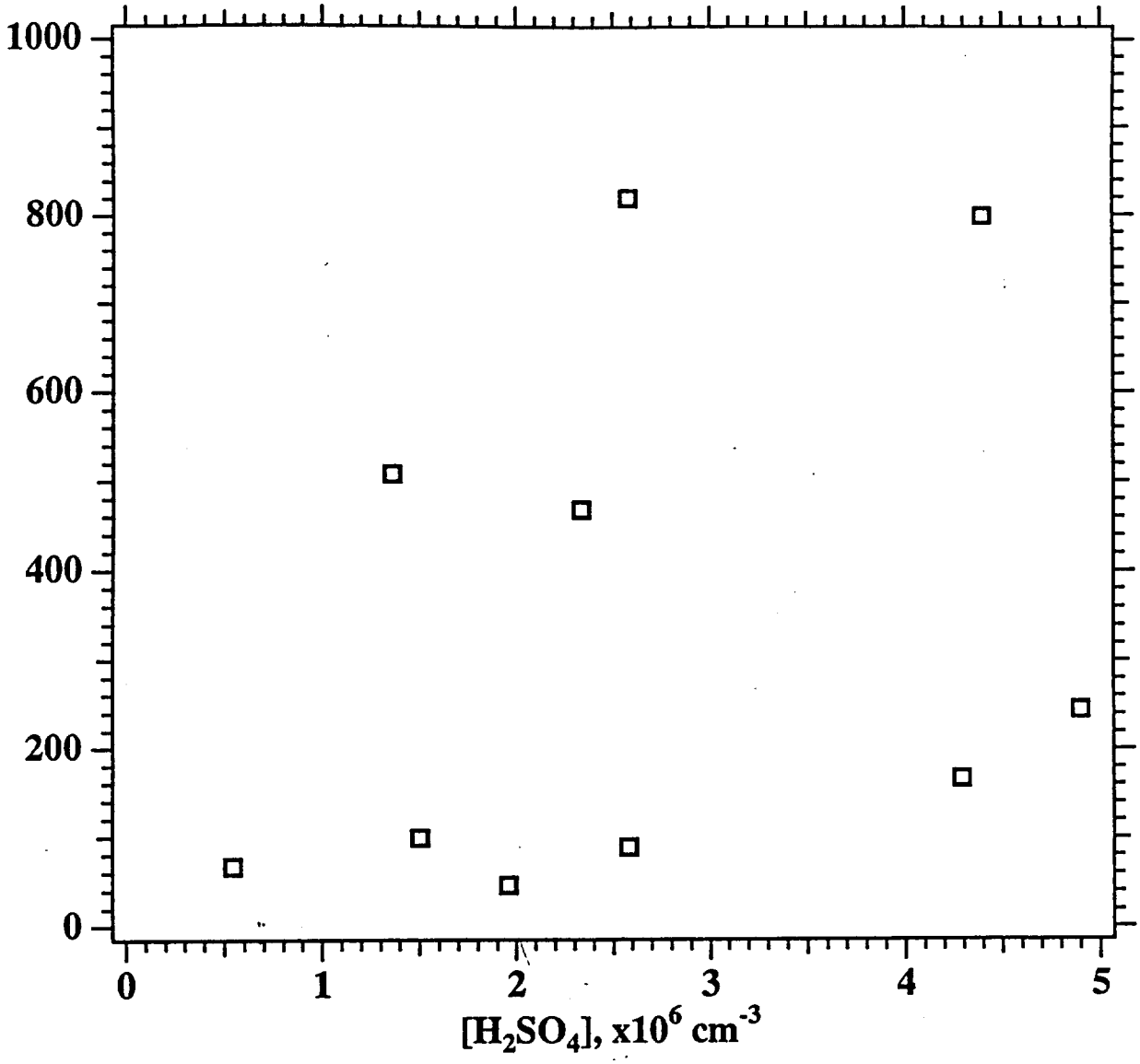

FIGURE 3.

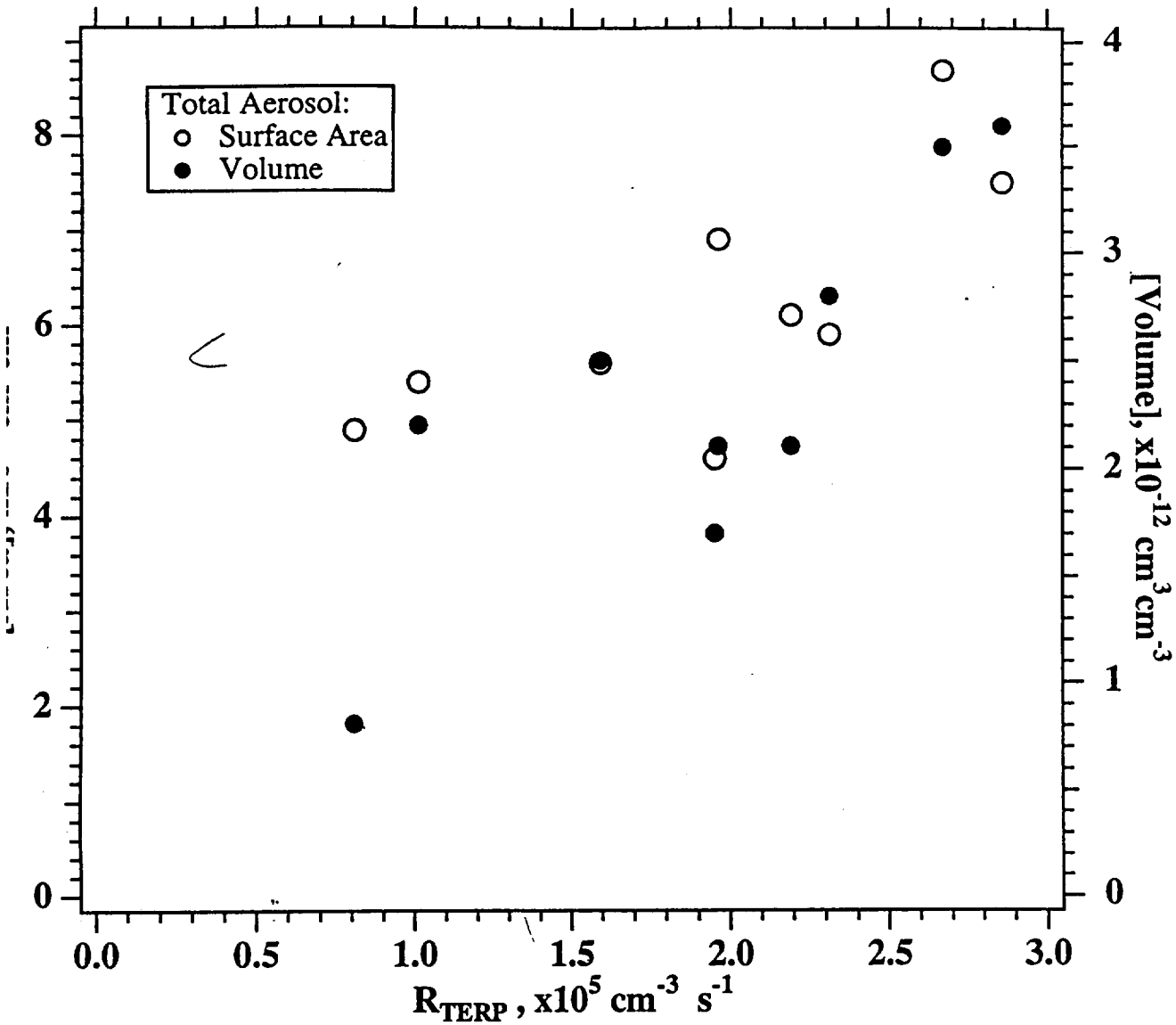
Total Aerosol:
Surface Area
Volume
0
2
4
6
8
0.0
0.5
1.0
1.5
2.0
2.5
3.0
0
1
2
3
4
R_TERP , x10^5 cm^-3 s^-1
[Volume], x10^-12 cm^3 cm^-3

FIGURE 4a.

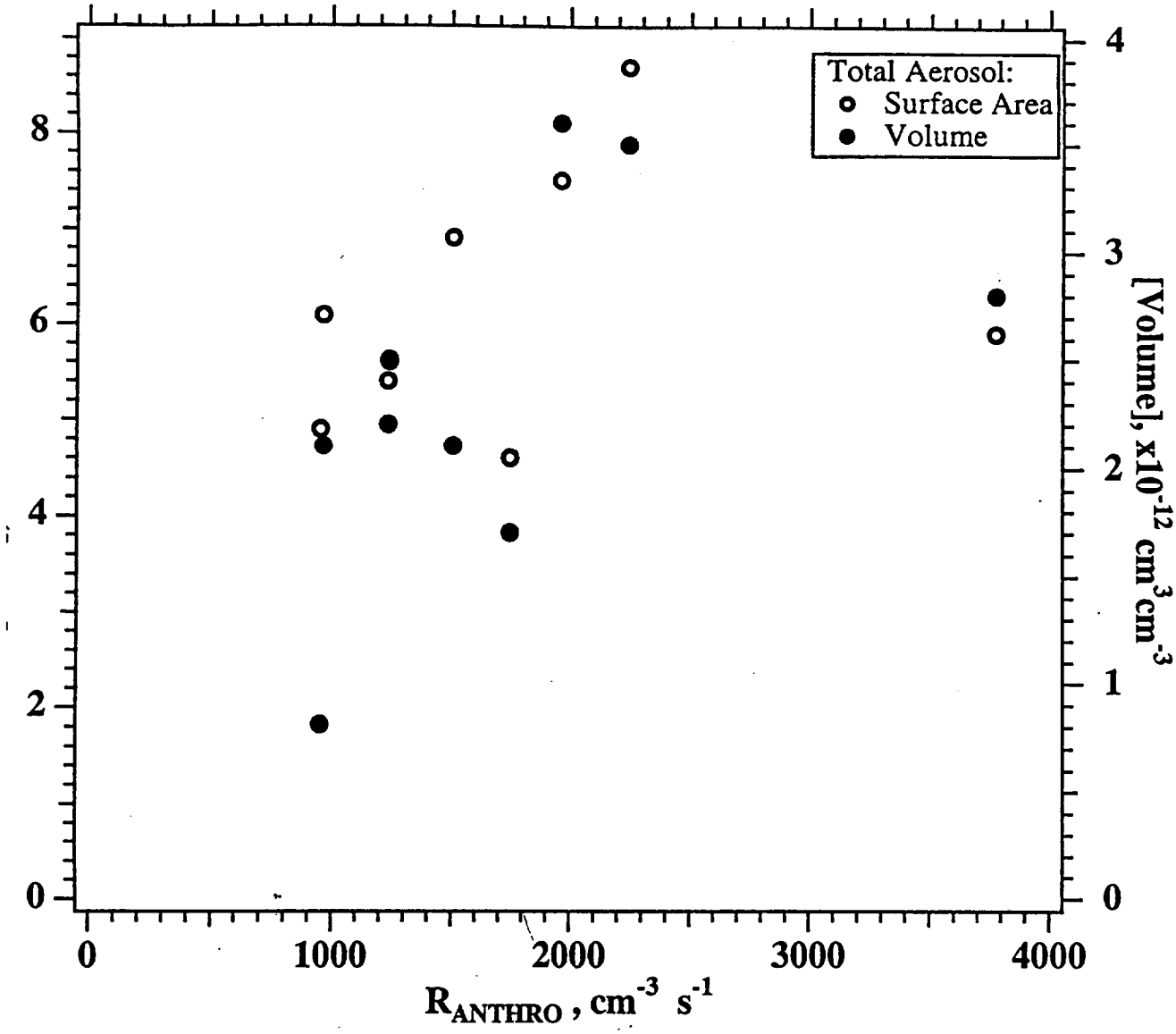
Total Aerosol:
Surface Area
Volume
0
2
4
6
8
0
1000
2000
3000
4000
R_{ANTHRO} , cm^{-3} s^{-1}
0
1
2
3
4
[Volume], $x10^{-12}$ cm^3 cm^{-3}

FIGURE 4b

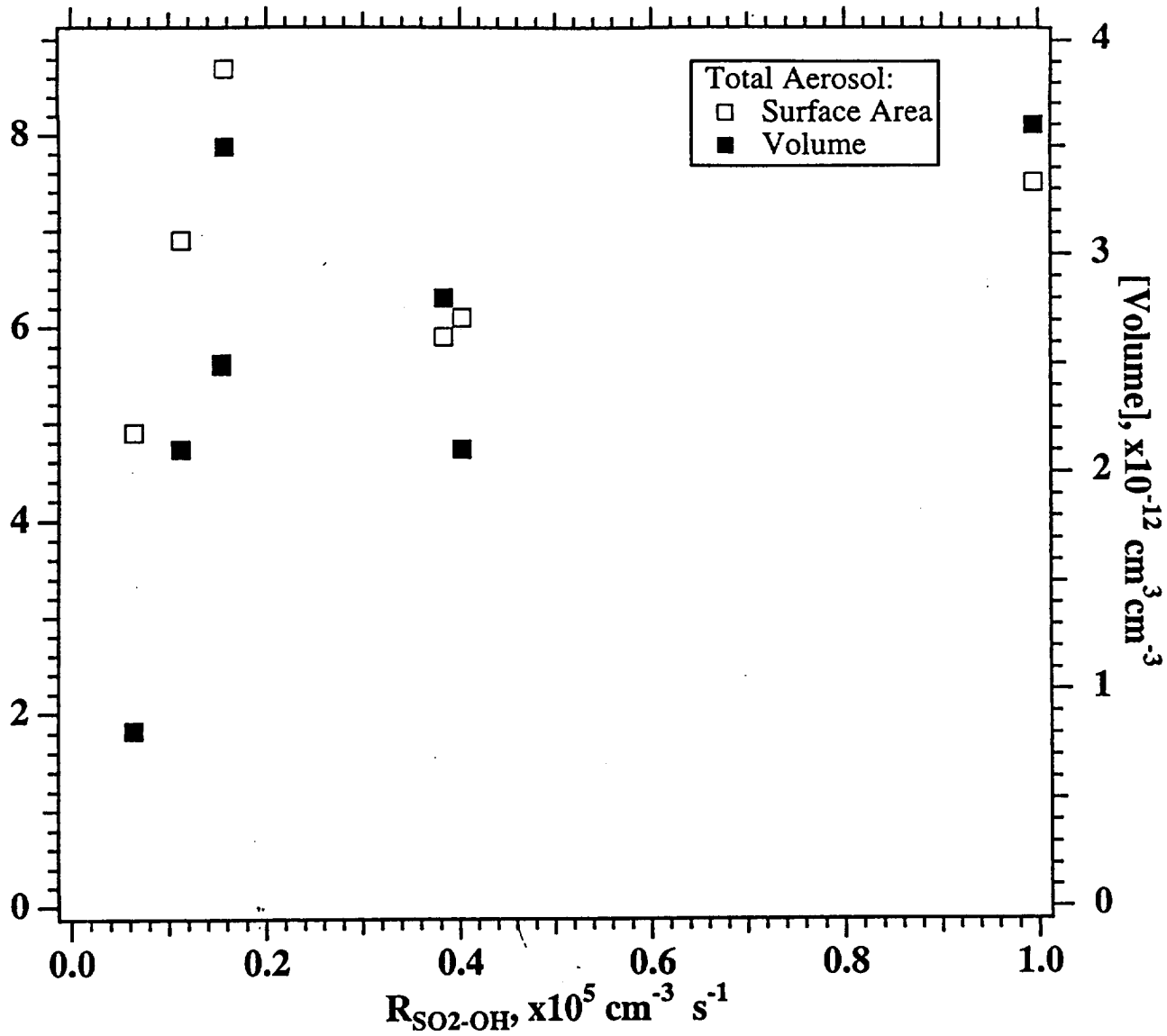
Total Aerosol:
Surface Area
Volume
0
2
4
6
8
0.0
0.2
0.4
0.6
0.8
1.0
0
1
2
3
4
R_{SO2-OH}, x10^5 cm^{-3} s^{-1}
[Volume], x10^{-12} cm^3 cm^{-3}

FIGURE 4c.

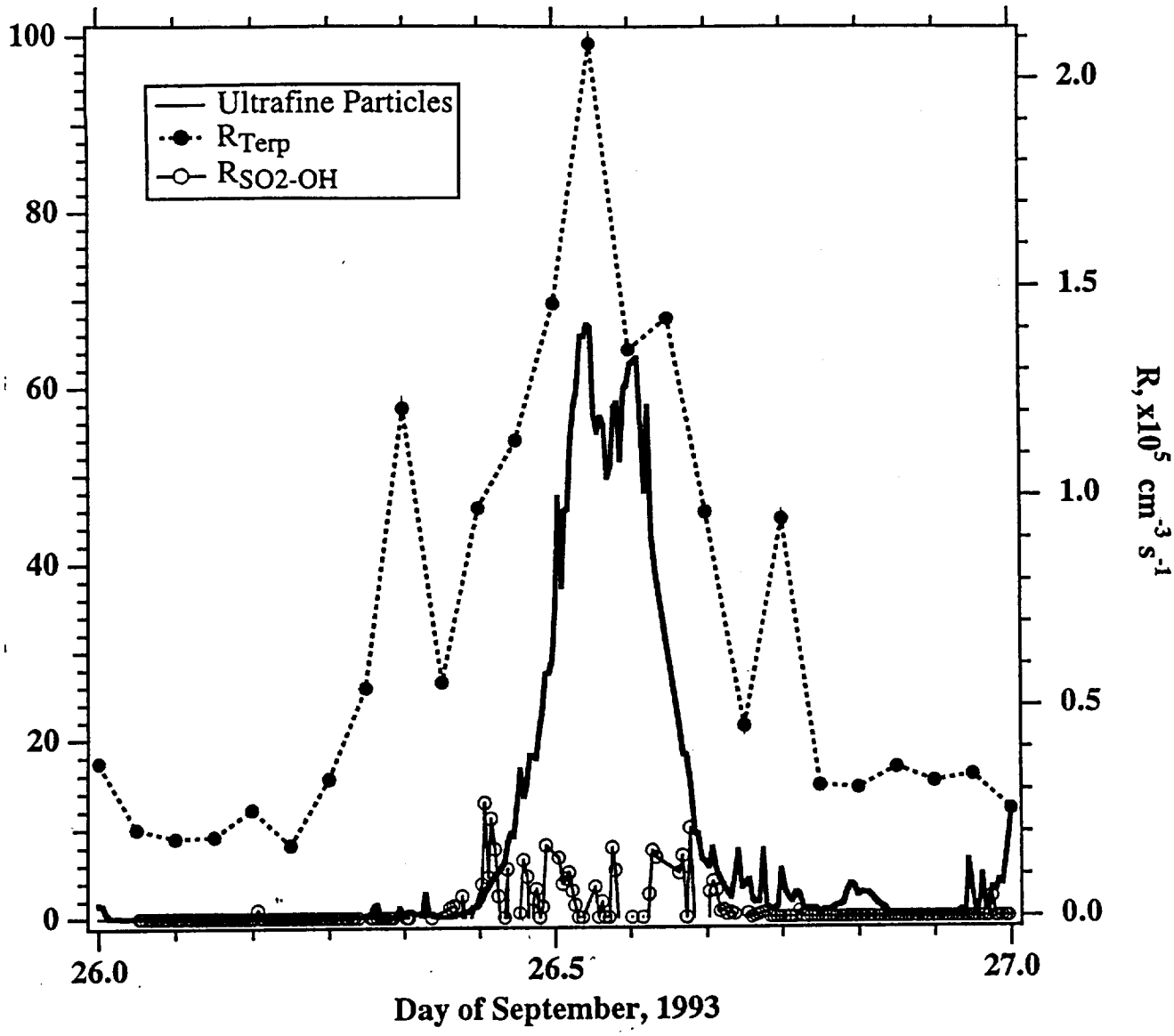
Ultrafine Particles
R_{Terp}
R_{SO2-OH}
100
80
60
40
20
0
2.0
1.5
1.0
0.5
0.0
R, x10^5 cm^{-3} s^{-1}
26.0
26.5
27.0
Day of September, 1993

FIGURE 5.

6 April 1996

Measurements of New Particle Formation and Ultrafine Particle Growth Rates at a Clean Continental Site

R. J. Weber†, J. J. Marti‡, P. H. McMurry*

Particle Technology Laboratory
Department of Mechanical Engineering
111 Church St. SE
University of Minnesota
Minneapolis, MN 55455

F. L. Eisele** D. J. Tanner. A. Jefferson

Atmospheric Chemistry Division
NCAR
P.O. Box 3000
Boulder, CO. 80307

Submitted to:

Journal of Geophysical Research: Atmospheres

PTL Publication No. 933

†Present address: Environmental Chemistry Division, Brookhaven National Laboratory, Building 426, Upton, NY 11973

‡Present address: Remote Sensing Division, Naval Research Laboratory, 4555 Overlook Ave. S.W., Washington, D. C. 20375-5320

*To whom correspondence should be addressed

**Also holds a joint appointment at EOEM2/GTRI
Georgia Institute of Technology
Atlanta, GA 30332

Abstract

Simultaneous measurements of aerosols and their expected gas phase precursors were made at Idaho Hill, Colorado, a remote continental site. This study used apparatus and techniques similar to those employed in an earlier study at the Mauna Loa Observatory, Hawaii (Weber et al., J. Atmos. Sci. 52:2242, 1995). New particle formation, identified by the presence of ultrafine particles (nominally 3 to 4 nm diameter), was commonly observed in downslope (westerly) air and was correlated with high sulfuric acid (H_2SO_4) concentrations, low relative humidity and low aerosol particle surface area concentrations. The data point to H_2SO_4 as a principle nucleation precursor species whereas water vapor (H_2O) apparently played a minor role. Particle production was observed at H_2SO_4 concentrations that are well below predicted values for binary nucleation of H_2O and H_2SO_4, suggesting that another species was involved.

Particle growth rates were estimated from the data with two independent approaches and in both cases were ~5 to 10 times higher than can be explained by condensation of H_2SO_4 and its associated water. This suggests that species in addition to H_2SO_4 are contributing ultrafine particle growth.

Finally, calculated steady-state H_2SO_4 concentrations were found to be in good agreement with measured values if the mass accommodation coefficient for H_2SO_4 on aerosol surfaces was assumed equal to ~1.

Introduction

Tropospheric aerosol particles influence global climate by scattering radiation directly [*Taylor & Penner*, 1994] and indirectly by altering the scattering characteristics of clouds [*Twomey et al.*, 1984]. Because both effects depend on particle size, processes which influence particle size distributions can influence climate. The formation of new particles from gas phase precursor species plays an important role in regulating aerosol populations; in the remote atmosphere it is thought to be the primary source for new particles. The growth rates of newly formed particles are also critical since new particles must grow by orders of magnitude to influence the earth's radiation balance.

A field study at the Mauna Loa Observatory, Hawaii, provided insight into particle formation in the remote marine troposphere [*Weber et al.*, 1995a]. This effort has been extended by measurements made at Idaho Hill, Colorado, a remote continental site. The approach in both cases has been to examine atmospheric new particle formation by measuring the expected nucleation gas phase precursor species with simultaneous measurements of ultrafine (nominally 3 to 4 nm diameter) and fine (~15 nm to ~0.5 μm diameter) aerosols. Together, these two studies provide insight into atmospheric new particle formation and also permit comparison of particle production at a remote marine and continental site.

Due in part to the extent of the earth's oceans, marine aerosols are thought to have a significant influence on global climate [*Charlson et al.*, 1987]. These aerosols have received special attention in both modeling and atmospheric measurements. Currently, classical binary nucleation theory involving sulfuric acid and water (H_2SO_4/H_2O) [*Jaecker-Voirol and Mirabel*, 1989] is used for predicting atmospheric particle formation rates. It has not been demonstrated, however, that remote tropospheric particles are formed by this mechanism. Measurements by various researchers have provided evidence of an in-situ source for marine aerosols. *Clarke* [1993] observed evidence of particle production in the Pacific free troposphere and modeling by *Raes and coworkers* [1992, 1995] suggests that the free troposphere is the major source for marine cloud condensation nuclei (CCN). On Pacific Ocean cruises *Covert et al.* [1995]

consistently observed evidence for particle formation in regions of subsiding air masses but saw no evidence of new particle formation in the marine boundary layer itself. Evidence of particle production has also been detected in the outflow regions of precipitating marine cumulus clouds [*Perry and Hobbs*, 1994] and in clear marine boundary layer air [*Hoppel et al.*, 1994a]. A common feature to the marine sites where researchers have detected new particle formation was low aerosol surface area concentrations (typically less than ~5 $\mu m^2\ cm^{-3}$).

Many of the phenomena observed for marine aerosols may also occur in clean continental air, although less attention has been given to these regions. Both gas phase species and aerosol concentrations are generally higher in continental than in marine environments. In addition, a greater variety of species, both natural and anthropogenic, may interact with aerosols making continental regions more complex chemical systems. For example, vegetation derived hydrocarbons may also contribute to particle formation [*Lopez et al.*, 1985] and growth. Based on measurements at a mountain site in Puerto Rico, *Novakov and Penner* [1993] speculated that the majority of particles less than 70 nm diameter were organic.

There is also evidence for new particle formation in clean continental air. A unique characteristic of these observations is a persistent diurnal variation in aerosol concentrations. This diurnal nature has been observed in a wide variety of continental settings and suggests a photochemical aerosol source [*Koutsenogii and Jaenicke*, 1994; *Marti*, 1990; *Hogan* 1968; *Bradbury and Meuron*, 1938]. As with marine environments, there is evidence of particle formation in the continental free troposphere [*Hofmann*, 1993] and evidence of possible nucleation events in the vicinity of continental cumulus clouds [*Radke and Hobbs*, 1991].

This work reports on measurements made at Idaho Hill, Colorado, from 5 September 1993 to 29 September 1993. Measurements representative of clean continental conditions are presented and compared to the earlier findings from the Mauna Loa Observatory.

Site

Idaho Hill is a remote continental site located on the eastern side of the Rocky Mountains (105°34'32" latitude, 39°58'56" longitude) slightly east of the continental divide and approximately 25 km west of Boulder. The site is situated just below the timber line at an average pressure elevation of 0.7 atmosphere (3070 m elevation). The local topography consists of generally higher elevations to the west and lower elevations to the east. The nearest populated areas (Boulder, Denver, etc.) are at lower elevations, east and south-east of the site. The western sector is sparsely populated and the prevailing westerly (downslope) winds were associated with relatively clean dry air. Upslope winds were typically from the SE, the direction of likely pollution sources. A more detailed description of the site is given by *Mount and Williams* [1995].

Instrumentation

Pertinent gas phase species that were measured in this study include sulfur dioxide (SO_2), the hydroxyl radical (OH), sulfuric acid (H_2SO_4), and water (H_2O). In addition, alpha and beta pinene, which are also aerosol precursors, were measured. An analysis of the role of the organic species in new particle formation is reported elsewhere [*Marti et al.*, 1995]. Here the focus is on the role of H_2SO_4.

Concentrations of molecular gas phase OH and H_2SO_4 were measured to an absolute uncertainty of ±35% using a unique chemical ionization mass spectrometer [*Eisele and Tanner*, 1993; *Tanner and Eisele*, 1995]. The instrument's lower detection limit was approximately 10^4 molecules per cm^3. Sulfur dioxide was measured by pulsed fluorescence (Model 43S, Thermo Environmental Instruments Inc. Hopkington, Mass.). This instrument had a lower detection limit of ~100 pptv (parts per trillion by volume). For the latter part of the study (24 September -29 September) hourly SO_2 zeros were performed. This permitted correcting for a temperature-dependent systematic offset error observed with this instrument. The validity of OH

measurements with this instrument was recently confirmed in a methods intercomparison study [*Mount and Williams*, 1995].

The ultrafine aerosol is defined here as particles in the narrow size range from 2.7 nm, the lower detection limit of the ultrafine condensation particle counter (UCPC), to nominally 4 nm diameter. Measurements of the ultrafine aerosol concentration were made with the prototype of the TSI 3025 UCPC [*Stolzenburg and McMurry*, 1991]. Ultrafine particle concentrations were determined by measuring the UCPC photo detector pulse heights [*Weber et al.*, 1995a] with a multichannel analyzer (MCA). This method of acquiring ultrafine particle size information is based on experimental work which showed that, for particles smaller than ~15 nm, the final droplet size (pulse height), after growth in the UCPC condenser, is uniquely related to the initial particle size [*Brockmann*, 1981; *Ahn and Liu*, 1990; *Stolzenburg* 1988; *Saros et al.*, 1995].

For this study, we diluted the sample aerosol prior to measuring the ultrafine concentration. Nevertheless, on rare occasions, significant particle coincidence (more then one particle in the UCPC optical scattering volume at a time) resulted in inaccurate sizing of the ultrafine aerosols. Based on laboratory experiments [*Saros et al.*, 1995], these episodes were identified by MCA dead times exceeding 15% and the data were ignored. The UCPC sample flow rate was 0.5 cm^3 s^{-1} and the typical sampling period was 2.5 minutes. Considering only those uncertainties associated with Poisson counting statistics, these settings result in an uncertainty of ±35% for a measured ultrafine concentration of 0.1 cm^{-3}. Uncertainties decrease for concentrations higher than this.

Because ultrafine particles of a given size produce a range of pulse heights, our method of measuring the ultrafine particle concentration does not count all particles in the ultrafine size range (i.e., ~3 to 4 nm diameter). This results in our underestimating the concentrations of these particles, typically by ~50%. This shortcoming, however, is far outweighed by the measurement's high sensitivity for detecting ultrafine particle concentrations.

Aerosol size distributions covering diameters between 15 and ~500 nm were measured with a scanning mobility particle spectrometer [*Wang and Flagan*, 1990]. A complete scan

through this size range was typically completed every 2.5 minutes. These data were inverted using the method of *Hagen and Alofs* [1983]; aerosol surface area concentrations were obtained by integrating over these distributions, assuming spherical particles. The concentrations of larger particles, ~0.5 μm up to 9 μm diameter, were measured by other researchers at the site. These larger sizes contributed at most 3% to the total aerosol surface area concentration when downslope conditions prevailed, although there were episodes when these larger particles (>0.5 μm diameter) made significant contributions to the total aerosol surface area when the wind was from the polluted sector (upslope).

Theory: Calculation of Particle Growth and Formation Rates

The data are used to calculate particle growth and formation rates in a manner similar to that performed earlier with the Mauna Loa measurements [*Weber et al.*, 1995a, 1995b].

If particle growth is limited by condensation of H_2SO_4 vapor, the ultrafine particle growth rate (i.e., free molecular regime) is [*Friedlander*, 1977]:

$$\frac{dD_p}{dt} = \frac{2\alpha v_1 (p_1 - p_d)}{(2\pi m k T)^{1/2}} \qquad (1)$$

where α is the H_2SO_4 mass accommodation coefficient, T the temperature, k is Boltzmann's constant, and m and v_1, the mass and volume respectively of the condensing vapor. The measured partial pressure of H_2SO_4 is p_1, and the equilibrium partial pressure, p_d. We assume an accommodation coefficient of one and that evaporation of H_2SO_4 from the droplet is small compared to condensation (i.e., $p_d = 0.0$). We also assume that growth is from condensation of only hydrated H_2SO_4 molecules which are in equilibrium with the H_2O vapor phase at 10°C. The degree of hydration is calculated using the equilibrium data of *Gmitro and Vermeulen* [1963]. These assumptions provide an upper limit if growth is only by condensation of hydrated H_2SO_4 vapor. Actual growth rates, however, could be higher if additional species were also involved, or if significant numbers of H_2SO_4 clusters also condense.

The rate at which particles grow through a certain size due to condensing vapor can be determined from the particle size distribution function and particle growth rate. The formation rate of nominally 3 nm particles is,

$$J(3nm) = \left.\frac{dN}{dD_P}\right)_{3.5nm} \cdot \left.\frac{dD_P}{dt}\right)_{3.5nm}, \qquad (2)$$

where dN/dD_P is the measured aerosol size distribution function at 3.5 nm and dD_P/dt is the diameter growth rate for 3.5 nm particles determined with Eq (1). We estimate the average size distribution function in the vicinity of 3.5 nm from our measurement of the ultrafine aerosol concentration by:

$$\left.\frac{dN}{dD_p}\right)_{3.5nm} \approx \bar{n} = \frac{\text{measured concentration in 3 to 4 nm diameter range}}{4\text{ nm} - 3\text{ nm}} \qquad (3)$$

Thus, our estimates of the 3 nm particle formation rate require simultaneous measurements of the H_2SO_4 vapor and ultrafine aerosol concentrations.

Results

Aerosol Concentrations Versus Wind Direction

At Idaho Hill, measured ultrafine aerosol concentrations were found to depend strongly on wind direction. Figure 1 shows as a function of angular wind direction the concentration of particles greater than ~3 nm (all counts from the UCPC) and the ultrafine aerosol concentration. In contrast to the total aerosol concentrations (Fig. 1a), which do not show a strong dependence on wind direction, high ultrafine concentrations were observed predominantly in downslope air (wind from western sector, Fig. 1b). The narrow angular band where the highest ultrafine concentrations were recorded was the most common downslope wind direction. Total aerosol surface area was on average higher and more variable in upslope air. During the daytime

between 600 and 1800 hours Mountain Standard Time (MST), the period when significant photochemically derived new particle formation is expected, the mean aerosol surface area concentration was 85±57 $\mu m^2\ cm^{-3}$ for upslope air compared to 49±18 $\mu m^2\ cm^{-3}$ for downslope air. In this case the surface areas were calculated from particle size distributions spanning 15 nm to 9 μm diameter. The higher aerosol surface areas associated with upslope air were likely the result of anthropogenic sources to the east and are a possible cause for the low ultrafine aerosol concentrations when the wind was from this sector. Since the focus of this work is on particle formation and growth in the clean continental troposphere, only downslope data are analyzed further.

Diurnal Variation of Species Concentrations at Idaho Hill

Analysis of All Downslope Flow Data: In Fig. 2 the concentrations of OH, SO_2, H_2SO_4, and ultrafine aerosol for periods of downslope flow are plotted as functions of the local time of day. Also included with each plot is the clear sky ultraviolet solar intensity (wavelength range: 290 to 385 nm). This can be interpreted as the envelope of UV solar intensity since interference from clouds will result in attenuated values.

The rapid increase and subsequent decrease in OH concentrations corresponding with sunrise (600 MST) and sunset (1800 MST) shown in Fig. 2a clearly indicate its photochemical source. Variations in OH concentrations are likely a result, in part, of variations in UV intensity. Similar observations of the diurnal variation of OH concentrations at the Mauna Loa Observatory are reported in *Tanner and Eisele* [1995]. Unlike OH, SO_2 had no diurnal pattern (Fig. 2b).

Sulfuric acid is thought to be produced primarily by the reaction of OH and SO_2 (support of this is provided in the following section on predicted H_2SO_4 concentrations). The diurnal variation of OH is responsible for the rapid rise in H_2SO_4 levels observed at sunrise, Fig. 2c. Note, there was practically no delay between the rise in OH and the earliest appearance of elevated H_2SO_4 concentrations at sunrise. Scatter in H_2SO_4 concentrations is probably from scatter in both the OH and SO_2, and also the variation in the aerosol surface area concentrations.

The ultrafine aerosol concentration also varied diurnally, Fig. 2d. Unlike the H_2SO_4 concentration, which increased at sunrise (~615 MST, Fig. 2c), the concentration of ultrafine particles did not begin to increase significantly until approximately 730 MST, more than an hour later We interpret this delay as the time required for the precursor vapor, H_2SO_4, (~1 nm diameter), to grow to the ultrafine size range (~3 nm diameter). In the following section this delay is use to estimate ultrafine particle growth rates.

By late afternoon the ultrafine concentrations began to decline and were low by nightfall. The median daytime ultrafine concentration was 48.2 cm^{-3} compared to 0.06 cm^{-3} during the night. These highly mobile ultrafine particles have short life spans because of scavenging by existing aerosol surface. The median surface areas during day and night for downslope conditions were comparable; 42 and 48 $\mu m^2\ cm^{-3}$ respectively. If there are no sources and the primary sink for the ultrafine aerosol is scavenging by preexisting particles, based on kinetic theory, the characteristic lifetime (e-folding time; τ) for a 3 nm particle is:

$$\tau = \frac{4\gamma}{\alpha \bar{c} A} \qquad (4)$$

The factor γ accounts for diffusional resistance to mass transfer that must be taken into account for preexisting particles that are on the order of or larger than the air mean free path. For the size distributions that we measured in this study, we found that γ=1.3±0.2. For the purpose of this discussion it is adequate to assume a fixed value of ~1.3. The average thermal speed, $\bar{c}$, for a 3 nm hydrated H_2SO_4 particle of density 1.4 g cm^{-3} is ~$2x10^3$ cm s^{-1} (assuming T=10°C, RH=32%). The preexisting aerosol surface area concentration is A. If we assume the ultrafine particles are always captured when they collide with the larger preexisting particles (i.e., α=1), the characteristic lifetime of a 3 nm particle at Idaho Hill was ~ 1.5 hour. This short life span likely accounts for the observed decay in numbers of ultrafine particles by afternoon.

A Representative Day: The H_2SO_4, ultrafine particle, and particle surface area concentrations on 21 September 1993 are shown in Fig. 3. Like most days at Idaho Hill, H_2SO_4

levels began to increase at ~ 615 MST. The ultrafine particle concentration did not begin to rise above nighttime levels until ~730 MST, about 1.25 hours later. During the day, the H_2SO_4 and ultrafine aerosol concentrations tracked well; changes in ultrafine concentrations followed changes in H_2SO_4 concentrations. This general correlation between these species was observed on all but one of the sampling days at Idaho Hill. It was also commonly observed at Mauna Loa. The measurements suggest that at both sites, H_2SO_4 was a precursor of the ultrafine particles.

The measured fine aerosol size distributions for 21 September are shown in Fig. 4. The data have been summarized by plotting the average distribution for three periods for which the distributions were fairly steady. From Fig. 4a, the largest changes in the number distributions were for particles with diameters less than approximately 50 nm. The concentrations of larger particles were fairly steady. Note that the concentration of the smallest particles plotted, ~20 nm, did not significantly increase until approximately 1000 MST. Recall the ultrafine concentration (3 nm particles) increased much earlier, at ~ 715 MST (see Fig. 3). Again, this delay may be the time required for growth from ~3 nm to ~20 nm diameter.

Another noteworthy feature of the particle size distributions is that at some point during the day they had a slight bimodal shape. The minimum between the modes was at ~60 nm. This bimodal distribution for fine aerosols is a common feature of marine boundary layer aerosols where it is understood to result from aerosol processing by non-precipitating marine clouds [*Hoppel et al.*, 1994b]. It was also a regular feature of the fine particle distributions recorded at Mauna Loa [*Weber and McMurry*, 1995]. Though such bimodality has not been commonly reported for continental aerosols, at Idaho Hill it was observed at some time during the day for nearly one-half the sampling days.

Figure 4b shows the fine aerosol surface area distributions corresponding to the three average number distributions. Plotted in this manner, the area under the curve is the calculated aerosol surface area concentration.

In summary, our data suggests that ultrafine particles were produced by recent nucleation and that H_2SO_4 was a precursor species. The ultrafine particle concentrations varied diurnally

due to the photochemical production of the precursor species and their short life spans. In the next section, the influence of parameters expected to affect the nucleation rate are studied by constructing scatter plots of ultrafine concentrations versus each parameter.

Correlations Between Ultrafine Concentrations and Measured Parameters

For all data free of local contamination and collected under downslope flow, the measured ultrafine concentrations are shown in Fig. 5 as a function of the preexisting aerosol surface area, relative humidity, and H_2SO_4 concentration. These plots illustrate the recorded range of each parameter and give some indication of their influence on the ultrafine aerosol concentration and thus the extent of new particle formation. A point of particular interest is the influence of these parameters on the maximum ultrafine concentration since this may provide insight about how individual parameters influenced nucleation. In all plots, an envelope roughly defining the maximum ultrafine concentration is indicated by a line. Similar scatter plots for Mauna Loa data can be found in *Weber et al.* [1995a].

Ultrafine Particle versus Aerosol Surface Area Concentrations: The effect of the aerosol surface area on ultrafine concentrations is shown in Fig.5. We found that generally lower ultrafine concentrations were recorded during periods of high aerosol surface area concentrations. The envelope defining the maximum measured ultrafine concentration decreases with increasing surface area. Note that "high" ultrafine aerosol concentrations were never detected at Idaho Hill during periods when the aerosol surface area was greater than ~80 $\mu m^2\ cm^{-3}$. Significant numbers of ultrafine particles were, however, recorded at surface areas up to this value. The observed decrease in ultrafine particle concentrations with increasing aerosol surface area is consistent with expectations. Concentrations of the nucleating species decrease due to heterogeneous condensation as preexisting aerosol concentrations increase; this leads to a reduction in particle production rates. Furthermore, the likelihood that a freshly formed nucleus grows to a detectable size before it is scavenged by the preexisting aerosol also decreases with increasing preexisting aerosol concentrations.

Scatter plots of Mauna Loa data (*Weber et al.* [1995a]) show a similar envelope with the same correlation between ultrafine and aerosol surface area concentrations, although the levels of both ultrafine particle and aerosol surface area concentrations were much lower at Mauna Loa. For example, high ultrafine concentrations were never observed at Mauna Loa during periods when the aerosol surface area was larger than ~30 $\mu m^2\ cm^{-3}$. Different production rates of precursor species (i.e., differing SO_2 concentrations) at these two sites probably accounts for these observed differences.

Ultrafine Particle Concentration versus Relative Humidity: From Fig. 5b, the highest ultrafine concentrations at Idaho Hill were observed at low relative humidities. Evidence of significant particle formation, indicated by high ultrafine particle concentrations, was observed at relative humidities as low as 15 to 30%. At both Idaho Hill and Mauna Loa there is no evidence that increases in relative humidity led to enhanced particle production, as would be expected if the ultrafine particles were formed by binary nucleation of H_2SO_4 and H_2O.

The observed negative correlation between ultrafine particle concentrations and relative humidity may be due to the observed positive correlation (correlation coefficient of +0.13) between these parameters. This correlation could result from two differing influences. First, because the degree of sulfate particle hydration increases with relative humidity, the swelling of particles with increasing relative humidity leads to higher aerosol surface areas at higher humidities; this effect becomes very significant as relative humidies increase beyond 85-90%, which is well in excess of values typically encountered in this study. Secondly, relative humidity at this site may have been an indicator of air mass origin; more pristine downslope air from higher elevations would also likely be dryer. In either case, the negative correlation between ultrafine particle concentration and relative humidity likely does not reflect the influence of water vapor concentration on atmospheric particle formation rates.

The observation of particle formation predominantly in dry downslope air (i.e., air originating from higher elevations) is similar to the marine observations of *Covert et al.* [1995]. They found evidence for new particle formation only in regions of subsiding air masses. In both

cases, the lower aerosol surface area concentrations associated with dry air from aloft may have been the prerequisite for significant particle production in these regions.

Ultrafine Particle versus Sulfuric Acid Concentrations: In Fig. 5c, the ultrafine particle concentration is plotted with respect to the H_2SO_4 relative acidity. Sulfuric acid relative acidity is the measured H_2SO_4 partial pressure divided by the saturation vapor pressure of pure H_2SO_4 at the measurement temperature [*Ayers et al.*, 1980]. Plotted in this way, the major influence of temperature on the tendency of H_2SO_4 and H_2O to nucleate is taken into account. A second abscissa showing H_2SO_4 concentrations is also shown. In principle, of course, concentration and relative acidity cannot be shown on the same graph if temperatures varied significantly. In this study the temperature did not vary widely; we used a characteristic value of 10 °C when evaluating concentrations for this plot. From Fig. 5c, it is evident that the measured ultrafine concentration and H_2SO_4 relative acidity were positively correlated; higher ultrafine concentrations were detected at higher H_2SO_4 concentrations. These results are consistent with expectations and our earlier observations [*Weber et al.* 1995a] that H_2SO_4 is a primary precursor species of the ultrafine particles generated by homogeneous nucleation.

At both sites, the H_2SO_4 concentrations typically ranged from ~10^5 to ~10^7 cm^{-3} and significant ultrafine concentrations were recorded at unexpectedly low acidities (or H_2SO_4 concentrations). Figure 5c shows that at Idaho Hill, high ultrafine concentrations were detected at acidities down to 10^{-6} which is much too low for nucleation by H_2SO_4 and H_2O. Another major inconsistency with binary nucleation is found when comparing measurements at Mauna Loa and Idaho Hill. The maximum ultrafine particle concentrations at a given H_2SO_4 relative acidity were about an order of magnitude higher at Idaho Hill than at Mauna Loa. This suggests that species other than H_2SO_4 and H_2O (e.g., ammonia), may also participate in particle formation. A conceptual framework for such a nucleation mechanism is discussed by *Weber and coworkers* [1995b; 1995c].

Discussion

Ultrafine Particle Growth Rates

In this section, the data are used to estimate average growth rates of sub-3 nm particles. These rates are compared to growth by condensation of only hydrated H_2SO_4 vapor calculated using Eq. (1) and the measured H_2SO_4 concentration and relative humidity. Two approaches are used to estimate the growth rate of ultrafine particles. First, growth rates are inferred from the observed time lag between the rise in H_2SO_4 concentration and the rise in ultrafine particle concentrations after sunrise. In the second approach, the observed effects of cluster scavenging by the preexisting aerosol surface area on ultrafine particle concentrations were used to estimate the ultrafine particle growth rate.

Growth Rates Inferred from the Delay Between H_2SO_4 and Ultrafine Particle Concentrations At Sunrise: As shown in Fig. 3, the H_2SO_4 concentration began to increase at ~615 MST on 21 September 1993 whereas the ultrafine concentration began to rise at ~730 MST. If we assume this delay is due solely to the time required for a H_2SO_4 vapor molecule of diameter ~1 nm to reach our lower detection limit of ~3 nm, then the observed average growth rate was 2 nm in 1.25 hours, or ~1.6 nm h^{-1}. From the measurements of H_2SO_4 and H_2O concentrations between 615 and 730 MST, Eq. (1) predicts an average growth rate from condensing H_2SO_4 vapor and its associated water of ~0.2 nm h^{-1} which is a factor of 8 below the observed growth rate. On this morning, if growth was solely due to condensation of H_2SO_4 vapor, the ultrafine particle concentration would not have begun to increase until about 1045 MST.

Recall that later in the morning of 21 September the concentrations of 20 nm particles did not increase until ~1000 MST (Fig. 4a). The number of ultrafine particles (~3 nm) had increased about 2.5 hours earlier at 730 MST. For 3 nm particles to reach 20 nm in 2.5 hours requires an average growth rate of ~7 nm h^{-1}. During this time the average growth rate by Eq. (1) based on measured H_2SO_4 concentrations was ~0.6 nm h^{-1}; the observed growth rate was roughly 11 times higher.

Observed growth rates for other days are compared in Table 1 with values calculated from Eq. (1). Results are shown for all days for which we had both H_2SO_4 and ultrafine aerosol concentrations in the morning. Note that growth rates of sub-3 nm particles were consistently 8 to 13 times higher than growth by condensation of only hydrated H_2SO_4 vapor.

Growth Rates Inferred From The Effects of Cluster Scavenging: Insights about particle growth rates can also be obtained by investigating the relationship between ultrafine particle concentrations and aerosol surface area. The probability that a freshly nucleated particle will grow to our minimum detectable size (~3 nm) decreases with increasing aerosol surface area. This probability also decreases with decreasing particle growth rates: lower growth rates lead to longer growth times during which losses to preexisting particles can occur.

The time-dependent concentration, N, of a population of uniformly-sized particles that is growing by gas-to-particle conversion and is being scavenged by preexisting particles can approximately be expressed as:

$$\frac{dN}{dt} \cong -\frac{N\bar{c}}{4} \cdot \frac{A}{\gamma} \qquad (5)$$

where $\bar{c}$ is the mean thermal speed of the particles and A is the surface area concentration of the preexisting particles. As was discussed above, we assume γ=1.3. From kinetic theory, the mean thermal speed for spherical particles of diameter D_p and density ρ is:

$$\bar{c}(D_p) = \left(\frac{48kT}{\pi^2 \rho D_p^3} \right)^{1/2} \qquad (6)$$

where k is Boltzmann's constant, and T is absolute temperature. As was discussed above (Eq. (1)), condensational growth rates are independent of size if evaporation is negligible relative

to condensation. Assuming that growth rates, dD_p/dt are also independent of time, the time-dependent size is:

$$D_p(t) = D_{p1} + \frac{dD_p}{dt} \cdot t \tag{7}$$

where D_{p1} is size of the freshly nucleated particle. Substituting (6) and (7) in (5) and solving for $N(D_{p2}(t))$ leads to the following result for the probability, P, that a particle will grow from D_{p1} to D_{p2} before it is scavenged by the preexisting aerosol:

$$P = \frac{N(D_{p2})}{N(D_{p1})} = \exp\left\{-\frac{2(A/\gamma)}{\pi \cdot dD_p/dt}\left(\frac{3kT}{\rho}\right)^{1/2}\left(\frac{1}{\sqrt{D_{p1}}} - \frac{1}{\sqrt{D_{p2}}}\right)\right\}. \tag{8}$$

Freshly nucleated particles probably consist of a few molecules. We will assume that $D_{p1} \equiv$ 1 nm; our discussion is not particularly sensitive to the assumed value. Furthermore, we assume that D_{p2} = 3 nm, our minimum detectable size. It follows that:

$$P = \frac{N(D_{p2})}{N(D_{p1})} = \exp\left\{-6.8 \times 10^{-2} \cdot \frac{A}{dD_p/dt}\right\}. \tag{9}$$

where A is in $\mu m^2 cm^{-3}$, dD_p/dt is in nm h^{-1}, and a density of 1.4 g cm^{-3} was assumed. If growth is due solely to condensation of H_2SO_4 vapor, then from (1) and (9):

$$P = \frac{N(D_{p2})}{N(D_{p1})} = \exp\left\{-9.2 \times 10^{5} \cdot \frac{A}{N_{H_2SO_4}}\right\} \tag{10}$$

where $N_{H_2SO_4}$ is the concentration of gas phase sulfuric acid in molecules cm^{-3}. An effective molecular weight of the condensing sulfuric acid and its associated water, etc., of 200 was assumed.

Figure 6 shows the relationship between the peak ultrafine particle concentration measured on each day at Idaho Hill and the preexisting aerosol surface area concentration, A. Based on the hypothesis that particles are produced by a multicomponent nucleation process that involves sulfuric acid, data are categorized by the peak sulfuric acid concentration that was measured at or prior to (typically within 1 to 2 hours) the time that the peak in ultrafine concentrations was observed. We confine our attention to the peak daily ultrafine concentrations since numerical calculations justify assuming steady state cluster size distributions that are dependent on the concentration of the nucleating vapor at this point (e.g., (McMurry, 1983; Rao and McMurry, 1989)). Note that there is a general trend towards decreasing peak ultrafine concentrations with increasing aerosol surface areas and with decreasing sulfuric acid concentrations, as expected.

Also shown in Figure 6 are two lines obtained from Equation 10 assuming $N_{H_2SO_4} = 3 \times 10^6$ and 10×10^6 cm^{-3}. Because we do not know how many particles are produced at a given sulfuric acid concentration, we have arbitrarily set $N(0) = 10^3$ cm^{-3} for both of these curves; our interest here is in comparing the slopes of these curves with trends in the data. Although there is too much scatter in the data to obtain accurate values for the logN versus A slopes, it appears that they are ~5 to 10 times smaller than predicted by Equation 10. This suggests that growth rates are 5 to 10 times higher than can be explained by H_2SO_4 condensation. This is consistent with the results in Table 1 that were obtained independently, and further supports our finding that a species in addition to H_2SO_4 is contributing to growth of freshly nucleated ultrafine particles. Our work (*Marti et al*, 1995) showed no relationship between concentrations of ultrafine particles and of alpha or beta pinene (or estimates of their reaction products). This suggests that, at this site, terpenes played a minor role in new particle formation compared to sulfates. Terpenes, however, were found to be correlated with the aerosol surface area and volume concentrations. This may indicate that these species contributed to particle growth. If the high growth rates were from heterogeneous condensation of organics, a significant fraction of the ultrafine particles would be organic.

Predicted H_2SO_4 Concentrations

If we assume that the only source of sulfuric acid is the OH, SO_2 reaction, and that the primary removal mechanism is condensation on preexisting particles with an accommodation coefficient of 1.0, the steady state sulfuric acid concentration is:

$$[H_2SO_4] = \frac{k[OH][SO_2]}{F} \qquad (11)$$

where k is the rate constant for the SO_2, OH reaction and $F \cdot [H_2SO_4]$ equals the rate of sulfuric acid transport to preexisting particles. We take $k = 1.1 \times 10^{-12}$ $cm^3 s^{-1}$ [*DeMore et al.*, 1992; *Gleason et al.*, 1987; *Wang et al.*, 1988]. The loss factor, F, was obtained by integrating the transition regime expression of Fuchs and Sutugin [1970] across the measured aerosol size distribution. The steady state assumption is justified since the characteristic time required to establish steady state is relatively short (~3 min). Sulfuric acid concentrations predicted with Eq. (11) are compared with measured values for 24 July 1992 (Mauna Loa) and 21 September 1993 (Idaho Hill) in Fig. 7. These two days were selected because, unlike most days, the recorded SO_2 concentrations were sufficiently above the instrument's lower detection limit to provide confidence in the measured values. Median daytime H_2SO_4 production rates were 6×10^3 and 3×10^4 $cm^3 s^{-1}$ at Mauna Loa (7/24) and Idaho Hill (9/21) respectively. Median fractional H_2SO_4 loss rates on these days were were 5×10^{-4} and 6×10^{-3} s^{-1}. Measured and calculated steady state concentrations are in very good agreement.

The loss Factor, F, in Eq. (11) is an implicit function of the H_2SO_4 mass accommodation coefficient on aerosol particle surfaces. In our analysis we have assumed that the accommodation coefficient equals 1.0. Previous researchers have used values for mass accommodation coefficients ranging from about 0.3 to 0.04 [*Hegg et al.*, 1990; *Raes et al*, 1992 and 1995]. These values would lead to increases in predicted steady-state sulfuric acid

concentrations by factors of ~3 to ~20. We conclude that given the good agreement between measured and calculated values, the assumed value of 1.0 is in the right range.

In deriving Equation (11) we also implicitly assumed that the equilibrium vapor pressure of sulfuric acid above the aerosol particles is small relative to the measured sulfuric acid concentrations. If this had not been the case, then the measured sulfuric acid concentrations would have systematically exceeded the calculated values. Again, there is no evidence to suggest that reevaporation was a significant source of sulfuric acid vapor on these days.

Conclusions

Measurements at a remote continental site indicate that elevated concentrations of ultrafine particles (nominally 3-4 nm diameter) resulted from recent new particle formation. The data points to H_2SO_4 as a precursor vapor of these newly formed particles.

The measured ultrafine particle concentration had a consistent diurnal pattern. There is evidence that this was due to the photochemical production of the precursor species (i.e., H_2SO_4 and possibly others) and the relatively short lifetime (~1.5 hour) of the ultrafine particles. Although the H_2SO_4 concentration was observed to increase just after sunrise, elevated ultrafine particle concentrations were delayed by approximately 1 hour. Growth rates of ultrafine particles were estimated from this delay and found to be roughly 8 to 12 times higher than growth by condensation of hydrated H_2SO_4 vapor. By a completely different approach, ultrafine particle growth rates were estimated from the influence of cluster scavenging on ultrfine particle concentrations. With this method, we estimate that growth rates of ultrafine particles were roughly 5 to 10 times higher than growth by H_2SO_4 vapor.

New particle formation, indicated by high ultrafine concentrations, was common at Idaho Hill in downslope air and was observed during periods of low relative humidity (median RH was 32%). Significant ultrafine concentrations were measured at H_2SO_4 relative acidities as low as 10^{-6}. These are water vapor and acidities for which classical H_2SO_4-H_2O nucleation theory would predict practically no nucleation.

At both Mauna Loa and Idaho Hill, the two major factors influencing particle formation were found to be the H_2SO_4 and preexisting aerosol surface area concentration. Sulfuric acid appeared to be a primary precursor species of the ultrafine particles and the highest ultrafine concentrations were recorded when the aerosol surface area was low (relative to typical surface area concentrations for that particular site). For a selected day at each site, the steady state H_2SO_4 concentration, calculated from the balance between H_2SO_4 photochemical production and H_2SO_4 scavenging by aerosol, agreed remarkably well with the measured values.

Compared to Mauna Loa, new particle formation was more vigorous at Idaho Hill despite similar H_2SO_4 relative acidities at both locations and much lower relative humidities at Idaho Hill. We speculate that additional species, such as ammonia, may have also participated in new particle production and that higher levels of these species at the continental site enhance nucleation there. Participation of ammonia, however, is not expected to significantly enhance particle growth rates, although other species, such as organics, may. These species may not have been involved in new particle formation, but could significantly enhance the growth rates of the newly formed particles and account for the high ultrafine particle growth rates observed at Idaho Hill.

Acknowledgments

This research was supported by a NSF Grant No. ATM 9205337, and by NASA through Grant No. NAGW-3767 and a NASA Global Change Fellowship. The authors thank Karsten Bauman and Eric Williams of the NOAA/Aeronomy Lab and CIRES, Boulder, CO for the solar and meteorological data. We also thank Gerd Hubler of NOAA for the Mauna Loa SO_2 data.

References

Ahn, K. and B. Liu, Particle activation and droplet growth processes in condensation nucleus counter-1. theoretical background, *J. Aerosol Sci.*, 21, 249-261, 1990.

Ayers, G. P., R. W. Gillett and J. L. Gras, On the vapor pressure of sulfuric acid, *Geophys. Res. Letters*, 7, 433-436, 1980.

Bradbury, N. E. and H. J. Meuron, The diurnal variation of atmospheric condensation nuclei, *Terr. Magn. Atmos. Electr.*, 43, 231-240, 1938.

Brockmann, J. E., Coagulation and deposition of ultrafine aerosols in turbulent pipe flow, *PhD Thesis, University of Minnesota*, , 1981.

Charlson, R. J., J. E. Lovelock, M. O. Andreae and S. G. Warren, Oceanic phytoplankton, atmospheric sulfur, cloud albedo and climate, *Nature*, 326, 655-661, 1987.

Clarke, A. D., Atmospheric nuclei in the Pacific midtroposphere: their nature, concentration and evolution, *J. Geophys. Res.*, 98, 20633-20647, 1993.

Covert, D. S., V. N. Kapustin, T. S. Bates and P. K. Quinn, Physical properties of marine boundary layer aerosol particles of the mid-pacific in relation to sources and meteorological transport, in press, 1995.

DeMore, W. B., S. P. Sander, D. M. Golden, R. F. Hampson, M. J. Kurylo, C. J. Howard, A. R. Ravishankara, C. E. Kolb and M. J. Molina, Chemical kinetics and photochemical data for use in stratospheric modeling, in Evaluation No. 10, *NASA/J.P.L.* Pub. 92-20, 1992.

Eisele, F. L. and D. J. Tanner, Measurement of the gas phase concentrations of H_2SO_4 and methane sulfonic acid and estimates of H_2SO_4 production and loss in the atmosphere, *J. Geophys. Res.*, 98, 9001-9010, 1993.

Friedlander, S. K., Smoke, Dust and Haze, *John Wiley and Sons*, New York, 1977.

Fuchs, N. A. and A. G. Sutugin, Highly Dispersed Aerosols, Ann Arbor Science Publishers, pp. 47-60, 1970.

Gleason, J. F., A. Sinha and C. J. Howard, J Phys. Chem., 91, 719, 1987.

Gmitro, J. and T. Vermeulen, Vapor-liquid equilibrium for aqueous sulfuric acid, *UCRL-10886, LRL REp. TID-4500 Univ. of Calif. Berkeley*, , 81, 1963.

Hagen, D. E. and D. J. Alofs, Linear inversion method to obtain aerosol size distributions from measurements with a differential mobility analyzer, *Aerosol Sci. Tech.*, 2, 465-475, 1983.

Hegg, D. A., L. F. Radke and P. V. Hobbs, Particle production associated with marine clouds, *J. Geophys. Res.*, 95, 13917-13926, 1990.

Hofmann, D. J., Twenty years of balloon-borne tropospheric aerosol measurements at Laramie, Wyoming, *J. Geophys. Res.*, 98, 12753-12766, 1993.

Hogan, A. W., An experiment illustrating that gas conversion by solar radiation is a major influence in the diurnal variation of Aitken nucleus concentrations, *Atmos. Envir.*, 2, 599-601, 1968.

Hoppel, W. A., G. M. Frick, J. W. Fitzgerald and R. E. Larson, Marine boundary layer measurements of new particle formation and the effects nonprecipitating cloud have on aerosol size distributions, *J. Geophys. Res.*, 99, 14443-14459, 1994a.

Hoppel, W. A., G. M. Frick, J. W. Fitzgerald and B. J. Wattle, A cloud chamber study of the effect that non-precipitating water clouds have on the aerosol size distribution, *Aerosol Sci. Techn.*, 20, 1-30, 1994b.

Jaecker-Voirol and A., P. Mirabel, Heteromolecular nucleation in the sulfuric acid-water system, *Atmos. Env.*, 23, 2053-2057, 1989.

Koutsenogii, P. K. and R. Jaenicke, Number concentrations and size distributions of atmospheric aerosols in Siberia, *J. Aerosol Sci.*, 25, 377-383, 1994.

Lopez, A., J. Fontan and M. O. Barthomeuf, Study of the formation of particles from natural hydrocarbons released by vegetation, *J. Atmos. Rech.*, 19, 295-307, 1985.

Marti, J., Diurnal variation in the undisturbed continental aerosol: results from a measurement program in Arizona, *Atm. Res.*, 25, 351-362, 1990.

Marti, J. J, R. J. Weber, P. H. McMurry, F. L. Eisele, D. J. Tanner and A. Jefferson, Particle formation at a remote continental site: assessing the contributions of SO_2 and terpene precursors, *J. Geophys. Res.* manuscript submitted June 1995.

McMurry, P. H. (1983). "New Particle Formation in the Presence of an Aerosol: Rates, Time Scales and sub-0.01 μm Size Distributions." *J. Colloid Interface Sci.* 95: 72-80.

Mount, G. and E. J. Williams, An overview of the tropospheric OH photochemistry experiment Fritze Peak/Idaho Hill, Colorado *J. Geophys. Res.* manuscript submitted June 1995.

Novakov, T. and J. E. Penner, Large contributions of organic aerosols to cloud-condensation nuclei concentrations, *Nature*, 28, 823-826, 1993.

Perry, K. D. and P. V. Hobbs, Further evidence for particle nucleation in clear air adjacent to marine clouds, *J. Geophys. Res.*, 99, 22803-22818, 1994.

Radke, L. F. and P. V. Hobbs, Humidity and particle fields around some small cumulus clouds, *J. Atmos. Sci.*, 48, 1190-1193, 1991.

Raes, F., Entrainment of free tropospheric aerosols as a regulating mechanism for cloud condensation nuclei in the remote marine boundary layer, *J. Geophys. Res.*, 100, 2893-2903, 1995.

Raes, F. and R. Van Dingenen, Simulations of condensation and cloud condensation nuclei from biogenic SO_2 in the remote marine boundary layer, *J. Geophys. Res.*, 97, 12901-12912, 1992.

Rao, N. P. and P. H. McMurry, Nucleation and Growth of Aerosol in Chemically Reacting Systems: A Theoretical Study of the Near- Collision-Controlled Regime, *Aerosol Science and Technology* 11: 120-132, 1989.

Saros, M. T., R. J. Weber, J. J. Marti and P. H. McMurry, Ultrafine aerosol measurements using a condensation nucleus counter with pulse height analysis, submitted to Aerosol Sci. Tech., Aug. 1995.

Stolzenburg, M. R., An ultrafine aerosol size distribution measuring system, *PhD Thesis, University of Minnesota*, 1988.

Stolzenburg, M. R. and P. H. McMurry, An ultrafine aerosol condensation nucleus counter, *Aerosol Sci. and Techn.*, 14, 48-65, 1991.

Tanner, D. J. and F. L. Eisele, Present OH measurement limits and associated uncertainties, *J. Geophys. Res.*, 100, 2883-2892, 1995.

Taylor, K. E. and J. E. Penner, Response of the climate system to atmospheric aerosols and greenhouse gases, *Nature*, 369, 734-737, 1994.

Twomey, S. A., M. Piepgrass and T. L. Wolfe, An assessment of the impact of pollution on global cloud albedo, *Tellus*, 36B, 356-366, 1984.

Wang, S. C. and R. C. Flagan, Scanning Electrical Mobility Spectrometer, *Aerosol Sci. and Techn.*, 13, 230-240, 1990.

Wang, X., Y. G. Jin, M. Suto, L. C. Lee, and H. E. O'Neal, Rate constant of the gas phase reaction of SO3 with H2O, *J. Chem. Phys.* 89, 4853, 1988.

Weber, R. J. and McMurry, Fine particle size distributions at the Mauna Loa Observatory, Hawaii, in press,1995.

Weber, R. J., P. H. McMurry, F. L. Eisele and D. J. Tanner, Measurement of expected nucleation precursor species and 3 to 500 nm diameter particles at Mauna Loa Observatory, Hawaii, *J. Atm. Sci.*, 52, 2242-2257, 1995a.

Weber, R. J., J. J. Marti, P. H. McMurry, F. L. Eisele, D. J. Tanner and A. Jefferson, Measured atmospheric new particle formation rates: implications for nucleation mechanisms, *Chem. Eng. Comm.*, in press, 1995b.

Weber, R. J., Studies of new particle formation in the remote troposphere, *PhD Thesis, University of Minnesota*, 1995c.

Table 1: Comparison of estimated observed growth rates of ultrafine particles and calculated growth rates based on measured H_2SO_4 and H_2O vapor concentrations assuming that growth is by condensation of hydrated H_2SO_4 vapor. The ratio of the observed growth rates to the calculated rates is shown in the right most column.

Day of Sept. 1993	Observed Growth, (nm/h)	Calculated Growth, (nm/h)	Ratio, Obs./Calc.
6	1	0.1	10
10	1.3	0.2	9
11	1.1	0.1	12
12	1.3	0.1	12
15	2	0.1	10
21	1.6	0.2	8
23	1.3	0.1	12
24	1.1	0.09	12
26	0.5	0.04	13

Figure Captions

Figure 1 Total aerosol number concentrations (diameters larger than 3 nm) (a), and ultrafine aerosol concentrations (diameters between nominally 3 nm and 4 nm) (b), as a function of wind direction. The plot shows that high ultrafine aerosol concentrations were observed predominantly in air from the western sector (downslope).

Figure 2 Recorded daily concentrations of OH (a), SO_2 (b), H_2SO_4 (c), and ultrafine particles (d). For all plots, only data during periods of downslope air flow is shown. Also plotted is the UV solar intensity on a clear day (26 September 1993). Both OH and H_2SO_4 concentrations often increased from nighttime levels at sunrise. Ultrafine aerosol concentrations, however, never began to rise until over an hour later. This delay is used to estimate the growth rate of ultrafine particles.

Figure 3 Measured H_2SO_4 (a), ultrafine aerosol (b), and aerosol surface area (c) concentrations on 21 September 1993. On this day the air flow was downslope from 000 through to 1700 MST.

Figure 4 Time average fine aerosol number and surface area distributions for periods 600 - 1000, 1000 - 1500, and 1500 - 1800 MST on 21 September 1993. Increased concentrations of the smallest particles did not begin until ~ 1000 MST; concentrations of the higher mode were fairly steady. The fine aerosol also appears to be bimodal; similar (albeit more strikingly bimodal) distributions have been reported for remote marine aerosols.

Figure 5 Scatter plots of the measured ultrafine concentration as a function of the aerosol surface area (a), the relative humidity (b), and the H_2SO_4 relative acidity (c). In plot (c), the corresponding H_2SO_4 concentration is shown assuming a temperature of 10°C. All plots contain data for periods of only downslope air flow.

Figure 6 Maximum ultrafine particle concentration observed on individual days versus preexisting aerosol surface area concentrations on those days. The data are categorized by the sulfuric acid concentrations that were measured about one hour prior to the peak ultrafine concentrations on the hypothesis that this was responsible for new particle production. The slopes of the solid lines (from Eq. (10)) show the expected sensitivity of ultrafine concentrations to aerosol surface area if growth rates are limited by H_2SO_4 concensation.

Figure 7 Comparison of the measured H_2SO_4 concentration and the predicted steady state concentration for 24 July 1992 at the Mauna Loa Observatory, Hawaii, and 21 September 1993 at Idaho Hill, Colorado. The predicted steady state H_2SO_4 concentration is determined from the balance between its production by the SO_2 - OH reaction and loss by aerosol scavenging.

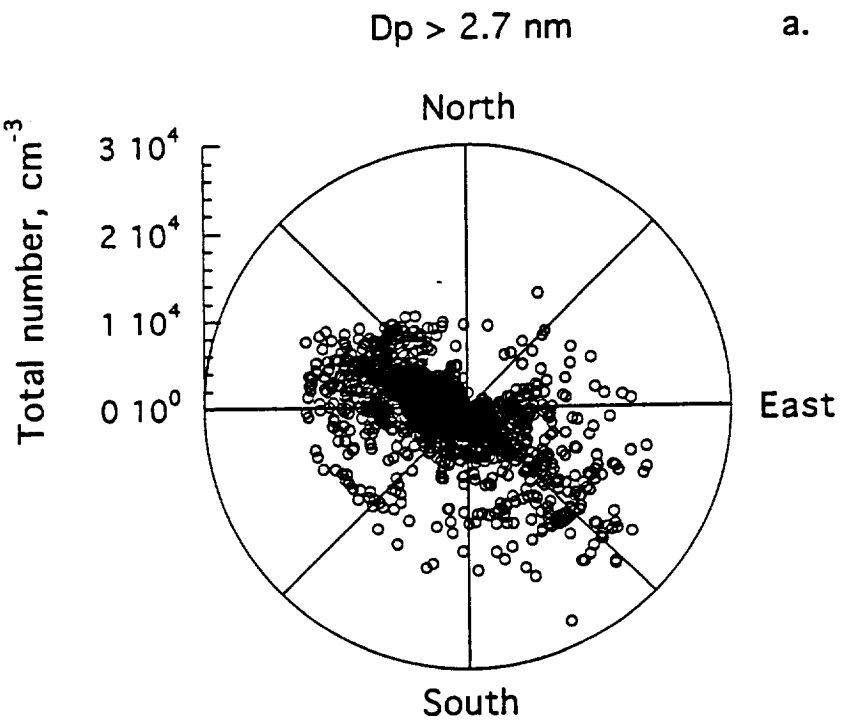
Dp > 2.7 nm
a.
North
3 10^4
2 10^4
1 10^4
0 10^0
Total number, cm^-3
East
South

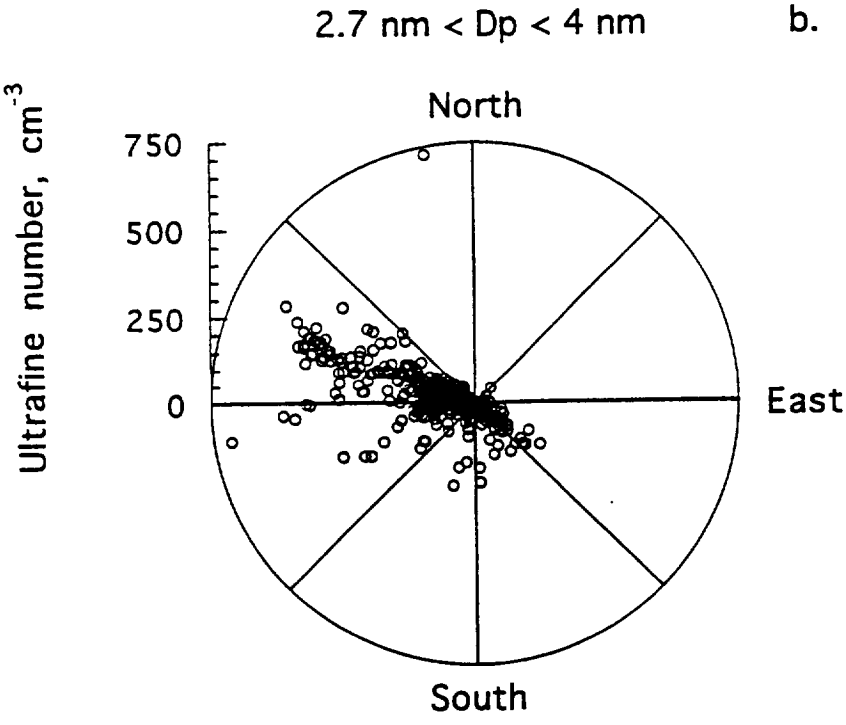
2.7 nm < Dp < 4 nm
b.
North
750
500
250
0
Ultrafine number, cm^-3
East
South

Figure 1

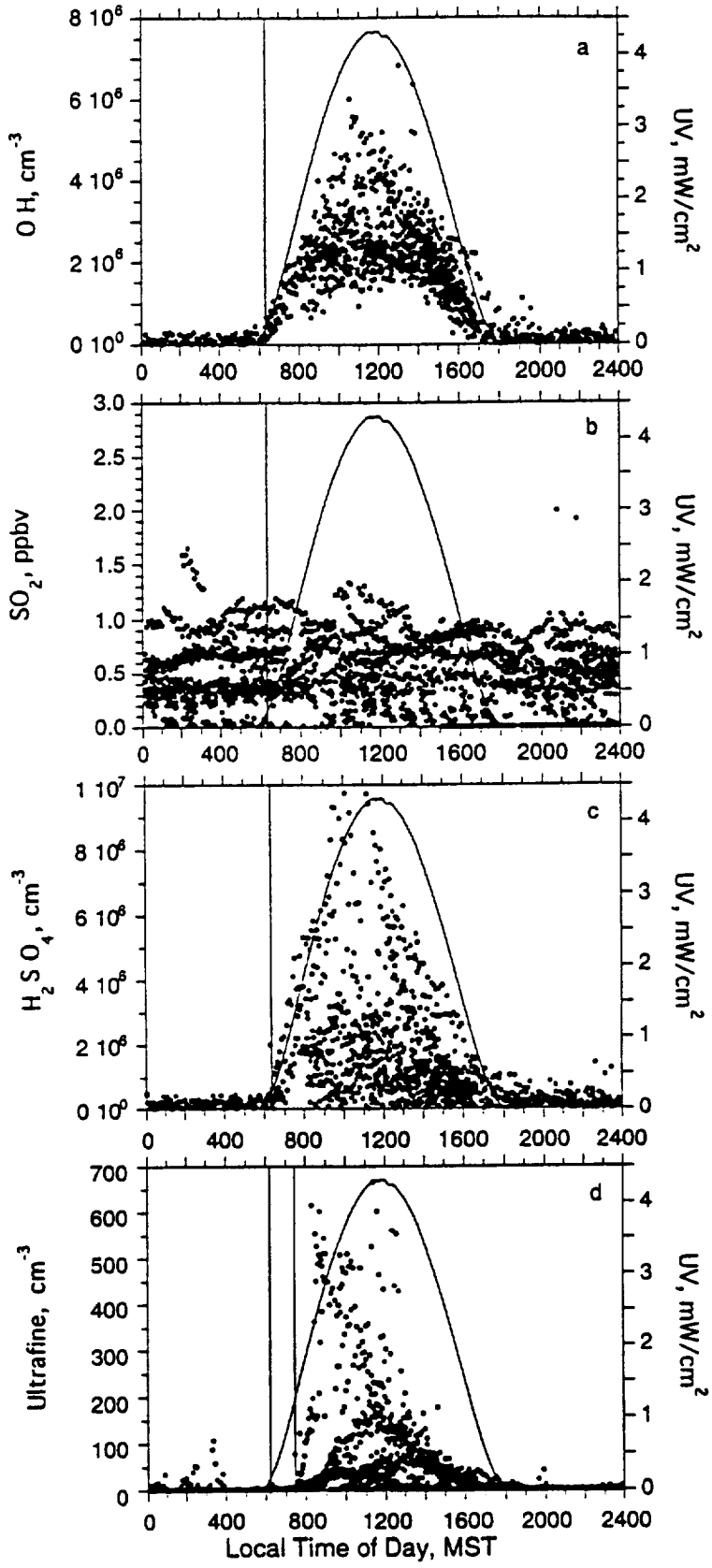
a
b
c
d
OH, cm-3
SO2, ppbv
H2SO4, cm-3
Ultrafine, cm-3
UV, mW/cm2
Local Time of Day, MST
0
400
800
1200
1600
2000
2400

Figure 2

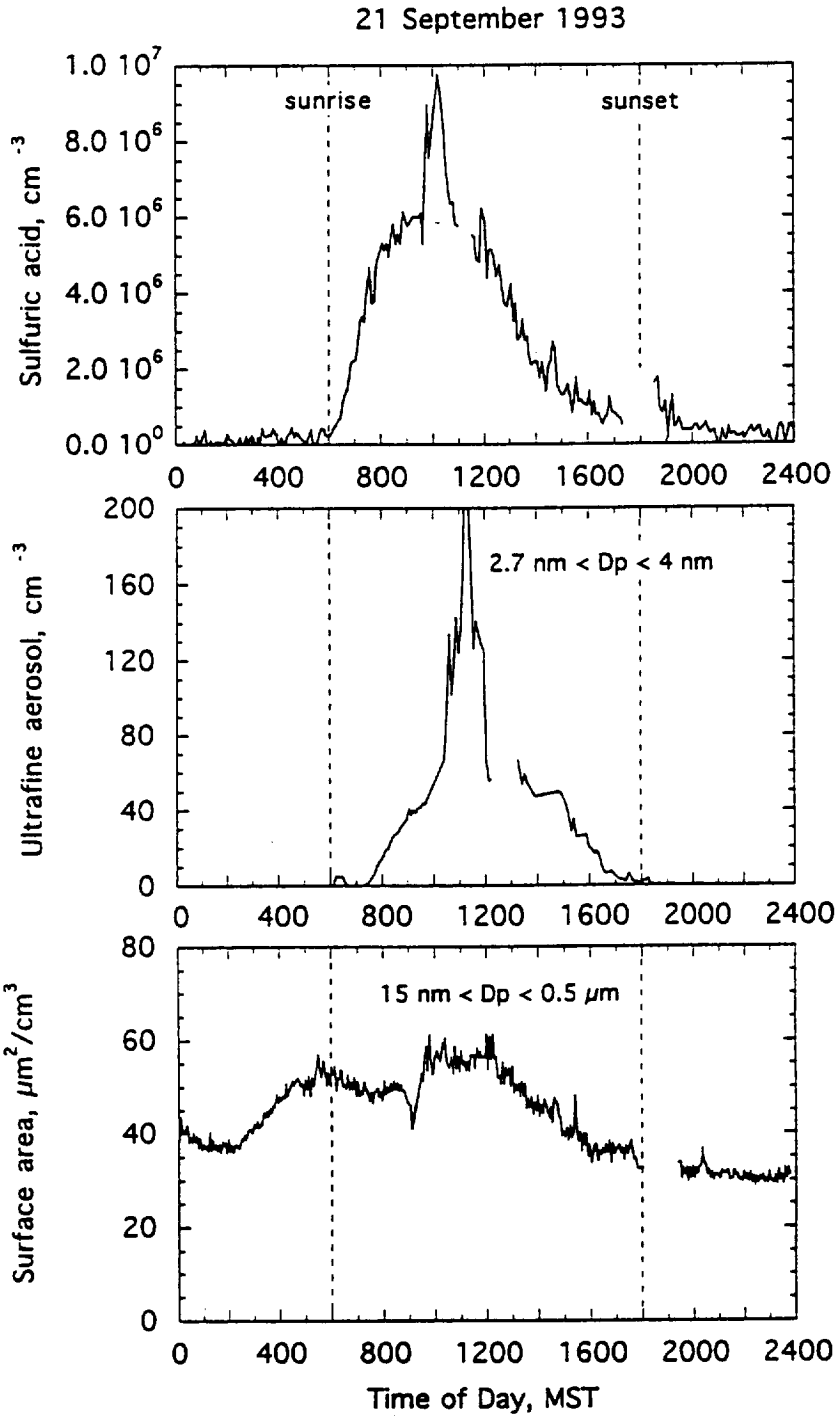
21 September 1993
Sulfuric acid, cm -3
1.0 10^7
8.0 10^6
6.0 10^6
4.0 10^6
2.0 10^6
0.0 10^0
sunrise
sunset
0
400
800
1200
1600
2000
2400
Ultrafine aerosol, cm -3
200
160
120
80
40
0
2.7 nm < Dp < 4 nm
Surface area, μm^2/cm^3
80
60
40
20
0
15 nm < Dp < 0.5 μm
Time of Day, MST

Figure 3

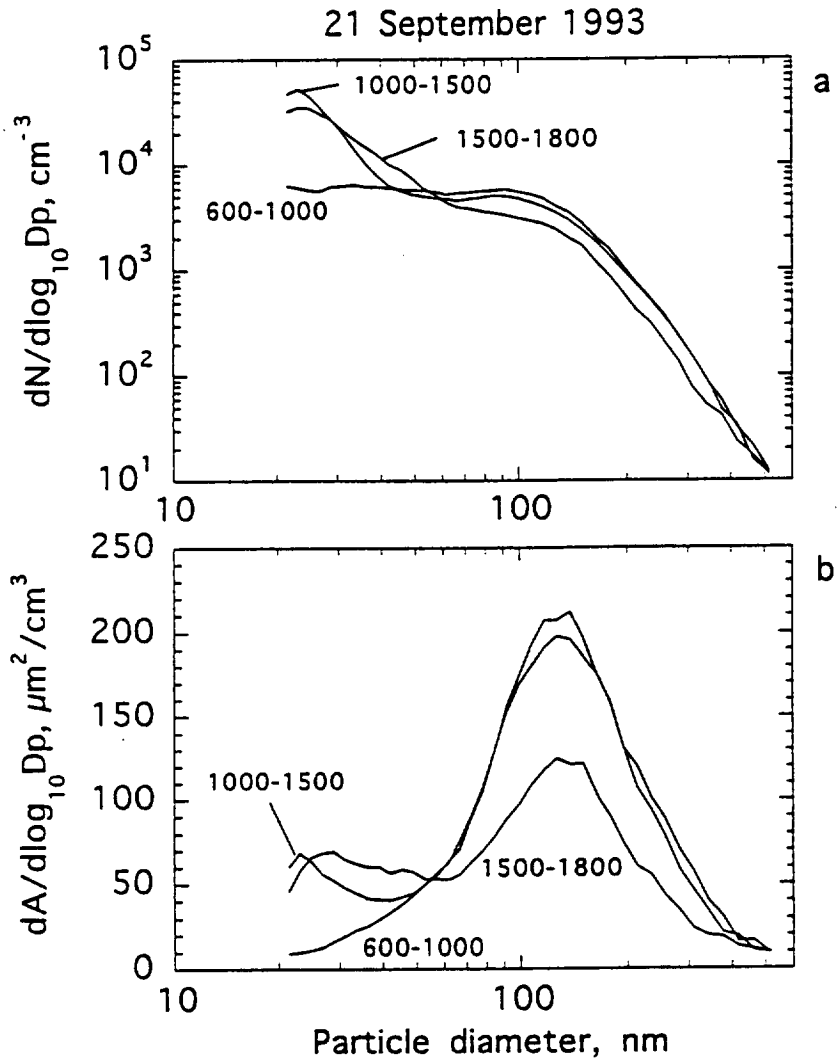
21 September 1993
a
b
1000-1500
1500-1800
600-1000
dN/dlog10Dp, cm-3
dA/dlog10Dp, μm2/cm3
Particle diameter, nm

Figure 4

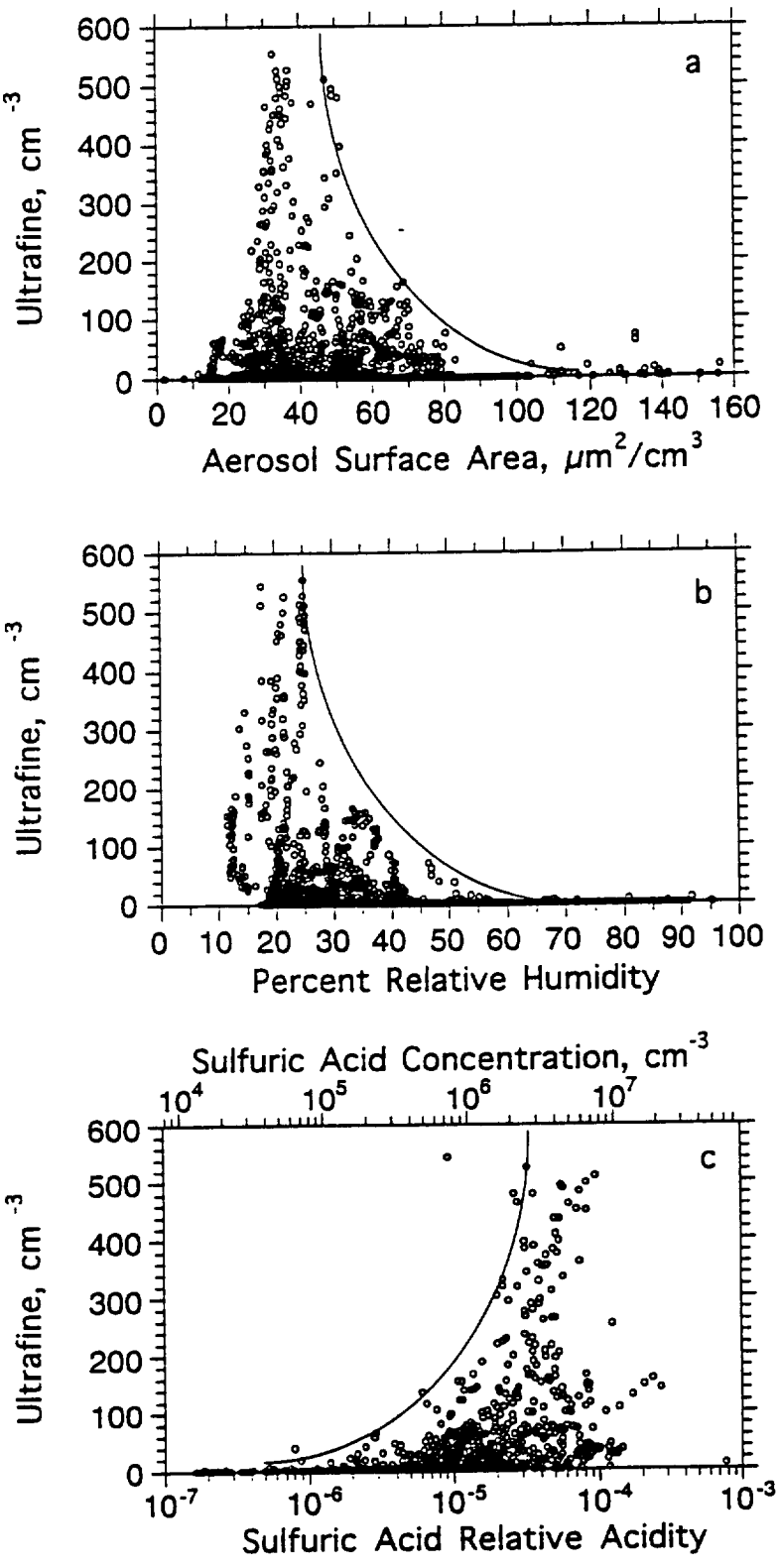
a
Ultrafine, cm^{-3}
600
500
400
300
200
100
0
0 20 40 60 80 100 120 140 160
Aerosol Surface Area, $\mu m^2/cm^3$
b
Ultrafine, cm^{-3}
0 10 20 30 40 50 60 70 80 90 100
Percent Relative Humidity
Sulfuric Acid Concentration, cm^{-3}
10^4 10^5 10^6 10^7
c
Ultrafine, cm^{-3}
10^{-7} 10^{-6} 10^{-5} 10^{-4} 10^{-3}
Sulfuric Acid Relative Acidity

Figure 5

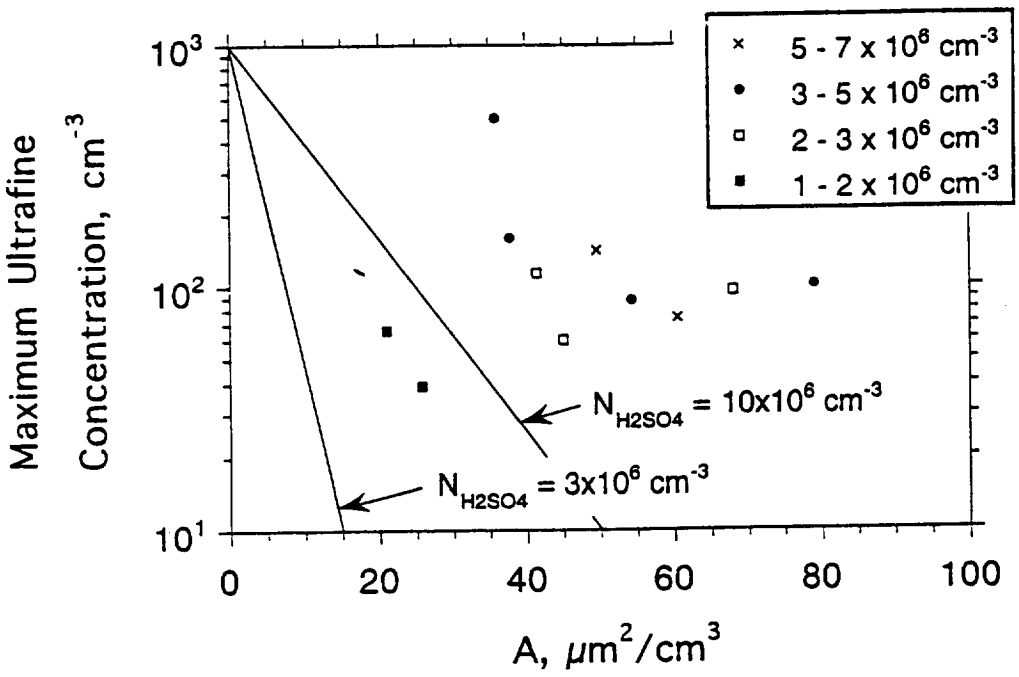
Maximum Ultrafine Concentration, cm^{-3}
10^3
10^2
10^1
0
20
40
60
80
100
A, $\mu m^2/cm^3$
5 - 7 x 10^6 cm^{-3}
3 - 5 x 10^6 cm^{-3}
2 - 3 x 10^6 cm^{-3}
1 - 2 x 10^6 cm^{-3}
N_{H2SO4} = 10x10^6 cm^{-3}
N_{H2SO4} = 3x10^6 cm^{-3}

Figure 6

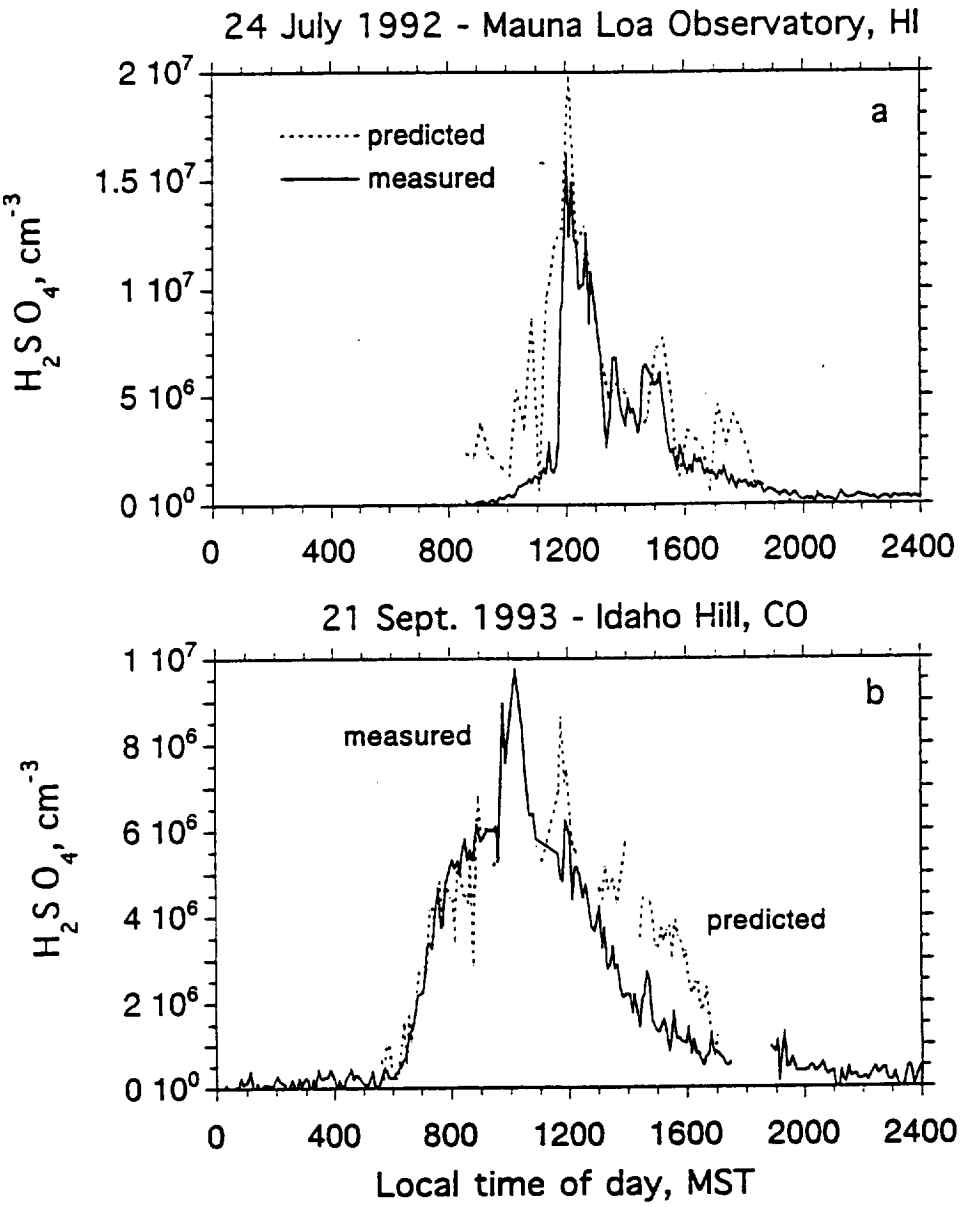
24 July 1992 - Mauna Loa Observatory, HI
predicted
measured
a
H_2SO_4, cm^{-3}
2 10^7
1.5 10^7
1 10^7
5 10^6
0 10^0
0
400
800
1200
1600
2000
2400
21 Sept. 1993 - Idaho Hill, CO
measured
predicted
b
H_2SO_4, cm^{-3}
1 10^7
8 10^6
6 10^6
4 10^6
2 10^6
0 10^0
0
400
800
1200
1600
2000
2400
Local time of day, MST

Figure 7

Revised 5/9/95

MEASURED ATMOSPHERIC NEW PARTICLE FORMATION RATES: IMPLICATIONS FOR NUCLEATION MECHANISMS

R. J. Weber, J. J. Marti, P. H. McMurry*

Particle Technology Laboratory
Department of Mechanical Engineering
111 Church St. SE
University of Minnesota
Minneapolis, MN 55455

F. L. Eisele,** D. J. Tanner, A. Jefferson

Atmospheric Chemistry Division
National Center for Atmospheric Research
P.O. Box 3000
Boulder, CO. 80307

Submitted to:

Chemical Engineering Communications Accepted

PTL Publication No. 917

January 1995

*To whom correspondence should be addressed

**Also holds a joint appointment at EOEML/GTRI
Georgia Institute of Technology
Atlanta, GA 30332

ABSTRACT

Measured production rates of tropospheric ultrafine particles (~3 nm diameter) are reported for the first time and are shown to be orders of magnitude greater than nucleation rates predicted by the binary theory of homogeneous nucleation for sulfuric acid and water. Furthermore, the functional dependence of observed particle formation rates on sulfuric acid vapor concentrations is much weaker than predicted by binary theory. We present arguments to show that these discrepancies might be due to the participation of a species such as ammonia which could stabilize subcritical clusters, thereby enhancing nucleation rates. The data suggest that atmospheric nucleation may occur by a collision-limited process, rather than by a condensation/evaporation controlled process as is assumed in the classical theory.

INTRODUCTION

New particle formation by nucleation of gas phase species significantly influences the size and numbers of tropospheric aerosols. These aerosols can affect the earth's radiation budget directly by scattering solar radiation (Charlson *et al.*, 1992; Kiehl and Briegleb, 1993) or indirectly by serving as cloud condensation nuclei (Twomey, 1977). Since in both cases the magnitude of the effect is sensitive to particle size and number density, accurate representation of nucleation is essential for accurate modeling of aerosol-climate coupling.

Atmospheric particle nucleation has been studied in the laboratory and simulated by numerous modeling studies, but *in situ* studies are more limited. Several recent field measurements have demonstrated without question that the formation of new particles by homogeneous nucleation occurs in the atmosphere. Table 1 lists work published since 1990 that presents evidence of new particle formation in a variety of environments. Much attention has been paid to nucleation in the marine boundary layer, and to a lesser extent, the marine free troposphere. Particle formation near marine clouds has received particular scrutiny. Nucleation over remote continental areas remains relatively unexplored.

Recent advances in instrumentation for detecting ultrafine particles has provided new insights into atmospheric nucleation phenomena. In particular, the ultrafine condensation particle counter (UCPC), developed in our laboratory (Stolzenburg and McMurry, 1991) and commercialized by TSI (St. Paul, MN) as the UCPC Model 3025, has played an important role in this work. With a 50% detection limit of less than 3 nm, the UCPC allows new particles to be counted sooner after nucleation than was previously possible.

Presently, despite little evidence for its applicability, most modeling studies of atmospheric aerosol nucleation and growth (e.g., Kreidenweis et al., 1991; Raes et al., 1992; Raes and van Dingenen, 1992; Hegg, 1993; Lin et al., 1993; Easter and Peters, 1994; Russell et al., 1994; Raes, 1995) use the classical binary theory of homogeneous nucleation for sulfuric acid (H_2SO_4) and water (H_2O) (Jaecker-Voirol and Mirabel, 1989). According to classical theory, new particles are born when molecular clusters grow past a stable (critical) size (Shugard et al. 1974). In binary H_2SO_4/H_2O nucleation, cluster growth rates are determined by the rates at which H_2SO_4 and H_2O are transported to and evaporate from subcritical clusters that contain only H_2SO_4 and H_2O. Because the atmosphere contains a complex spectrum of species that could participate in the nucleation process, there is no *a priori* reason to expect the H_2SO_4/H_2O theory to be

generally valid.

In this paper we show that actual atmospheric rates of new particle formation measured at Mauna Loa, HI and Idaho Hill, CO are far faster than predicted by the theory for binary nucleation of H_2O and H_2SO_4. Furthermore, the observed dependence of particle production rates on H_2SO_4 concentrations is inconsistent with classical theoretical expectations, but is more nearly consistent with a collision-controlled process. We provide evidence to show that NH_3 is likely to participate in nucleation, and may be responsible for the observed high rates.

When Peter McMurry began his doctoral research under the supervision of Sheldon Friedlander at Caltech in 1972, Friedlander suggested that he work on the problem of nucleation in chemically reacting systems. This problem has been an enduring theme of McMurry's research since that time. Chemical nucleation is important in the atmosphere, in semiconductor processing equipment, and in aerosol reactors used for material synthesis. While a great deal of elegant work has been done to evaluate the classical liquid droplet model for nucleation, it is well known that there are significant discrepancies between theory and experiment remain. Furthermore, the multicomponent thermodynamic data needed to apply this theory to aerosol systems of practical importance is often unavailable. This is because vapor pressures for species that nucleate under many practical circumstances are exceedingly low and difficult to measure. In addition, nucleation frequently occurs under circumstances for which the classical theory is invalid. For example, if the vapor pressures of chemically-produced condensable species are sufficiently low, then the nucleation process will be collision-controlled rather than condensation/evaporation controlled as is assumed in the classical theory. Alternatively, the classical theory is invalid when particle growth is dominated by surface reactions (as likely occurs in semiconductor processing equipment) rather than by condensation. Validated approaches for modeling such phenomena are generally not available. The present paper summarizes our most recent thinking on atmospheric nucleation. Our ultimate objective in this research is to obtain data that can be used to develop and verify theories for nucleation in the atmosphere.

EXPERIMENT

In this paper we estimate particle formation rates from measurements made at a remote marine site (Mauna Loa Observatory, Hawaii 1992) and a remote continental site (Idaho Hill, Colorado, 1993). These estimates were made possible by the recent development of instrumentation for measuring concentrations of gas phase H_2SO_4 and

3 to 4 nm ultrafine particles. The H_2SO_4 was measured using an atmospheric pressure-selected ion chemical ionization mass spectrometric technique (Eisele and Tanner, 1993). The ultrafine particles were measured using the ultrafine condensation particle counter (UCPC) described by (Stolzenburg and McMurry, 1991) in the pulse height analysis (PHA) mode.

The PHA technique has been described previously (Brockmann, 1981; Stolzenburg, 1988; Ahn and Liu, 1990; Wiedensohler *et al.*, 1994); the reader is referred to these previous publications for details. In summary, particles larger than ~15 nm are activated (i.e., begin to grow by condensation) near the entrance to the UCPC condenser and all grow to about the same final droplet size. However, curvature effects become significant for particles smaller than this. Therefore, such "ultrafine" particles must travel further into the UCPC condenser before saturation ratios are sufficiently high to initiate their condensational growth. Because growth times decrease with initial size, the final droplet size at the exit from the condenser also decreases with initial size. This final droplet size can be measured with the photo detector that is used to count individual particles exiting from the condenser. Thus, by measuring the UCPC pulse height distributions it is possible to obtain quantitative information on ultrafine particle size distributions.

For the data reported in this paper, counting intervals were 15 minutes (Mauna Loa) and 2.5 minutes (Idaho Hill). We confine our attention to a range of pulse heights that excludes all particles exceeding 4.5 nm. Because the minimum detectable size for this instrument is ~2.7 nm, we assume that the mean size of the counted particles is ~3.5 nm. We also assume that all particles in the 3 to 4 nm diameter range are counted, although we know from measured instrument PHA response functions that a fraction of the particles in this range will produce pulse heights that exceed our lower limit. Because of these factors, our reported particle formation rates are somewhat smaller than actual values. Uncertainties introduced by these approximations , however, are likely to be small compared to the variability in the data. A more complete discussion of the PHA technique that was used for these measurements is discussed by (Weber, 1995).

The PHA method offers considerable advantages over methods mentioned in Table 1 for measuring size distributions and concentrations of ultrafine atmospheric particles. Techniques that rely on calculating the difference between concentrations measured with two CPCs having differing lower detection limits (e.g. $N_{ultrafine}=N_{3025}-N_{3760}$) are severely limited by counting-statistical uncertainties and flow uncertainties. For example, if the concentration of particles larger than 15 nm is ~200 cm^{-3} (a typical value in the remote troposphere) and if a time resolution of 5 minutes is required, then

counting statistical uncertainties limit the minimum ultrafine (3-15 nm) concentration that can be measured with 15% accuracy to ~>10 cm^{-3}. This value will increase when the flow uncertainties of the two instruments are taken into account. In contrast, using the PHA technique under the same sampling conditions, ultrafine concentrations as small as 0.1 cm^{-3} can be measured to within ~10-15%. Furthermore our measurements are only weakly dependent on flow uncertainties, and provide information on size as well as concentration. Techniques that employ differential mobility analysis (i.e., DMPS or SMPS systems) can provide excellent size resolution, but are limited by counting rates: only a very small fraction of the smallest particles are charged, and only charged particles are classified and counted with this technique. Thus, far more time is require to measure size distributions. Diffusion batteries require time to scan through a series of sampling ports, and also require a steady size distribution for accurate measurements. In summary, the PHA technique provides information on 3 to 12 nm size distributions with better time resolution and sensitivity than is possible with other methods.

THEORY

In this section the approach that is used to estimate rates of 3-4 nm particle formation from our field measurements is discussed. The rate at which particles grow past the minimum detectable size (~3 nm diameter) by vapor condensation is:

$$J(3\ nm) = \left.\frac{dN}{dD_P}\right|_{3.5\ nm} \cdot \left.\frac{dD_P}{dt}\right|_{3.5\ nm} \qquad [1]$$

where dN/dD_P is the measured aerosol size distribution function at 3.5 nm and dD_P/dt is the diameter growth rate for 3.5 nm particles. The average size distribution function in the vicinity of 3.5 nm, $\bar{n}$, can be estimated from our ultrafine measurements by:

$$\left.\frac{dN}{dD_p}\right|_{3.5\ nm} \equiv \bar{n}(3.5\ nm) \approx \frac{\text{measured concentration in 3 to 4 nm diameter range}}{4\ nm - 3\ nm}. \qquad [2]$$

We have previously shown that the appearance of ultrafine particles is correlated with H_2SO_4 vapor concentrations, suggesting that H_2SO_4 participates in new particle production (Weber et al., 1995). If condensation of H_2SO_4 vapor is much faster than evaporation (a reasonable assumption in our case where particle size greatly exceeds the

critical size for binary H_2SO_4/H_2O homogeneous nucleation), and if the rate limiting step for particle growth is uptake of H_2SO_4, then from kinetic theory (e.g., Present, 1958):

$$\frac{dv}{dt} = \frac{\text{collisions}}{\text{area} \cdot \text{time}} \cdot \frac{\text{total volume added}}{\text{collision}} \cdot \text{particle surface area}$$
$$= \alpha_{H_2SO_4} \frac{[H_2SO_4]\bar{c}}{4} v_1 \pi D_p^2 = \frac{\pi D_p^2}{2} \frac{dD_p}{dt}. \quad [3]$$

Therefore:

$$\frac{dD_p}{dt} = 2\alpha_{H_2SO_4} v_1 \frac{[H_2SO_4]}{4} \bar{c} \quad [4]$$

where $[H_2SO_4]$ is the molecular gas phase concentration of H_2SO_4, $\alpha_{H_2SO_4}$ is the H_2SO_4 mass accommodation coefficient, $\bar{c}$ is the mean thermal speed of the condensing H_2SO_4 species, and v_1 is the amount that the particle volume increases upon the addition of a single H_2SO_4 molecule. This volume increment includes species that are transported to the particle with the H_2SO_4 as well as species that are absorbed afterwards to maintain phase equilibrium, such as H_2O and possibly NH_3. Actual diameter growth rates will exceed the value given by Eq. [4] if additional species that are not associated with H_2SO_4 are involved. Assuming that every collision between 3 nm particles and the hydrated H_2SO_4 molecule is effective ($\alpha_{H_2SO_4} = 1$), the "measured" rate of new particle formation is:

$$J_{measured} = \bar{n} \cdot 2v_1 \frac{[H_2SO_4]}{4} \bar{c}. \quad [5]$$

Note that rates calculated by Eq. [5] are based on instantaneous point data, and are therefore not affected by advection.

RESULTS AND DISCUSSION

Figure 1 shows particle formation rates calculated using Eq. [5] versus measured H_2SO_4 concentration for all data obtained at Mauna Loa and Idaho Hill that were judged free of local anthropogenic influences. In both cases the data are bounded by two lines. The maximum measured particle formation rates vary approximately with the square of the H_2SO_4 concentration (line of slope ~2 in Figure 1). No significance regarding nucleation can be drawn from the apparent lower boundary (line of slope 1) which is an

artifact of the measurement procedure. This lower boundary corresponds to measurements in which only one particle was detected by the UCPC during the measurement interval. Sulfuric acid concentrations for cases when no ultrafine particles were detected are given at $J = 10^{-10}$ cm^{-3} s^{-1}.

Predicted rates of homogeneous nucleation according to the classical hydrate theory for binary (H_2SO_4/H_2O) nucleation are also shown in Figure 1. The measured particle formation rates significantly exceed the theoretical rates. While classical theory predicts practically no nucleation for $[H_2SO_4] < 10^7$ cm^{-3} (at 50% RH), we observed new particle formation at H_2SO_4 concentrations down to 10^4 cm^{-3}. Because the critical size for homogeneous nucleation (~1.5 nm diameter) (Mirabel and Katz, 1974) is significantly below our minimum detectable size (~3 nm), the predicted rates of homogeneous nucleation are not directly comparable with our reported rates of new particle formation. In particular, a fraction of the newly-formed particles is scavenged by preexisting particles before they grow to 3 nm. Therefore, if binary theory were used to model aerosol production, predicted rates of 3 nm particle production would be lower than the theoretical rates of binary nucleation shown on Figure 1. Thus scavenging by preexisting particles will further increase discrepancies between our measured rates, which include scavenging, and the theoretically-predicted values which do not.

Although the experimental values in Figure 1 were obtained assuming a H_2SO_4 mass accommodation coefficient of 1.0, the discrepancy between theory and experiment would not be resolved if the actual value were smaller than this. The accommodation coefficient would not affect the functional dependence of our reported rates on H_2SO_4 vapor concentrations. Furthermore, nucleation rates from binary theory would also need to be decreased to account for nonaccommodation, thus not resolving the discrepancy between theory and measurements.

The dependence of new particle formation rates measured in Colorado on aerosol surface area is shown in Figure 2. Note that higher aerosol surface areas led to reduced rates of particle production. This is consistent with expectations, since clusters formed by nucleation can be scavenged by preexisting particles before they grow to our minimum detectable size. Thus, aerosol surface area accounts for some but not all of the scatter in the Colorado particle formation rate results. A similar dependence on surface area was not observed in Hawaii. This may be because of the higher measurement uncertainties associated with the lower concentrations in that environment.

The observation that the maximum measured new particle formation rates vary in proportion to $[H_2SO_4]^2$ is intriguing. This suggests that the nucleation process may be collision-controlled rather than evaporation/condensation controlled, as is assumed in

classical nucleation theory. McMurry (1980) has discussed the problem of aerosol formation in a reaction system when nucleation is collision-controlled, and Rao and McMurry (1989) have discussed the transition between the collision-controlled and condensation/evaporation-controlled limiting regimes Assuming a steady-state cluster distribution, the upper limit for the new particle formation rate is the rate at which H_2SO_4 collides with itself, $\beta[H_2SO_4]^2$, where the collision frequency function β is about 3×10^{-10} $cm^3\ s^{-1}$ (McMurry and Friedlander, 1978; McMurry, 1983a). Observed maximum new particle formation rates at Hawaii and Colorado were, respectively, approximately six and five orders of magnitude below this, (Figure 1). Phenomena that will reduce rates below the H_2SO_4 collision rate include cluster evaporation, nonaccommodation for H_2SO_4 collisions, cluster scavenging by preexisting aerosol as clusters grow up to our minimum detectable size (~3 nm), or the participation of species other than H_2SO_4 and H_2O in the nucleation process. The latter is the only explanation consistent with our data. The binary theory, while accounting for the effects of cluster evaporation, produces results that are inconsistent with our measurements; including nonaccommodation in the binary theory would increase discrepancies with our data. The Colorado data in Figure 2 show that cluster scavenging by preexisting particles led to reduced rates of particle production at given H_2SO_4 concentrations during our measurements, but not when new particle formation rates were maximum (i.e., along the $J \sim [H_2SO_4]^2$ line shown in Figure 1).

Scenarios that will lead to the observed results can be found if a stabilizing species such as NH_3 were to react with clusters containing one or more H_2SO_4 molecules and H_2O. Such species would decrease rates of H_2SO_4 evaporation from clusters, thereby increasing nucleation rates. For example, nucleation rates could be determined by collision rates of a thermodynamically-determined NH_3-stabilized fraction, γ, of the H_2SO_4 monomer. The resulting steady state rate of particle formation in the absence of cluster scavenging by preexisting particles would then be:

$$\frac{dN}{dt} = \beta\gamma^2[H_2SO_4]^2 \qquad [6]$$

where β is the collision frequency function for the molecular clusters that contain the stabilized H_2SO_4 molecule. Assuming that $\beta \sim 3 \times 10^{-10}$ cm^3/s, it follows from the data in Figure 1 that $\gamma \sim 0.001$ for Hawaii and 0.003 for Colorado. Alternatively, stabilization might occur at a later step in cluster growth. In this case only a fraction of the clusters produced by H_2SO_4 collisions would be stabilized and begin growth towards the detectable size. Unfortunately, NH_3 was not measured during the field studies discussed

here. Previous measurements have shown, however, that NH_3 concentrations in regions similar to those at Idaho Hill are roughly an order of magnitude higher than values found over the Pacific (Ayers and Gras, 1983; Tanner and Eisele, 1991; Langford and Fehsenfeld, 1992). It is interesting to note that the maximum particle formation rates shown in Figure 1 are also about an order of magnitude higher in Colorado than in Hawaii.

There is good reason to believe that NH_3 may participate in atmospheric nucleation (Hoppel, 1975; Scott and Cattell, 1979). Characteristic values for concentrations of H_2O, NH_3, and H_2SO_4 in the remote troposphere are ~10^{17} cm^{-3}, 10^9 to 10^{10} cm^{-3}, and 10^4 to 10^7 cm^{-3}, respectively. Because the NH_3 and H_2O are typically greatly in excess of H_2SO_4, these species collide with molecular clusters at much higher rates than does H_2SO_4. Laboratory experiments have shown that the reaction probability for NH_3 with aqueous H_2SO_4 droplets is close to 1.0 (Huntzicker et al., 1980; McMurry et al., 1983b); it is likely that NH_3 also reacts efficiently with atmospheric H_2SO_4/H_2O clusters. Furthermore, we recently completed laboratory experiments which showed that vapor pressures of H_2SO_4 over $H_2O/H_2SO_4/(NH_4)_2SO_4$ solutions drop by orders of magnitude as ammonium-to-sulfate ratios rise above one (Marti et al., 1995). These observations suggest that tropospheric NH_3 is probably present in sufficient quantities to stabilize clusters, thereby leading to higher nucleation rates than would occur in its absence. It is also possible that additional species not considered here play a role in nucleation. Our previous work has shown, however, that one candidate species, methane sulfonic acid, is not correlated with ultrafine particles at Mauna Loa (Weber et al., 1995).

Our field measurements have the limitation that they were made at a fixed location. This can complicate our interpretations because there is about a 1 hour growth period between the time particles are produced by homogeneous nucleation and the time they are detected with our instrumentation. Therefore, the H_2SO_4 concentration present during the nucleation event could have been different from the H_2SO_4 concentrations measured at our site. Although this would not affect the local particle formation rates calculated with Equation [5], it could affect the inferred functional dependence of particle formation rates on H_2SO_4 concentrations. However, supplemental measurements strongly suggest that homogeneous nucleation was occurring at the measurement site. A mass spectrometer was used to detect sub-3 nm ($2x10^3$ to 10^4 amu) molecular clusters for a portion of the measurement period at Mauna Loa (Weber et al., 1995). We found that clusters were typically present when ultrafine particles were detected. Furthermore, at both sites, the observed delay times between increases in H_2SO_4 concentrations and the appearance of 3 nm particles were often comparable to expected values, based on

diameter growth rates given by Equation [3]. Therefore, while transport may have contributed to scatter in the observed relationships between particle formation rates and H_2SO_4 concentrations shown in Figure 1, the evidence that some of the measurements were made during nucleation events and the consistency of the results obtained in two distinctly different locations supports our conclusion that the results of Figure 1 were determined primarily by local transformations and not by transport.

CONCLUSIONS

In summary, our data shows that although H_2SO_4 is involved with the formation of new particles in the troposphere, observed rates of new particle formation typically exceed rates of homogeneous nucleation predicted by the classical hydrate theory for the H_2SO_4/H_2O system. Furthermore, particle formation is observed at lower H_2SO_4 concentrations than predicted by binary nucleation theory. We postulate that these discrepancies between observation and theory can be attributed to the stabilizing influence of species such as NH_3. Ammonia is known to react at a near collision-controlled rate with H_2SO_4/H_2O droplets, and markedly reduces equilibrium H_2SO_4 vapor pressures when incorporated into H_2O/H_2SO_4 solutions. It is also possible that other species not considered here also participate in the nucleation process. Thus, because new particle formation plays a key role in regulating aerosol size distributions and concentrations of cloud condensation nuclei, species such as NH_3 may significantly influence our view of the dynamic interaction between aerosols and climate. Future work incorporating these results into atmospheric aerosol models may lead to new insights regarding the impact of aerosols on climate.

ACKNOWLEDGMENTS

We thank the Mauna Loa Observatory and NOAA Aeronomy Lab for the use of their facilities. This work was funded by: the National Science Foundation under grants ATM 9021522 and ATM 9205337, the Department of Energy grant No. DE-FG02-91ER61205, and NASA grant No. NAGW-3767. In addition, RJW was supported by a NASA Global Change Fellowship.

REFERENCES

Ahn, K.-H. and B.Y.H. Liu (1990) Particle Activation and Droplet Growth Process in Condensation Nucleus Counter-I. Theoretical Background, J. Aerosol Science **21**: 249-261.

Ayers, G. P. and J. L. Gras (1983) "The concentration of ammonia in southern ocean air." J. Geophys. Res. **88**: 10655-10659.

Brockmann, J.E. (1981) Coagulation and Deposition of Ultrafine Aerosols in Turbulent Pipe Flow, Ph.D., University of Minnesota.

Charlson, R.J., *et al.*, (1992) Climate Forcing by Anthropogenic Aerosols, Science **255**:423-430.

Clarke, A. D. (1993). "Atmospheric Nuclei in the Pacific Midtroposphere - Their Nature, Concentration, and Evolution." Journal of Geophysical Research - Atmospheres **98**(D11): 20633-20647.

Covert, A. D., et al. (1992) "New particle formation in the marine boundary layer." Journal of Geophysical Research **97**: 20581-20589.

Covert, D. S., et al. (1995) "Aerosol number size distributions from 3 to 500 nm diameter in the summer Arctic marine boundary layer." Tellus B : in press.

Easter, R. C. and L. K. Peters (1994) "Binary homogeneous nucleation: Temperature and relative humidity fluctuations, nonlinearity, and aspects of new particle production." J. Applied Meteorology **33**(7): 775-790.

Eisele, F. L. and Tanner, D. J. (1993) "Measurement of the gas phase concentrations of H_2SO_4 and Methane Sulfonic acid and estimates of H_2SO_4 production and loss in the atmosphere" J. Geophys. Res. **98**: 9001-9010.

Hegg, D. A., L. F. Radke and P. V. Hobbs (1990) "Particle production associated with marine clouds." J. Geophys. Res. **95**(D9): 13917-13926.

Hegg, D. A., L. F. Radke and P. V. Hobbs (1991) "Measurements of Aitken nuclei and cloud condensation nuclei in the marine atmosphere and their relation to the DMS-cloud-climate hypothesis." G. Geophys. Res. **96**(D10): 18727-18733.

Hegg, D. (1993) "A Model Study of the Formation of Cloud Condensation Nuclei in Remote Marine Areas - Comment." Journal of Geophysical Research - Atmospheres **98**(D11): 20813-20814.

Hoppel, W. A., et al. (1990) "Aerosol size distributions and optical properties found in the marine boundary layer over the Atlantic Ocean." J. Geophys. Res. **95**: 3659-3686.

Hoppel, W. A. and G. M. Frick (1990) "Submicron Aerosol Size Distributions Measured Over the Tropical and South Pacific." Atmos. Env. **24A**(3): 645-660.

Hoppel, W. A., et al. (1994) "Marine Boundary Layer Measurements of New Particle Formation

and the Effects Nonprecipitating Clouds Have on Aerosol Size Distribution." Journal of Geophysical Research - Atmospheres 99(D7): 14443-14459.

Hoppel, W. A. (1975) "Growth of condensation nuclei by heteromolecular condensation" J. Rech. Atmos. 9: 167-180.

Huntzicker, J. J., Caryke, R. A. and Ling, C. S. (1980) "Neutralization of sulfuric acid aerosol by ammonia" Envir. Sci. Technol. 14: 819-824.

Jaecker-Voirol, A., and Mirabel, P (1989) "Heteromolecular nucleation in the sulfuric acid-water system" Atmos. Envir. 23: 2053-2057.

Kiehl, J. T. and Briegleb, B. P. (1993) "The relative roles of sulfate aerosols and greenhouse gases in climate forcing" Science 260: 311-314.

Koutsenogii, P. K. and R. Jaenicke (1994) "Number Concentration and Size Distribution of Atmospheric Aerosol in Siberia." Journal of Aerosol Science 25(2): 377-383.

Kreidenweis, S. M., et al. (1991) "The Effects of Dimethylsulfide Upon Marine Aerosol Concentrations." Atmospheric Environment 25A(11): 2501-2511.

Langford, A. O. and Fehsenfeld, F. C. (1992) "Natural vegetation as a source or sink for atmospheric ammonia: a case study" Science 255: 581-583.

Lin, X., et al. (1993) "A Model Study of the Formation of Cloud Condensation Nuclei in Remote Marine Areas - Reply." Journal of Geophysical Research - Atmospheres 98(D11): 20815-20816.

Marti, J. (1990) "Diurnal variation in the undisturbed continental aerosol: Results from a measurement program in Arizona." Atmospheric Research 25: 351-362.

Marti, J. J., McMurry, P. H., Jefferson, A., and Eisele, F. (1995) "Vapor pressures of sulfuric acid-ammonium sulfate solutions and implications for atmospheric aerosols," manuscript in preparation.

McMurry, P. H. and Friedlander, S. K. (1979) "New Particle Formation in the Presence of an Aerosol." Atmospheric Environment 13: 1635-1653.

McMurry, P. H. (1980) "Photochemical aerosol formation from SO2: A theoretical analysis of smog chamber data," J. Colloid Interface Sci. 78(2) 513-527.

McMurry, P. H. (1983a) "New particle formation in the presence of an aerosol: rates, time scales, and sub-0.01 μm size distributions" J. Colloid Interface Science 95: 72-80.

McMurry, P. H., Takano, H. and Anderson, G. R. (1983b) "Study of the ammonia (gas) - sulfuric acid (aerosol) reaction rate" Envir. Sci. Tech. 17: 347-352.

Mirabel, P. and Katz, J. (1974) "Binary homogeneous nucleation as a mechanism for the formation of aerosol" J. Chem. Phys. 60, 1138-1144.

Perry, K. D. and P. V. Hobbs (1994) "Further evidence for particle nucleation in clear air

adjacent to marine cumulus clouds." Journal of Geophysical Research - Atmospheres 99(D11): 22803-22818.

Present, R. D. (1958) Kinetic Theory of Gases, McGraw-Hill Book Company, Inc.

Putaud, J. P., et al. (1993) "Dimethylsulfide, Aerosols, and Condensation Nuclei over the Tropical Northeastern Atlantic Ocean." Journal of Geophysical Research - Atmospheres 98(D8): 14863-14871.

Quinn, P. K., et al. (1993) "Dimethylsulfide, cloud condensation nuclei, climate system: Relevant size resolved measurements of relevant chemical and physical properties of atmospheric aerosol particles." J. Geophys. Res. 98: 10411-10427.

Radke, L. F. and P. V. Hobbs (1991) "Humidity and particle fields around some small cumulus clouds." J. Atmos Sci. 48: 1190-1193.

Radke, L. F. and P. V. Hobbs (1991) "Humidity and particle fields around some small cumulus clouds." J. Atmos Sci. 48: 1190-1193.

Raes, F. (1995) "Entrainment of free tropospheric aerosols as a regulating mechanism for cloud condensation nuclei in the remote marine boundary layer." Journal of Geophysical Research - Atmospheres 100(D2): 2893-2903.

Raes, F., A. Saltelli and R. van Dingenen (1992) "Modelling formation and growth of H2SO4-H2O aerosols: Uncertainty analysis and experimental evaluation." J. Aerosol Sci. 23(7): 759-771.

Raes, F. and R. van Dingenen (1992) "Simulations of Condensation and Cloud Condensation Nuclei From Biogenic SO_2 in the Remote Marine Boundary Layer." Journal of Geophysical Research 97(D12): 12901-12912.

Rao, N. P. and P. H. McMurry (1989) "Nucleation and growth of aerosol in chemically reacting systems." Aerosol Sci. Technol. 11: 120-132.

Russell, L. M., S. N. Pandis and J. H. Seinfeld (1994) "Aerosol production and growth in the marine boundary layer." Journal of Geophysical Research - Atmospheres 99(D10): 20989-21003.

Scott, W. D. and Cattell, F. D. R. (1979) "Vapor pressure of ammonium sulfates" *Atmos Envir.* 13: 307-317.

Shugard, W. J., Heist, R. H. and Reiss, H. (1974) "Theory of vapor phase nucleation in binary mixtures of water and sulfuric acid" J. Chem. Phys. 61: 5298-5305.

Stolzenburg, M.R. (1988) An Ultrafine Aerosol Size Distribution Measuring System, Ph.D., University of Minnesota

Stolzenburg, M. R. and McMurry, P. H. (1991) "An ultrafine aerosol condensation nucleus counter" Aerosol Sci. Tech. 14: 48-65.

Tanner, D. J. and Eisele, F. L. (1991) "Ions in oceanic and continental air masses" J.

Geophys. Res. 96:1023-1031.

Twomey, S. (1977) "Atmospheric Aerosols" (Elsevier, Amsterdam).

Weber, R. J. (1995) Studies of New Particle Formation in the Remote Troposphere, Ph.D. Thesis, University of Minnesota, Minneapolis, MN 55455.

Weber, R. J., McMurry, P. H., Eisele, F. L. and Tanner, D. J. (1995) "Measurement of expected nucleation precursor species and 3 to 500 nm diameter particles at Mauna Loa Observatory, Hawaii" *J. Atmos. Sciences* in press.

Wiedensohler, A., Aalto, P., Covert, D., Heintzenberg, J. and McMurry, P. H. (1994) "Intercomparison of four methods to determine size distributions of low concentration (~100 cm^{-3}), ultrafine aerosols (3<Dp<10nm) with illustrative data from the Arctic" Aerosol Sci. Tech. 21: 95-109.

FIGURE CAPTION:

Figure 1 Measured rates of new particle formation at a remote marine site, Mauna Loa Observatory, Hawaii (a), and a remote continental site, Idaho Hill, Colorado, located on the eastern face of the Rocky Mountains (b). The median relative humidities and temperatures at Mauna Loa and Idaho Hill for the data shown were: 48%, 8°C and 32%, 6°C respectively. The measured particle formation rates are compared to classical hydrate binary (H_2SO_4/H_2O) nucleation theory for relative humidities of 100, 50 and 10%, and with the collision rate of hydrated (50% RH) H_2SO_4 molecules, $\beta[H_2SO_4]^2$.

Figure 2. Dependence of averaged particle formation rates (from Figure 1b) on preexisting aerosol surface area concentrations.

Table 1: Recent field measurements of new particle formation .

Location	Reference	Comment
Arctic marine boundary layer	Covert *et al.*(Covert et al., 1995)	
Marine boundary layer	Weber *et al.* (Weber, McMurry et al., 1995)	Simultaneous CN and H_2SO_4 measurements
Marine boundary layer	Hoppel *et al.* (Hoppel et al., 1994)	In clear air and near stratiform clouds
Marine free troposphere	Perry and Hobbs (Perry and Hobbs, 1994)	In clear air, adjacent to marine cumulous clouds
Arctic marine boundary layer	Wiedensohler *et al.* (Wiedensohler et al., 1994)	Intercomparison of 4 ultrafine aerosol measurement techniques
Remote continental boundary layer	Koutsenogii and Jaenicke (Koutsenogii and Jaenicke, 1994)	
Marine upper troposphere	Clarke (Clarke, 1993)	
Marine boundary layer	Putaud *et al.* (Putaud et al., 1993)	Simultaneous CN and gas phase measurements
Open ocean and coastal surface; coastal boundary layer	Quinn et al (Quinn et al., 1993)	
Marine boundary layer	Covert *et al.* (Covert et al., 1992)	
Lower continental troposphere	Radke and Hobbs (Radke and Hobbs, 1991)	Near small cumulus clouds
Marine free troposphere	Hegg *et al.* (Hegg et al., 1990; Hegg et al., 1991)	In clear air and near stratiform clouds
Marine boundary layer	Hoppel et al (Hoppel et al., 1990)	Tropical Atlantic ocean
Marine boundary layer	Hoppel and Frick (Hoppel and Frick, 1990)	Tropical Pacific ocean
Background continental boundary layer	Marti (Marti, 1990)	Mountain station, above surface inversion layer

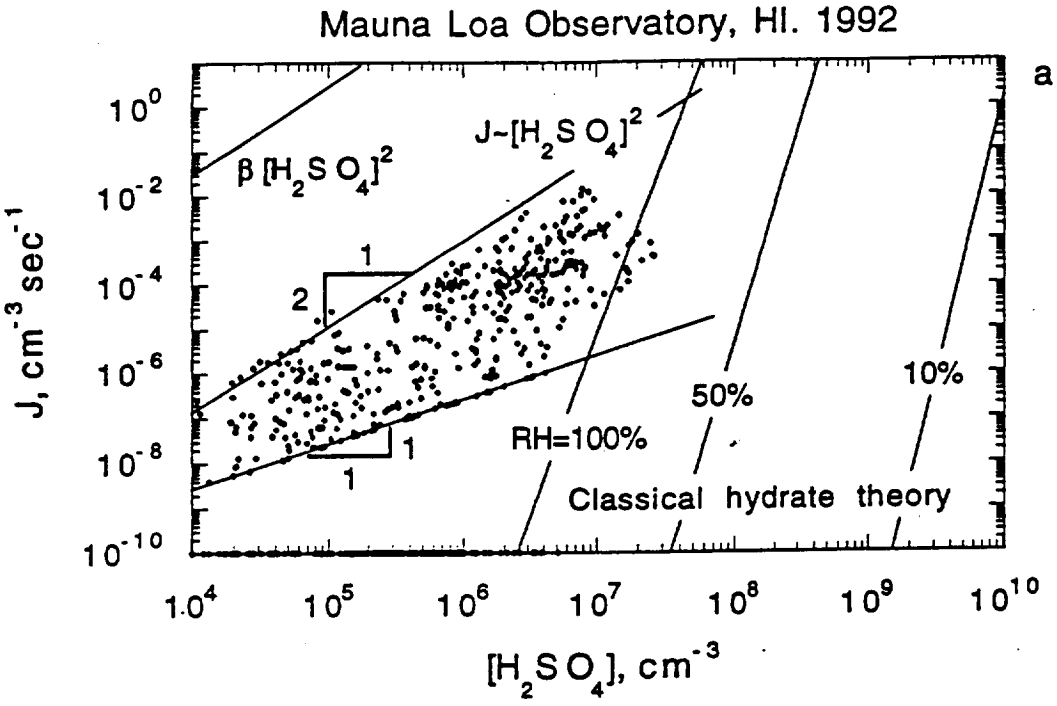
Mauna Loa Observatory, HI. 1992
a
J, cm^{-3} sec^{-1}
10^{0}
10^{-2}
10^{-4}
10^{-6}
10^{-8}
10^{-10}
$\beta [H_2SO_4]^2$
$J \sim [H_2SO_4]^2$
1
2
1
1
RH=100%
50%
10%
Classical hydrate theory
10^{4}
10^{5}
10^{6}
10^{7}
10^{8}
10^{9}
10^{10}
$[H_2SO_4]$, cm^{-3}

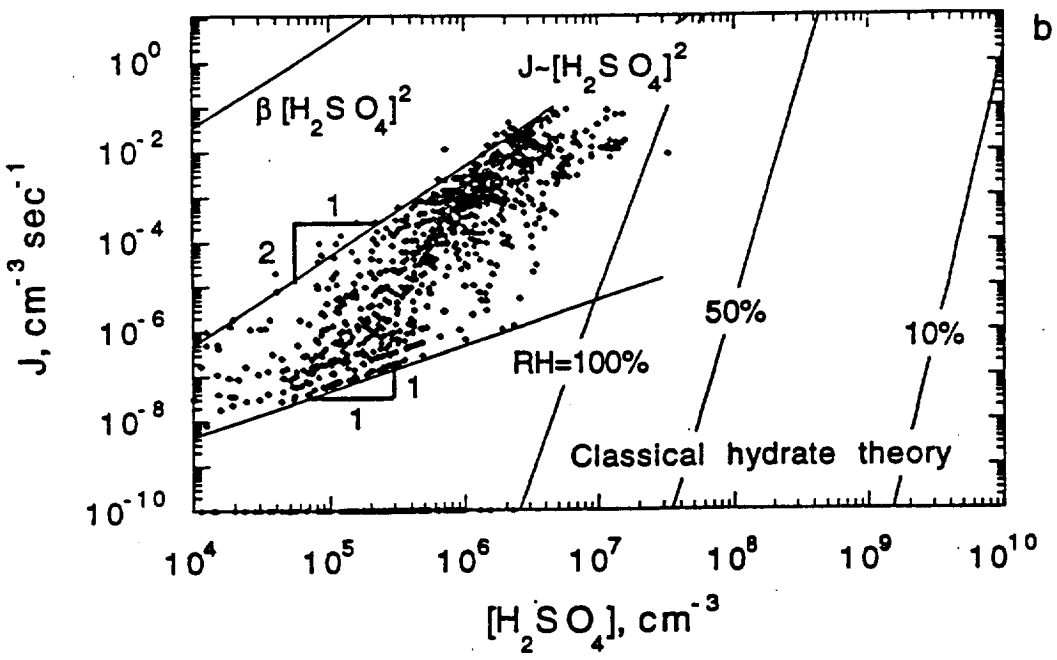
Idaho Hill, CO. 1993
b
J, cm^{-3} sec^{-1}
10^{0}
10^{-2}
10^{-4}
10^{-6}
10^{-8}
10^{-10}
$\beta [H_2SO_4]^2$
$J \sim [H_2SO_4]^2$
1
2
1
1
RH=100%
50%
10%
Classical hydrate theory
10^{4}
10^{5}
10^{6}
10^{7}
10^{8}
10^{9}
10^{10}
$[H_2SO_4]$, cm^{-3}

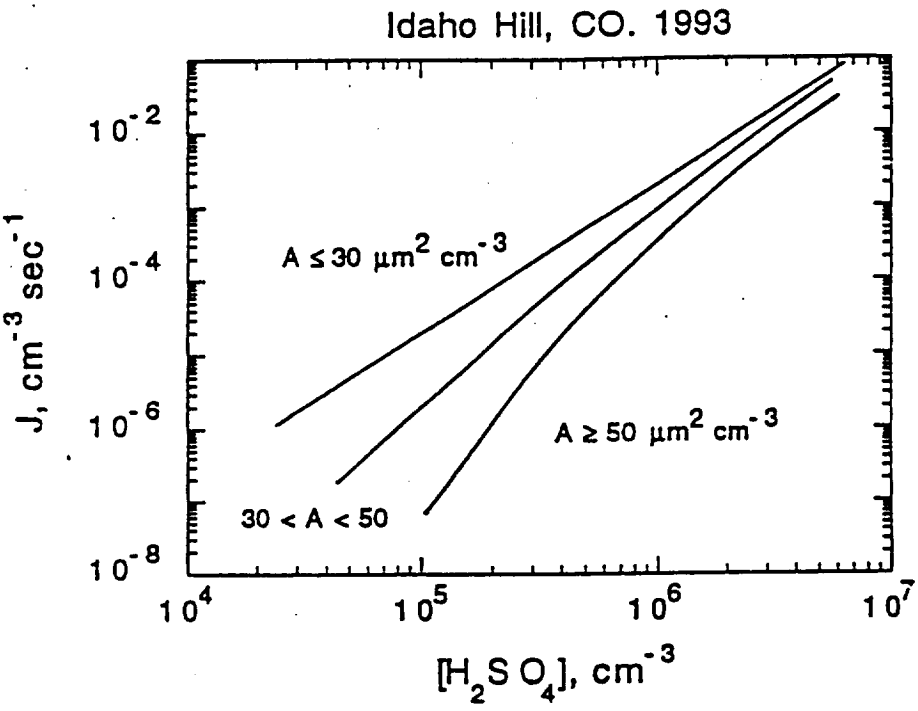
Idaho Hill, CO. 1993
10^{-2}
10^{-4}
10^{-6}
10^{-8}
J, cm^{-3} sec^{-1}
$A \leq 30\ \mu m^2\ cm^{-3}$
$A \geq 50\ \mu m^2\ cm^{-3}$
$30 < A < 50$
10^4
10^5
10^6
10^7
$[H_2SO_4]$, cm^{-3}

The H_2SO_4 Vapor Pressure Above Sulfuric Acid and Ammonium Sulfate Solutions

James J. Marti[1], Anne Jefferson[2], Xiao Ping Cai[1], Chad Richert[1], Peter H. McMurry[1*], and Fred Eisele[2]

[1]Particle Technology Laboratory,
Department of Mechanical Engineering,
University of Minnesota,
Minneapolis, MN

[2]Atmospheric Chemistry Division,
National Center for Atmospheric Research,
Boulder, CO

October 1995

Submitted to: Journal of Geophysical Research

PTL Publication No. 986

*To whom correspondence should be addressed.

Abstract

Sulfates make up a major part of the submicron atmospheric aerosol across a wide range of environments. The sulfate aerosol often consists of aqueous sulfuric acid solutions or acidic solutions neutralized with sodium, calcium or ammonium. Due to the very low pressures involved (below 10^{-4} Pa, or 10^{-6} torr), few measurements of H_2SO_4 vapor pressure have been made for sulfuric acid in the temperature and concentration ranges of atmospheric interest, and no such measurements appear to have been made for sulfuric acid solutions neutralized with ammonia. This work presents measurements of H_2SO_4 vapor pressure for aqueous sulfuric acid solutions between 55 and 77 wt% H_2SO_4 (corresponding to about 5 to 25% relative humidity), pure ammonium sulfate solids at low humidities, and partially neutralized solutions with $[NH_4^+]$:$[SO_4^=]$ ratios between 0.13 and 1.0. The vapor pressure data collected over sulfuric acid solutions generally agree with the predictions of Ayers, et al [1980], although positive deviation was observed for the more dilute solutions. The good agreement between this and previous measurements by absolute techniques suggests that the evaporative coefficient for the H_2SO_4-H_2O system is near unity. H_2SO_4 vapor pressures over solid ammonium sulfate were measured between 27 and 60C; the data were fit to $\log p = A/T + B$, with $A = -2671 \pm 369$ and $B = -1.287 \pm 0.093$. The H_2SO_4 vapor pressures of mixed H_2SO_4-H_2O-$(NH_4)_2SO_4$ solutions dropped significantly as the $[NH_4^+]$:$[SO_4^=]$ ratio exceeded 0.5. The results suggest that ammonia could very effectively stabilize molecular clusters of sulfuric acid and water in the atmosphere against evaporation, leading to rates of new particle formation higher than predicted by binary H_2SO_4-H_2O theory.

Introduction

The background atmospheric aerosol varies in composition geographically and temporally. Aerosols are commonly found to contain sulfates, including sulfuric acid (H_2SO_4), ammonium sulfate ($(NH_4)_2SO_4$) and partially neutralized species such as ammonium bisulfate (NH_4HSO_4). Stratospheric aerosols are usually sulfuric acid solutions in the 75 wt% H_2SO_4 range [Junge, 1954, 1963], while the tropospheric sulfate aerosol may occur as sulfuric acid or as neutralized solutions [Twomey, 1971; Meszaros and Vissy, 1974; Weiss et al., 1977]. Conventional theory holds that these particles nucleate from sulfuric acid and water vapor [Raes and Van Dingenen, 1992; Easter and Peters, 1994; Raes, 1995] and then undergo neutralization by gas phase ammonia. The resulting aerosol consists of a solution of sulfuric acid, water, and ammonium sulfate in varying proportions depending on growth history.

Because of the important roles that aerosols play in the Earth's radiative balance and atmospheric chemistry, the nucleation and growth of the sulfate aerosol must be included in global atmospheric models. Key to the success of these aerosol models is a thorough understanding of the thermodynamics of the H_2SO_4-H_2O-$(NH_4)_2SO_4$ system. In particular, the values used for equilibrium vapor pressures of the system components will profoundly affect predicted aerosol nucleation rates. Hence it is important to establish vapor pressure relations for all the components of this system within the temperature and solution strength range likely to be found in the troposphere.

Measurements of water vapor pressure over sulfuric acid solutions have been available for decades [Grollman and Frazier, 1925; Hornung and Giauque, 1955; Giauque et al., 1960], in addition to values calculated from thermodynamic quantities [Gmitro and Vermeulen, 1964]. The interested reader is referred to the comprehensive review of water activity measurements by Bolsaitis and

Elliot [1990]. Water activities and vapor pressures have recently become available for the H_2SO_4-H_2O-$(NH_4)_2SO_4$ system [Kim et al., 1994; Spann and Richardson, 1985] and for pure aqueous $(NH_4)_2SO_4$ [Apelblat, 1993]. These studies all addressed water, the system component that is by far the majority of vapor phase. The vapor pressure of ammonia in these systems is lower by many orders of magnitude and is more difficult to measure. Scott and Cattell [1979] succeeded in doing so for pure ammonium sulfate between 45 and 180° C; more recently, ammonia vapor pressures over ammonium sulfate/acid solutions were reported by Koutrakis et al [1993].

The vapor pressure of H_2SO_4 also lies far lower than that of water for the H_2SO_4-H_2O-$(NH_4)_2SO_4$ system, and is concomitantly difficult to measure. Data on H_2SO_4 vapor pressures over mixed H_2SO_4-H_2O-$(NH_4)_2SO_4$ solutions appear to be entirely missing from the literature. Vapor pressure measurements over unneutralized, concentrated H_2SO_4-H_2O solutions have been accomplished through several ingenious techniques, including radioisotope labeling [Roedel, 1979], cold trapping of acid vapor [Ayers et al., 1980], and particle shrinkage during levitation [Richardson et al., 1986]. These measurements, however, are generally limited to solutions much more concentrated (greater than 90% acid by weight) or temperatures much higher (over 50°C) than those normally encountered in the atmosphere. In general, atmospheric scientists have made use not of the experimental data but of thermodynamic derivations of the H_2SO_4 vapor pressure over sulfuric acid. Older literature cites the derivation of Gmitro and Vermeulen [1964], who calculated H_2SO_4 vapor pressures of sulfuric acid-water solutions starting from pure component thermodynamic values. Later work [Verhoff and Banchero, 1972; Banchero and Verhoff, 1975] noted that the Gmitro and Vermeulen formulation was inconsistent with previous experimental data, and suggested this may be due to uncertainties in the thermodynamic quantities on which the formulation was based. Ayers et al [1980] fit their experimental data to the same form as Gmitro and Vermeulen, resulting in a formulation that was consistent with the Roedel [1979] measurement, but predicted H_2SO_4 vapor pressures lower than the Gmitro and Vermeulen values by over an order of magnitude. The Ayers et al equation for H_2SO_4 vapor pressures over sulfuric

acid solutions has been used extensively in sulfate aerosol nucleation modeling, although it is based on data obtained at high temperatures (65 to 172 C) and nearly pure acid solutions (98.01 wt%). To make useful predictions for the troposphere requires an extrapolation in pressure over several orders of magnitude. Experimental verification of the Ayers et al fit at lower temperatures and solution strengths would be desirable. In addition, there is a clear need for data on H_2SO_4 vapor pressures over mixed H_2SO_4-H_2O-$(NH_4)_2SO_4$ solutions, which probably make up much of the submicron atmospheric aerosol.

This paper presents measurements of H_2SO_4 vapor pressures over aqueous sulfuric acid solutions, solid ammonium sulfate, and mixed H_2SO_4-H_2O-$(NH_4)_2SO_4$ solutions. Vapor pressure measurements were made in temperature and solution composition ranges close to those found in the atmosphere, and should be relevant to two current questions regarding the atmospheric aerosol. Firstly, which of the H_2SO_4 vapor pressure formulations found in the literature should be used in nucleation models? Secondly, how does H_2SO_4 vapor pressure change as the solution is progressively neutralized with the ammonia? The addition of ammonia would presumably cause H_2SO_4 vapor pressure to drop, thereby stabilizing the solution against evaporation. Hence the quantitative behavior of the ternary solution must be known to properly model the formation and growth of atmospheric sulfate aerosols.

Apparatus and Procedure

Two different experimental approaches were used to measure sulfuric acid vapor pressures. Both techniques involved measuring the rates of evaporation of sub micron solid particles and liquid droplets into a carrier gas that was initially free of H_2SO_4. Vapor pressure data on H_2SO_4-H_2O-$(NH_4)_2SO_4$ solutions, and most of the data for sulfuric acid-water solutions, were obtained by measuring the rate at which gas phase H_2SO_4 evaporating from 0.25 μm particles accumulated in a short residence time (2-6 second) flow system. Gas phase measurements were made with a chemical ionization mass spectrometer (CIMS), which is described in detail elsewhere [Eisele,

1986, 1988, 1993; Eisele and Tanner, 1991]. The CIMS system enabled detection of H_2SO_4 vapor down to below 10^5 molecules per cm^3. These measurements of initial evaporation rate yielded equilibrium H_2SO_4 vapor pressure through application of mass transfer theory, as will be discussed below.

Vapor pressures for sulfuric acid-water solutions were also obtained with a tandem differential mobility analyzer (TDMA) [Rader and McMurry, 1986]. This technique measured the initial and final sizes of monodisperse sulfuric acid solution droplets which flowed through a conditioning tube for 30 to 250 seconds. Mass transfer theory was used to calculate equilibrium vapor pressure from particle shrinkage. The TDMA technique has been used to measure vapor pressures of organic compounds [Rader and McMurry, 1987; Tao and McMurry, 1989]; the approach was first applied to the H_2SO_4-H_2O system by Richert [1991].

Both the CIMS and TDMA experiments applied the appropriate mass transfer relations. Since mass transfer between particle and gas phase is a function of particle radius (see below), monodispersity of sample particles is required. The aerosols (solid crystalline particles or liquid droplets) used in the both sets of experiments were size selected by a differential mobility analyzer (DMA) [Liu and Pui, 1974]. While the TDMA measurements required significant particle shrinkage (in excess of 10%), the mass spectrometric technique required only enough evaporation to yield detectable gas phase concentrations; the final sizes of the particles in the CIMS experiments were virtually unchanged.

CIMS measurements. The flow system and detection apparatus are shown in Figure 1. Major components included gas phase detection system (the CIMS), an atmospheric pressure flow tube system with movable injector, and a particle generation and size selection system, which provided monodisperse aerosols of variable composition.

Liquid droplets of aqueous sulfuric acid or sulfuric acid-ammonium sulfate mixtures were formed by atomizing bulk solutions with the desired $[NH_4^+]$:$[SO_4^=]$ molar ratios. The droplets were passed through a diffusion dryer containing silica gel, resulting in a somewhat more concentrated solution droplet. The particles were then imparted with an electrostatic charge by a polonium source and size selected with a DMA. A condensation nucleus counter (CNC) (Model 3760, TSI, St. Paul, MN) was used to monitor output particle concentration. Filtered dry nitrogen was used as the carrier gas for aerosol formation and maintained at a flow rate of 1.0 liters per minute.

The flow system consisted of a temperature controlled Pyrex tube, 80 cm in length by 8 cm in diameter, and a movable 2.5 cm diameter glass injector. Monodisperse aerosol from the DMA was mixed with particle free nitrogen gas within the injector, which was designed to ensure turbulent mixing of aerosol and flow gas through use of a constriction that raised the flow Reynolds number to around 10^4. A wire mesh covered the flared opening of the injector to distribute the well mixed aerosol into the full bore of the flow tube.

Following particle-gas mixing in the injector, the liquid water content of the droplets very rapidly equilibrated with the water partial pressure in the nitrogen carrier gas [Richert, 1991], subject to any Kelvin curvature correction. Hence for liquid particles, the flow tube relative humidity controlled droplet water content and, by extension, the H_2SO_4 concentration of the droplet. Droplet water vapor pressures were calculated by reference to thermodynamic tables of water vapor pressures for aqueous sulfuric acid solutions [Gmitro and Vermeulen, 1964]. The relative humidity of the nitrogen flow was controlled by passing some of the gas over a distilled water reservoir. Flow gas RH was varied from near zero to about 25% in this manner, and was measured by a dew point hygrometer (General Eastern Instruments Model Hygro M-3) at the flow tube exit.

Sulfuric acid-water solution droplets were generated in the 55 to 77 wt% (18 to 36 mol%) range,

corresponding to the relative humidity range quoted above. Compositions of the mixed H_2SO_4-H_2O-$(NH_4)_2SO_4$ solutions, expressed as the molar $[NH_4^+]$:$[SO_4^=]$ ratio, ranged from zero (i.e., unneutralized sulfuric acid-water solutions) to 2.0 (pure ammonium sulfate). These measurements were performed at relative humidities below 15%, which is well below both the deliquescence point (80% RH) and the crystallization point (39%) of ammonium sulfate [Tang and Munkelwitz, 1984] and the deliquescence point (39% RH) of ammonium bisulfate ($[NH_4^+]$:$[SO_4^=]$ ratio = 1) [Tang and Munkelwitz, 1977]. Hence mixed H_2SO_4-H_2O-$(NH_4)_2SO_4$ particles with composition ratio 1.0 to 2.0 were almost certainly solid, crystalline particles; all other aerosols measured in the experiment were liquid solution droplets.

Flow tube temperature was maintained with a circulating water bath; the carrier gas stream was passed through a heat exchanger at bath temperature before passing into the injector. Gas temperature was checked at the flow tube inlet and exit with calibrated thermocouples. Particle residence time in the flow tube was determined by turning the DMA off and on at various injector positions, resulting in a rapid decay or rise in particle concentration at the CNC located at the flow tube exit. By varying the injector position and establishing the delay between DMA transition and measured changes in particle counts, flow tube residence times for each injector position were established. These times, ranging between 2 and 6 seconds, were equal (within measurement error) to those predicted by laminar flow.

The flow tube was directly coupled to the CIMS system. The mass spectrometer measured count rates at mass 97 (the HSO_4^- ion) and mass 62 (the NO_3^- ion). The (97)/(62) count ratio, multiplied by a predetermined calibration factor, yielded the total H_2SO_4 concentration in the gas flow stream with an absolute accuracy of about 30 to 35%. Instrument background was obtained by measuring the count rates from several masses, such as mass 10 and 106, where no signal was expected to occur. Calibration of the mass spectrometer is described by [Tanner and Eisele, 1995]. A CNC (TSI 3760) measured aerosol concentration at the flow tube exit. Measurements of both

particle and gas phase concentration were typically integrated over 30 second intervals.

TDMA measurements. The TDMA technique has been discussed in detail by [Rader and McMurry, 1986], [Tao and McMurry, 1989], and [Richert, 1991]. The TDMA apparatus is shown in Figure 2. Cleaned, filtered air flow from an air purifier (Aadco Model 737) was split and bubbled separately through reservoirs of distilled water and fuming sulfuric acid, the latter becoming enriched in sulfur trioxide, SO_3. The flows were then turbulently combined in a small mixing volume, forming droplets of concentrated sulfuric acid-water solution. These particles were electrostatically charged and passed through a DMA to produce a monodisperse aerosol; sizes between 0.05 and 0.3 μm diameter were used in the experiment. The ability of the DMA to accurately size particles above about 0.1 μm is limited by multiple charging. For this portion of the experiments, particles were charged with the low ion concentration, bipolar device described by Gupta and McMurry [1989] to reduce the effects of multiple charging.

The 1.5 lpm aerosol flow was then mixed with 8.5 lpm of purified air and passed into a 3 m conditioning tube, 10 cm in diameter. The conditioning tube temperature was controlled by a circulating bath. The 10 lpm tube flow was laminar; however, residence time measurements, similar to those described above, yielded particle residence times somewhat longer than predicted by laminar flow. As with the flow tube experiments described above, the conditioning tube flow gas was humidified as desired, and droplet composition was determined assuming the water vapor pressure of the droplets to be in equilibrium with the flow gas.

Theory

Transition regime mass transfer. Equilibrium vapor pressure of H_2SO_4 was determined from the experimentally measured quantities by mass transfer theory. With particle radius set at 0.125 μm, the Knudsen number Kn of the system (= molecular mean free path/particle radius) is about 0.25, placing mass transfer in the transition regime. Several transition regime mass transfer expressions

exist in the literature. These expressions describe the mass flux density J from a particle

$$J = \frac{1}{area}\frac{dm}{dt} \tag{1}$$

in terms of continuum mass flux density J_C via a transition term F(Kn):

$$J = F(Kn)J_c = F(Kn)\frac{2D_{vg}M}{D_pRT}(p_{vs} - p_\infty) \tag{2}$$

where D_{vg} is the diffusivity of the vapor species, M the vapor molecular weight, D_p the particle diameter, p_{vs} the equilibrium vapor pressure and p_∞ the partial pressure of the vapor far from the particle. Two expressions for F(Kn) were considered in this work, those of Fuchs and Sutugin [1970]

$$F(Kn) = \frac{J}{J_c} = \left(1 + Kn\left(\frac{1.333 + .71Kn^{-1}}{1 + Kn^{-1}} + \frac{4(1-E)}{3E}\right)\right)^{-1} \tag{3}$$

and Bademosi and Liu [1971a,b]

$$\frac{J}{J_c} = \left\{1 + \frac{J_c}{J_k} - \frac{1}{\left(1 - \frac{0.13\,J_c}{\beta Kn\,J_k}\right)^{-1} + 6.04\frac{J_k}{J_c}}\right\}^{-1} \tag{4}$$

The ratio J_C/J_K is that of continuum to free molecular mass transfer expressions, which can be written as [Davis and Ray, 1978]

$$\frac{J_c}{J_k} = \frac{4\beta Kn}{E} = \frac{4D_{vg}}{Eac} \tag{5}$$

where β is a constant obtainable from Enskog-Chapman theory for molecular diffusivity, a is particle radius and c is the mean molecular velocity. In expressions (3) and (5), E is the evaporative coefficient, which will be addressed in detail below. Substituting (5) in (4) yields a function of E and Kn analogous to equation (3):

$$\frac{J}{J_c} = \left\{ 1 + \frac{4D_{vg}}{Eac} - \frac{1}{\left(1 - \frac{0.52}{E}\right)^{-1} + 24.16\frac{E}{Kn}} \right\}^{-1} \qquad (6)$$

The transition regime corrections given by equations (3) and (6) agreed to within about 10%. While the Fuchs-Sutugin expression is widely used for transition mass transfer, Davis and Ray [1978] found that the Bademosi-Liu relation better fit their experimental data for Kn > 0.1. For this reason equation (6) was employed in this work.

CIMS Measurements. Each experimental run with the CIMS system measured the accumulation of gas phase H_2SO_4 molecules during evaporation from an ensemble of 1000-3000 particles cm^{-3}. The total mass flux from n_p monodisperse particles of diameter D_p is

$$\frac{dm}{dt} = n_p \pi D_p^2 J = n_p \pi D_p^2 F(Kn) J_c \qquad (7)$$

This mass flux evolves a (very low) partial pressure given adequately by the ideal gas law

$$\frac{dm}{dt} = \frac{MV}{kT}\frac{dp}{dt} \qquad (8)$$

Combining equations 4, 7, and 8, we get

$$\frac{dp}{dt} = 2F(Kn)N\pi D_p D_{vg}(p_{vs} - p_\infty(t)) \qquad (9)$$

where $N = n_p/V$, the number density of aerosols. The experimentally measured quantities in (9) are aerosol concentration N (fixed), H_2SO_4 partial pressure P_∞(at $t=t_{final}$), and D_p (fixed). F(Kn) is a constant for fixed D_p. Equation 9 may be integrated to yield an expression for equilibrium vapor pressure [Cammenga, 1980]

$$P_{vs} = \frac{p_m - p_0 \exp(-Ct)}{1 - \exp(-Ct)} \qquad (10)$$

where C is the collection of constants in (9)

$$C = 2F(Kn)N\pi D_p D_{vg},$$

p_m is the H_2SO_4 pressure measured at the end of the flow tube, and p_0 is the very small initial concentration of H_2SO_4 brought into the injector along with the aerosol flow (a result of the sulfate aerosol beginning to evaporate before reaching the flow tube entrance). This initial pressure was estimated to be less than 10^{-9} Pa, based on expected evaporation rates of the concentrated acid solution droplets before they were mixed with humidified flow gas. The ratio p_0/p_m was generally below 10%, keeping any error introduced by this estimate tolerably small. In general, equation 10 should include a correction for the elevation of droplet vapor pressures due to the Kelvin effect. For the droplets used in this portion of the study ($D_p = 0.25$ μm) the Kelvin correction amounted to less than a tenth of a percent, and was ignored.

TDMA Measurements. After evaporation times of 30 to 250 seconds, the sulfuric acid solution droplets were sampled from the TDMA conditioning tube and their final size determined by a second DMA. The change in particle diameter D_p is related to mass flux density J by

$$\frac{dD_p}{dt} = \frac{J}{\rho} \qquad (11)$$

where ρ is solution droplet density. Using the Bademosi-Liu transition regime mass transfer equation (3) and incorporating a Kelvin curvature term (droplets used in TDMA experiments were small enough to require the Kelvin correction), equation 11 can be rewritten and integrated [Tao and McMurry, 1989]:

$$P_{v,0} = P_{\infty} + \frac{\rho RT}{4D_{vg}Mt}\int_{D_f}^{D_i} \frac{J_c}{J} \exp\left(\frac{-4\sigma M}{\rho RTD_p}\right) D_p dD_p \qquad (12)$$

where the integration limits are initial to final droplet diameter. Equation 9 was solved numerically, using measurements of D_i, D_f, residence time t and tube temperature, and estimates of P_{∞}, the "back pressure" of H_2SO_4 that accumulated in the conditioning tube over time. Since the solution droplet composition was fixed by carrier gas relative humidity, any H_2SO_4 evaporation would be accompanied by associated water to keep the droplet composition constant. To accurately account for particle shrinkage, both the H_2SO_4 and H_2O mass fluxes were calculated separately.

The mass transfer expressions (3) and (6) contain the evaporation coefficient E. For simple liquids, E is taken to be equal to the coefficient of condensation α_c. Either coefficient must be determined experimentally for individual compounds; E (α_c) is defined as the measured rate of evaporation (condensation) divided by the rate theoretically predicted with E (α_c) set equal to unity. While the value of α_c for sulfuric acid solutions has been reported as much less than unity, between 0.02 and 0.09 [Van Dingenen and Raes, 1991], there is a considerable body of work that suggests that for single component liquids, E is unity or very close to unity [Mozurkewich, 1986]; Cammenga, 1980; Pound, 1972; Maa, 1967] and that experimental results to the contrary may be due to sample cooling and contamination. The systems described in this work are multicomponent

solutions, so these arguments may have limited applicability. However, Mozurkewich [1986] has argued that α_c for any polar species on an aqueous surface should be near unity. This would imply that E for a sulfuric acid solution or an ammonium sulfate-sulfuric acid mixture should be near unity, even though they are not pure liquids. Due to the undetermined state of E for the sulfate systems examined in these experiments, the vapor pressure data presented in this work have been calculated with E assumed to be unity. The validity of such an assumption may be judged by comparing the results of this work with extrapolations of measurements at higher temperatures and solution strengths [Ayers et al., 1980; Roedel, 1979] which did not rely on mass transfer considerations.

Results

The vapor pressures of H_2SO_4 over aqueous sulfuric acid solutions at 25, 30 and 35°C are shown in Figures 3a-c. The data in each figure are for a single temperature, with solution concentration varied from about 55 to 77 wt%. Figure 3a shows vapor pressures measured with the CIMS only. Figures 3b and 3c include both CIMS and TDMA derived data. In all cases, the data fall closer to the predictions of Ayers et al than to the earlier Gmitro and Vermeulen work. However, the data agree with the Ayers et al formulation only for solution concentrations above 70 wt%. Below this solution strength the vapor pressure data appear to be up to 5 times higher than the predictions of Ayers et al, although still well below those of Gmitro and Vermeulen. Reasons for the discrepancy are explored below in Discussion.

Vapor pressure measurements obtained with the TDMA generally support those from the CIMS experiments (Figures 3b, 3c). However, the figures show the high scatter that the TDMA technique was prone to, scatter well in excess of random error. Both the present experiment and previous work [Richert, 1991] found that calculated H_2SO_4 vapor pressures often depended on particle residence time within the TDMA. Vapor pressures derived after shorter evaporation times

(t< 30 seconds) were usually nearer to those predicted by Gmitro and Vermeulen but dropped as evaporation time increased over 60 seconds, reaching near zero after the full 250 second tube residence time. TDMA results such as these suggested the presence of a droplet contaminant that lowered the H_2SO_4 vapor pressure, such as ammonia gas, the effects of which would become more pronounced with dropping particle size. The TDMA system and associated plumbing was mechanically and thermally cleaned and examined for possible contamination problems. These efforts reduced data scatter somewhat and yielded the data shown in Figures 3b and 3c. However, the performance of the TDMA with the H_2SO_4-H_2O system did not approach that of the CIMS, as is evident in the Figures. The better repeatability and accuracy of the CIMS system led to reliance on this technique for the bulk of the H_2SO_4-water measurements and all the measurements of mixed systems.

Measured H_2SO_4 vapor pressures of pure $(NH_4)_2SO_4$ are shown in Figure 4 for the temperature range 28 to 60° C The relative humidity for all measurements was kept below about 6%. The data are plotted as log pressure (in Pa) versus inverse temperature (K^{-1}). Although possessing substantial uncertainties, the points form a convincing regression line of the Clausius-Clayperon form

$$log\ p = \frac{A}{T} + B \qquad (13)$$

with A = -2670 ± 369 and B = -1.29 ± 0.0925. The extremely low vapor pressures measured in this temperature range were near the lower detection limit of the apparatus, as evidenced by the large error bars on the data.

As noted above, the $(NH_4)_2SO_4$ particles were most likely solid, since the relative humidity of the system was well under the crystallization point of ammonium sulfate. The particles' vapor pressure-temperature relationship is unlikely to change with relative humidity as long as they

remain in the solid phase. Starting as such, ammonium sulfate aerosols can be expected to stay solid until the ambient relative humidity reaches the deliquescence point. Hence the relationship in equation 13 should hold for atmospheric humidities below the deliquescence point. The only prediction of H_2SO_4 vapor pressure over ammonium sulfate found in the literature is that of Scott and Cattell [1979], who calculate a vapor pressure of about 10^{-13} Pa for nearly pure $(NH_4)_2SO_4$ at 25 °C. This is two orders of magnitude lower than given by the experimental fit equation above.

In Figure 5 are shown vapor pressure data from mixed solutions of sulfuric acid, ammonium sulfate and water, collected across a range of relative humidity while keeping the temperature fixed at 30° C. The data are grouped by $[NH_4^+]$:$[SO_4^=]$ ratio, hereafter called the ionic ratio. The vapor pressures measured over solutions with low ionic ratios (below 0.2) were only slightly below those measured for unneutralized sulfuric acid solutions, especially at higher humidities. Solutions with ionic ratio = 0.33 and lower also possessed vapor pressures close to the sulfuric acid values. It was not until the ionic ratio increased over 0.5 that H_2SO_4 vapor pressure was appreciably depressed vis-a-vis the unneutralized acid. Particles with ratio = 0.8 had H_2SO_4 vapor pressures less than one quarter of those for sulfuric acid solutions at 15% relative humidity; at 5% relative humidity they were over an order of magnitude lower than their unneutralized acid counterparts. Particles with ionic ratio of 1.0 (probably ammonium bisulfate, NH_4HSO_4) exhibited H_2SO_4 vapor pressures in the mid 10^{-10} Pa range that were nearly constant between 5 and 15% relative humidity. Data taken at this temperature for ammonium sulfate, although sparse, also show no apparent change with relative humidity, as would be expected for the solid below its deliquescence point. The vapor pressures for the pure ammonium sulfate solid appears to be below 10^{-10} Pa at these relative humidities.

Discussion

The H_2SO_4 vapor pressure measurements presented in this paper depend in part on two key parameters, the evaporation coefficient E and the H_2SO_4 diffusion coefficient D. The values

selected for these parameters affect the outcome of equilibrium vapor pressure calculations. As addressed above in the Theory section, this work assumed an evaporative coefficient of unity. The vapor pressures derived with this assumption, shown in figures 3a-c, are in substantial agreement with the extrapolation of the Ayers et al fit line in the higher solution concentration range. The latter is a fit to vapor pressure measurements obtained at higher temperatures and solution strengths; these measurements were absolute, i.e., they did not rely on mass transfer assumptions. Thus if the Ayers et al results can be extrapolated, the present work offers evidence that E is close to unity for the H_2SO_4-H_2O system. There is a clear need for further experiments in this area.

Vapor pressures presented in this paper were derived using value of the diffusion coefficient D for H_2SO_4 in nitrogen/air calculated from Enskog-Chapman theory [Present, 1958]. One obstacle to using this approach is the selection of a suitable diameter for the collision volume of the highly aspherical H_2SO_4 molecule; small variations in the choice result in large changes to the calculated D_{vg}. In addition, conditions in this experiment were such that the gas phase H_2SO_4 molecules were hydrated with one or more water molecules [Heist and Reiss, 1974]. For this work, a collision diameter for H_2SO_4 was chosen as that of a hydrated H_2SO_4 cluster from the work of Heist and Reiss [1974]. The value of D_{vg} so obtained was 0.103 ± 0.01 cm^2 sec^{-1} at 25C, ranging up to 0.110 at 60C. This compares with D suggested (but not explicitly derived) by Roedel [1979], 0.08 ± 0.02 cm^2 sec^{-1} at 23C, which has become widely used in the atmospheric science literature.

The vapor pressures of sulfuric acid solutions (Figures 3a-c) are largely consistent with the predictions of Ayers et al [1980] at solution concentrations greater than 70 wt%. In this range the data clearly support the 1980 Ayers et al formulation for H_2SO_4 vapor pressure over the Gmitro and Vermeulen predictions. Below 70 wt% however the data positively diverge from the Ayers et al line, moving closer to, but still substantially below, its older counterpart. Two possible causes for such an effect are droplet cooling, which should lower the vapor pressure of the more volatile

(higher wt%) droplets, and particle shrinkage, which would give erroneous calculated vapor pressures through its effect on particle surface area and thus mass flux density. Final droplet temperatures were estimated by means of a coupled mass-heat transfer calculation [Vesala, 1991]. Thermal conductivity and specific enthalpy were assumed constant over the relatively narrow temperature range examined in this study. The results indicated a negligible cooling effect even for the most concentrated (77 wt%) solution droplets. The very low decrease in droplet temperature (less than 10^{-6} K) was due to the minute amounts of liquid phase material that volatilized in the short tube residence time. These short evaporation times likewise kept calculated particle shrinkage to be less than 0.1% of initial volume. It seems then that the divergence of H_2SO_4 vapor pressures with more dilute solutions, shown in Figure 3, may be real.

Recent field measurements have shown a low but nonzero nocturnal partial pressure of H_2SO_4 [Eisele, 1993]. This is an unexpected result since the production of gas phase H_2SO_4 relies on the oxidation of SO_2 by OH; the latter, being in rapid photochemical equilibrium, vanishes quickly after sunset, thereby turning off the major H_2SO_4 source. In the absence of a photochemical source, the H_2SO_4 may be present due to the vapor pressure of the background aerosols. Eisele and co-workers [1993] measured roughly $4x10^{-9}$ Pa H_2SO_4 at a clean marine site in Washington state and about $4x10^{-10}$ Pa at a station in the mountains of Colorado. Although both sites probably had relative humidities in excess of those used in this present experiment, the data in Figure 4 may be extrapolated for use as a rough guide to H_2SO_4 vapor pressures for moister conditions. The H_2SO_4 partial pressures measured in at these field sites may be more consistent with a partially neutralized sulfate droplet; an extrapolation of the data in Figure 5 to higher relative humidities suggest an aerosol with $[NH_4^+]$:$[SO_4^=]$ ratio of 0.8 or less.

Data for H_2SO_4-H_2O-$(NH_4)_2SO_4$ mixed solutions (Figure 5) are also subject to the evaporation coefficient concerns outlined above. Regardless of their absolute values, however, the vapor pressures over H_2SO_4-H_2O-$(NH_4)_2SO_4$ mixed solutions convey important information from the

relative placement of the curves. As Figure 5 shows, addition of the ammonium ion to a sulfuric acid-water solution begins to significantly depress H_2SO_4 vapor pressure as the ammonium to sulfate ion ratio exceeds about 0.5. These data were obtained using sub micron droplets, a collection of about 10^7 molecules. If clusters of 1 to 10 H_2SO_4 and H_2O molecules behave in an analogous manner, Figure 5 suggests that a few ammonium ions could substantially stabilize such molecular clusters. The result would be smaller critical cluster sizes and higher observed particle formation and growth rates in the presence of ammonia. Since levels of atmospheric ammonia have been found to be at least an order of magnitude greater than measured H_2SO_4 concentrations at continental sites [Tanner and Eisele, 1991; Langford and Fehsenfeld, 1992], it is reasonable to suppose that ammonia may play a significant role in new particle formation at these sites. Recent field measurements by the authors [Weber et al., 1995b] indicate that new particle formation rates frequently exceeded those predicted by binary nucleation theory at a remote continental site. These measurements offer strong evidence that some other substance may be involved in stabilizing H_2SO_4-H_2O clusters. The present work provides quantitative support for atmospheric ammonia as one such stabilizing agent.

Acknowledgments. The authors wish to thank David Tanner for able assistance with the CIMS system. This work was supported by NASA grant No. NAGW-3767 and the Department of Energy grant No. DE-FG02-91ER61205.

References

Apelblat, A., The Vapor Pressures of Saturated Aqueous Solution of Potassium Bromide, Ammonium Sulfate, Copper (II) Sulfate, Iron (II) Sulfate, and Manganese (II) Dichloride, at temperatures from 283 to 308 K, Journal of Chemical Thermodynamics, 25, 1513-1520, 1993.

Ayers, G. P., R. W. Gillett and J. L. Gras, On the vapor pressure of sulfuric acid, Geophysical Research Letters, 7, 433-436, 1980.

Bademosi, F. and B. Y. H. Liu, A Universal Law for Transfer Processes in Knudsen Aerosols, University of Minnesota, Particle Technology Laboratory Publication, 1971b.

Banchero, J. T. and F. H. Verhoff, Evaluation and interpretation of the vapour pressure data for sulfuric acid solutions with applications to flue gas dewpoints, J. Inst. Fuel, 48, 76-80, 1975.

Bolsaitis, P. and J. F. Elliott, Thermodynamic Activities and Equilibrium Partial Pressures for Aqueous Sulfuric Acid Solutions, Journal of Chemical Engineering Data, 35, 69-85, 1990.

Cammenga, H. K. (1980). Evaporation mechanism of liquids. Current Topics in Materials Science. North-Holland Publishing Co. 335-446.

Davis, E. J. and A. K. Ray, Submicron droplet evaporation in the continuum and non-continuum regimes, Journal of Aerosol Science, 9, 411-422, 1978a.

Easter, R. C. and L. K. Peters, Binary homogeneous nucleation: temperature and relative humidity fluctuations, nonlinearity, and aspects of new particle production, Journal of Applied Meteorology, 33, 775-790, 1994.

Eisele, F. L., Identification of tropospheric ions, Journal of Geophysical Research, 91, 7897, 1986.

Eisele, F. L., First tandem mass spectrometric measurements of tropospheric ions, Journal of Geophysical Research, 93, 716, 1988.

Eisele, F. L., D. J. Tanner, Measurement of the gas phase concentrations of H2SO4 and Methane Sulfonic acid and estimates of H2SO4 production and loss in the atmosphere, Journal of Geophysical Research, 98, 9001-9010, 1993.

Eisele, F. L. and D. J. Tanner, Ion assisted tropospheric OH measurements, Journal of Geophysical Research, 96, 9295-9308, 1991.

Fuchs, N. A., A. G. Sutugin (1970). Highly Dispersed Aerosols. Ann Arbor, Ann Arbor Science Publishers.

Giauque, W. F., E. W. Hornung, J. E. Kunzler and T. R. Rubin, The Thermodynamic Properties of Aqueous Sulfuric Acid Solutions from 15 to 300K, J. Amer. Chem. Soc., 82, 62-70, 1960.

Gmitro, J. T. and T. Vermeulen, Vapor-liquid equilibria for aqueous sulfuric acid, American Institute of Chemical Engineers Journal, 10, 740-746, 1964.

Grollman, A. and J. C. Frazier, The Vapor Pressure Lowering of Aqueous Sulfuric Acid Solutions at 25 C, J. Am. Chem. Soc., 47, 712-717, 1925.

Gupta, A. and P. H. McMurry, A device for generating singly charged particles in the 0.1 - 1.0 micron diameter range, Aerosol Science and Technology, 10, 451-462, 1989.

Heist, R. H. and H. Reiss, Hydrates in supersaturated binary sulfuric acid-water vapor, Journal of Chemical Physics, 61, 573-581, 1974.

Hornung, E. W. and W. F. Giauque, The vapor pressure of water over aqueous sulfuriv acid at 25C, Journal of the American Chemical Society, 77, 2744, 1955.

Junge, C., The Chemical Composition of Atmospheric Aerosols I. Measurements at Round Hill Field Station, June-July 1953, Journal of Meteorology, 11, 323, 1954.

Junge, C. E. (1963). Air Chemistry and Radioactivity. New York, Academic Press.

Kim, P. K., B. K. Pun, C. K. Chan, R. C. Flagan and J. H. Seinfeld, Determination of Water Activity in Ammonium Sulfate and Sulfuricc Acid Mixtures Using Levitated Single Particles, Aerosol Science and Technology, 20, 275-284, 1994.

Koutrakis, P. and B. Aurian-Blajeni, Measurement of Partial Vapor Pressure of Ammonia over Acid Ammonium Sulfate Solution by an Intregral Method, Journal of Geophysical Research, 98, 2941-2948, 1993.

Langford, A. O. and F. C. .Fehsenfeld, Natural vegetation as a source or sink for atmospheric ammonia: a case study, Science, 255, 581-583, 1992.

Liu, B. Y. H. and F. Bademosi, Diffusion Charging of Knudsen Aerosols II. Theoretical, University of Minnesota, Particle Technology Laboratory Pulblication, 1971a.

Liu, B. Y. H. and D. Y. H. Pui, A submicron aerosol standard and the primary, absolute

calibration of the CNC, Journal of Colloid and Interface Science, 47, 155-171, 1974.

Maa, J. R., Evaporation Coefficient of Liquids, Industrial and Engineering Chemistry Fundamentals, 6, 504, 1967.

Meszaros, A. and K. Vissy, Concentrations, Size Distributions and Chemical Nature of Atmospheric Aerosol Particles in Remote Oceanic Areas, Aerosol Science, 5, 101-109, 1974.

Mozurkewich, M., Aerosol growth and the condensation coefficient for water: A review, Aerosol Science and Technology, 5, 223-236, 1986.

Pound, G. M., Selected values of evaporation and condensation coefficients for simple substances, Journal of Physical Chemistry Reference Data, 1, 135-140, 1972.

Present, R. D. (1958). Kinetic Theory of Gases. New York, McGraw-Hill Book Company.

Rader, D. J. and P. H. McMurry, Application of the tandem differential mobility analyzer to studies of droplet growth or evaporation, Journal of Aerosol Science, 17, 771-787, 1986.

Rader, D. J. and P. H. McMurry, Evaporation rates of monodisperse organic aerosols in the 0.02- to 0.2 micron diameter range, Aerosol Science and Technology, 6, 247-260, 1987.

Raes, F., Entrainment of free tropospheric aerosols as a regulating mechanism for cloud condensation nuclei in the remote marine boundary layer, Journal of Geophysical Research, 100, 2893-2903, 1995.

Raes, F. and R. Van Dingenen, Simulations of condensation and cloud condensation nuclei from

biogenic SO2 in the remote marine boundary layer, Journal of Geophysical Research, 99, 20989-21003, 1992.

Richardson, C. B., R. L. Hightower and A. L. Pigg, Optical measurement of the evaporation of sulfuric acid droplets, Applied Optics, 25, 1226-1229, 1986.

Richert, C. A., Measurements of the relative humidity dependent vapor pressure of sulfuric acidusing the tandem differential mobility analyzer, Department of Mechanical Engineering, University of Minnesota, M.S. Thesis, 1991.

Roedel, W., Measurement of sulfuric acid saturation vapor pressure; Implications for aerosol formation by heteromolecular nucleation, Journal of Aerosol Science, 10, 375-386, 1979.

Scott, W. D. and F. C. R. Catell, Vapor Pressure of Ammonium Sulfates, Atmospheric Emvironment, 13, 307-317, 1979.

Spann, J. F. and C. B. Richardson, Measurement of the Water Cycle in Mixed Ammonium Acid Sulfate Particles, Atmospheric Environment, 19, 819-825, 1985.

Tang, I. N. and H. R. Munkelwitz, Aerosol Growth Studies III--Ammonium Bisulfate Aerosols in a Moist Atmosphere, Journal Aerosol Science, 8, 321-330, 1977.

Tang, I. N. and H. R. Munkelwitz, An Investigation of Solute Nucleation in Levitated Solution Droplets, Journal of Colloidal and Interfacial Science, 98, 430-438, 1984.

Tanner, D. J. and F. L. Eisele, Ions in oceanic and continental air masses, Journal of Geophysical Research, 96, 1023-1031, 1991.

Tanner, D. J. and F. L. Eisele, Present OH measurement limits and associated uncertainties, Journal of Geophysical Research, 100, 2883-2892, 1995.

Tao, Y. and P. H. McMurry, Vapor pressures and surface free energies of C14-C18 monocarboxylic acids and C5 and C6 dicarboxylic acids, Environmental Science and Technology, 23, 1519-1523, 1989.

Twomey, S., The composition of cloud nuclei, Journal of the Atmospheric Sciences, 28, 377-381, 1971.

Van Dingenen, R. and F. Raes, Determination of the condensation accommodation coefficient of sulfuric acid on water-sulfuric acid aerosol, Aerosol Science and Technology, 15, 93-106, 1991.

Verhoff, F. H. and J. T. Banchero, A Note on the Equilibrium Partial Pressures of Vapors Above Sulfuric Acid Solutions, American Institute of Chemical Engineers Journal, 18, 1265-1268, 1972.

Vesala, T. (1991). Binary droplet evaporation and condensation as phenomenological processes. Helsinki, The Finnish Society of Arts and Letters.

Weber, R. J., J. J. Marti, P. H. McMurry, F. L. Eisele, D.J.Tanner and A. Jefferson, Measured atmospheric new particle formation rates: Implications for nucleation mechanisms, Submitted to : Chemical Engineering Communications, , 1995.

Weiss, R. E., A. P. Waggoner, R. J. Charlson and N. C. Ahlquist, Sulfate Aerosol: Its Geographical Extent in the Midwestern and Southern United States, Science, 195, 979-981, 1977.

Figure Captions.

Figure 1. Chemical ionization mass spectrometer and flow tube apparatus used in vapor pressure measurements. Aerosol flows are given with solid arrows; sheath or carrier gas flows are depicted with open arrow symbols.

Figure 2. Tandem differential mobility analyzer apparatus used in vapor pressure measurements.

Figure 3. H_2SO_4 vapor pressures (in Pascals) measured over sulfuric acid solutions of varying concentration. Labeled lines show two vapor pressure formulations from the literature.

3a. H_2SO_4 vapor pressures at 25 °C.

3b. H_2SO_4 vapor pressures at 30 °C. Both CIMS and TDMA derived data are included.

3c. H_2SO_4 vapor pressures at 35 °C. Both CIMS and TDMA derived data are included.

Figure 4. H_2SO_4 vapor pressures over samples of ammonium sulfate at low (<5%) relative humidity.

Figure 5. H_2SO_4 vapor pressures of partially to fully neutralized sulfuric acid. Data are grouped by the ionic ratio (see text).

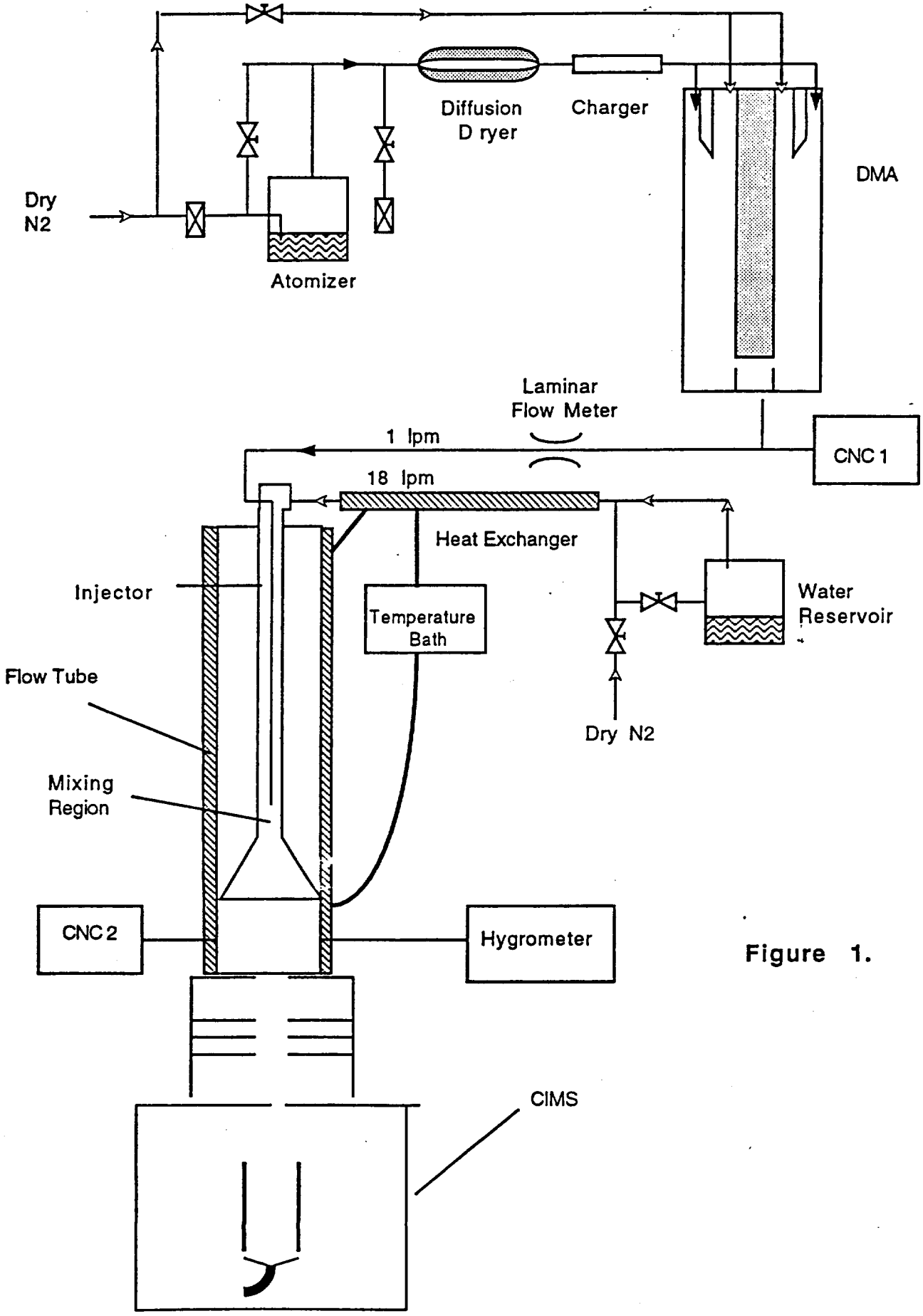
Dry
N2
Atomizer
Diffusion
D ryer
Charger
DMA
Laminar
Flow Meter
1 lpm
CNC 1
18 lpm
Heat Exchanger
Injector
Temperature
Bath
Water
Reservoir
Flow Tube
Dry N2
Mixing
Region
CNC 2
Hygrometer
CIMS

Figure 1.

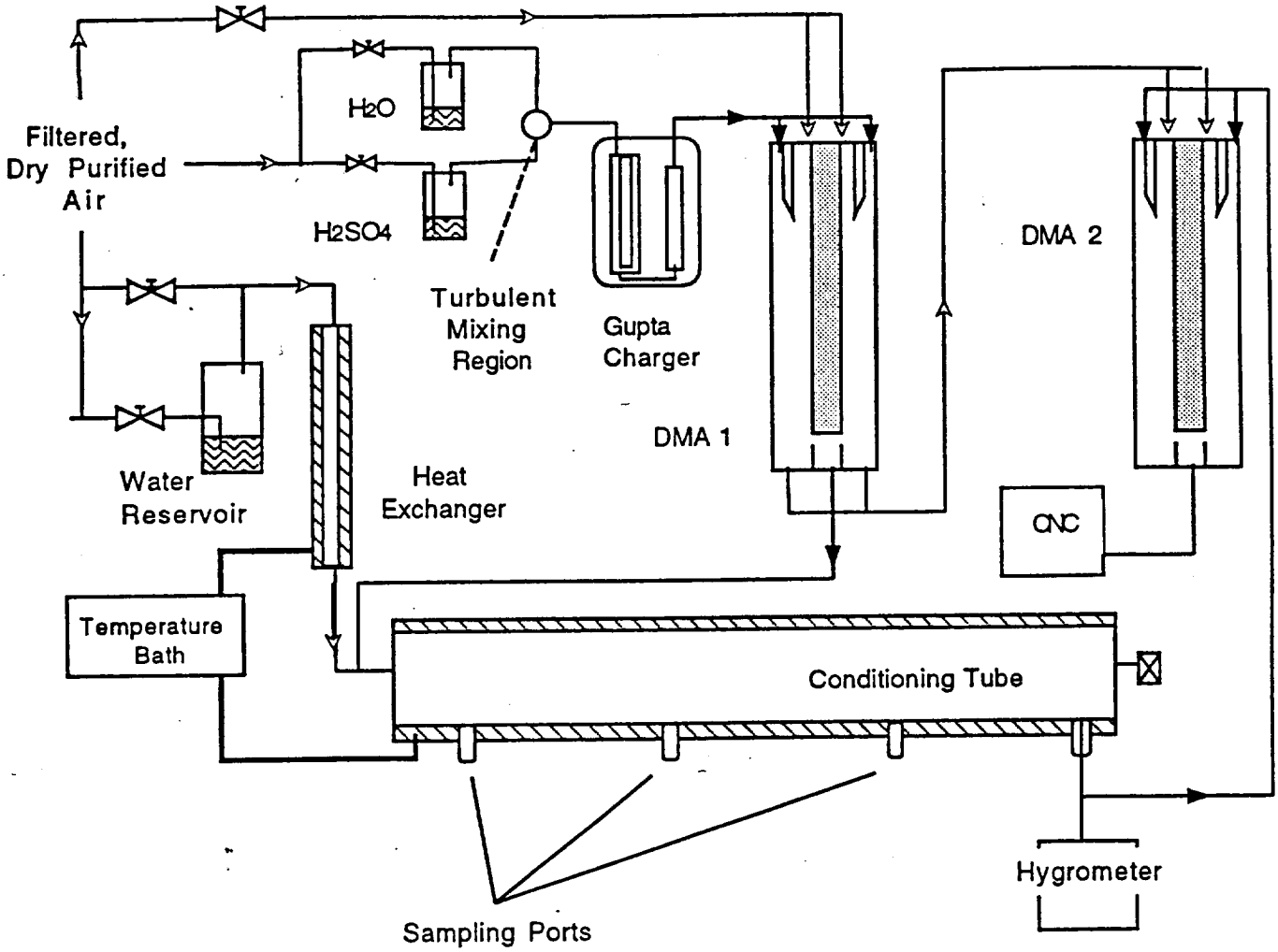
Filtered,
Dry Purified
Air
H2O
H2SO4
Turbulent
Mixing
Region
Gupta
Charger
DMA 1
DMA 2
CNC
Water
Reservoir
Heat
Exchanger
Temperature
Bath
Conditioning Tube
Hygrometer
Sampling Ports

Figure 2.

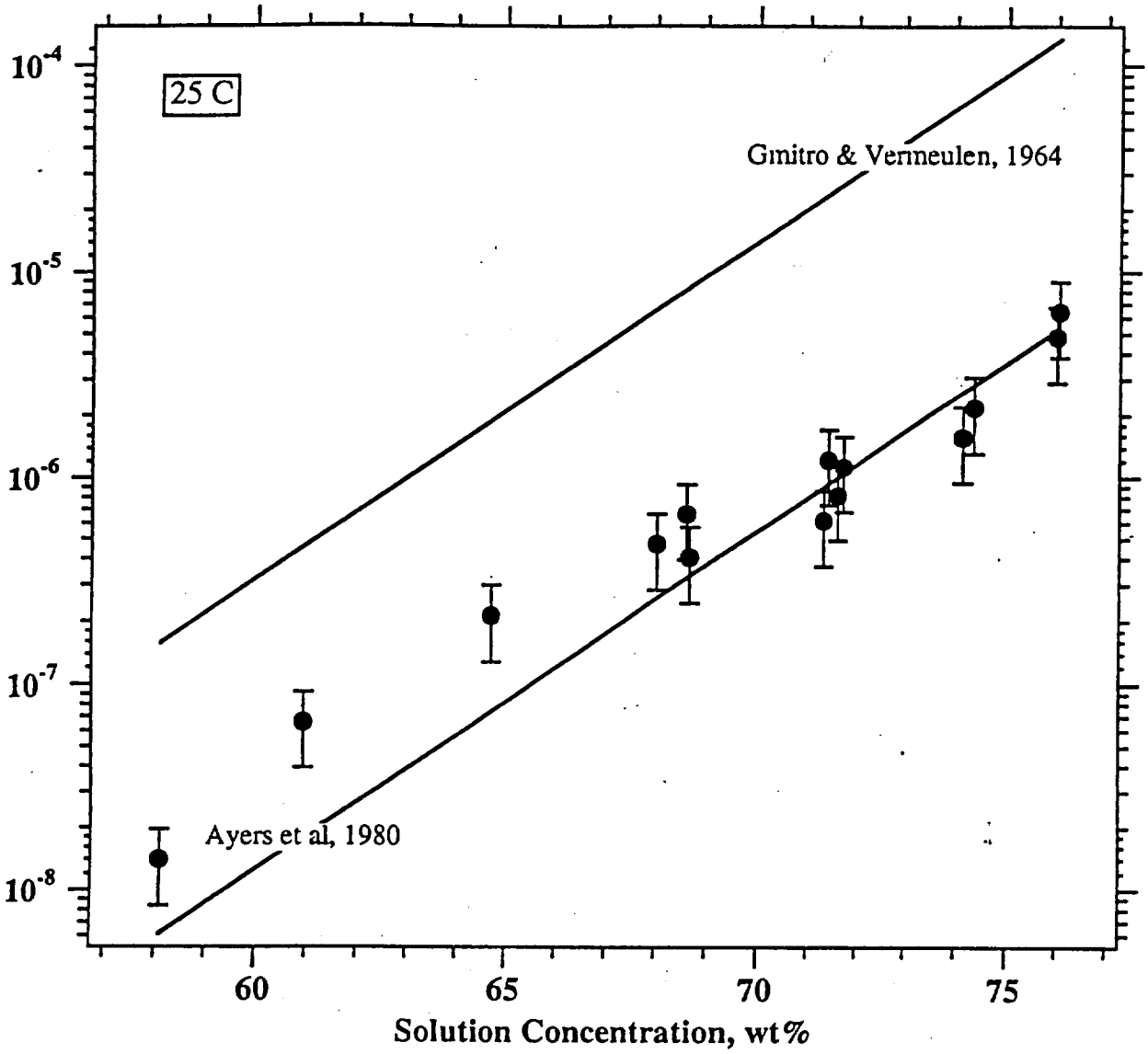
25 C
Gmitro & Vermeulen, 1964
Ayers et al, 1980
10^{-4}
10^{-5}
10^{-6}
10^{-7}
10^{-8}
60
65
70
75
Solution Concentration, wt%

FIGURE 3a.

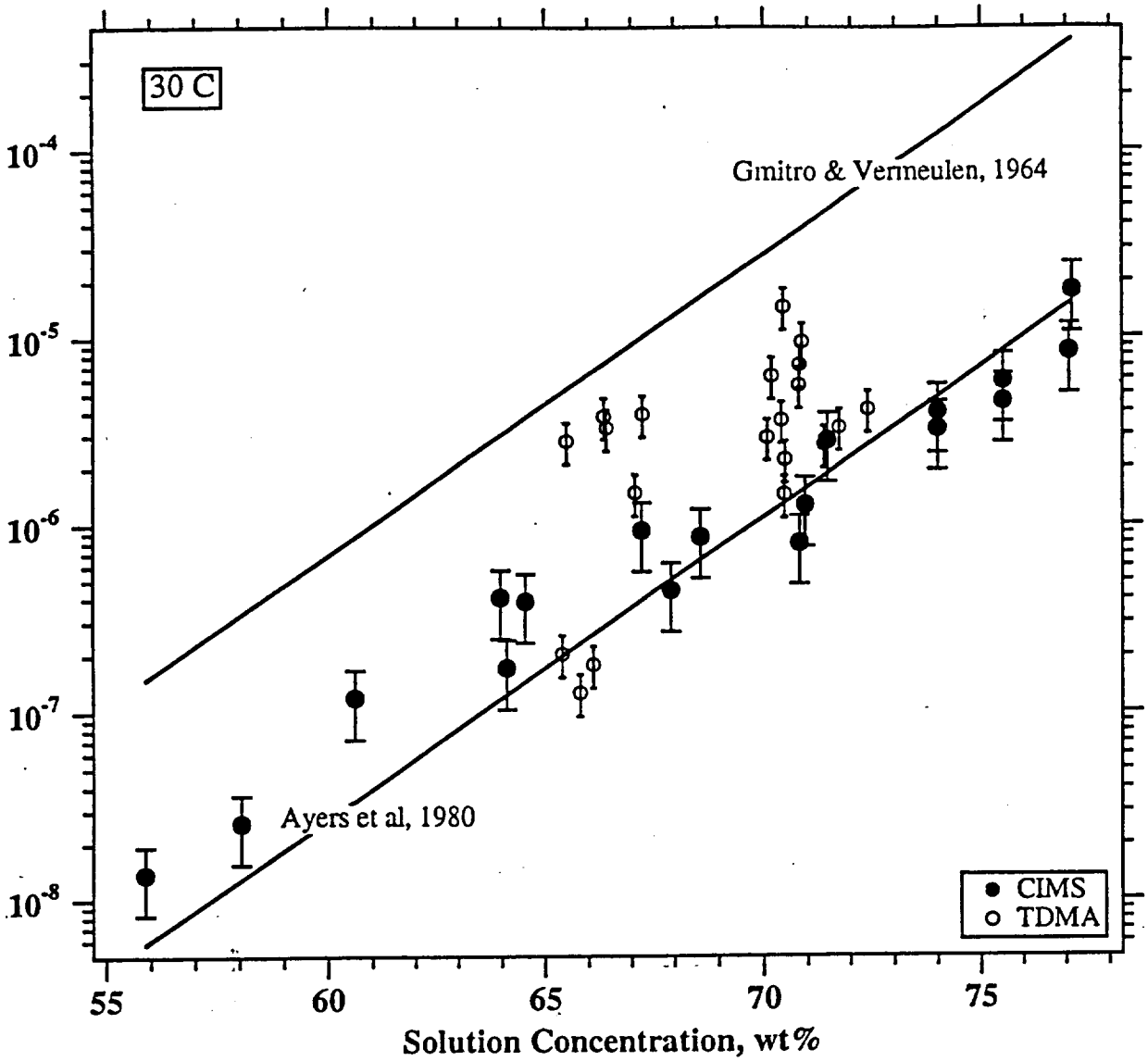
30 C
Gmitro & Vermeulen, 1964
Ayers et al, 1980
CIMS
TDMA
10^{-4}
10^{-5}
10^{-6}
10^{-7}
10^{-8}
55
60
65
70
75
Solution Concentration, wt%

FIGURE 36

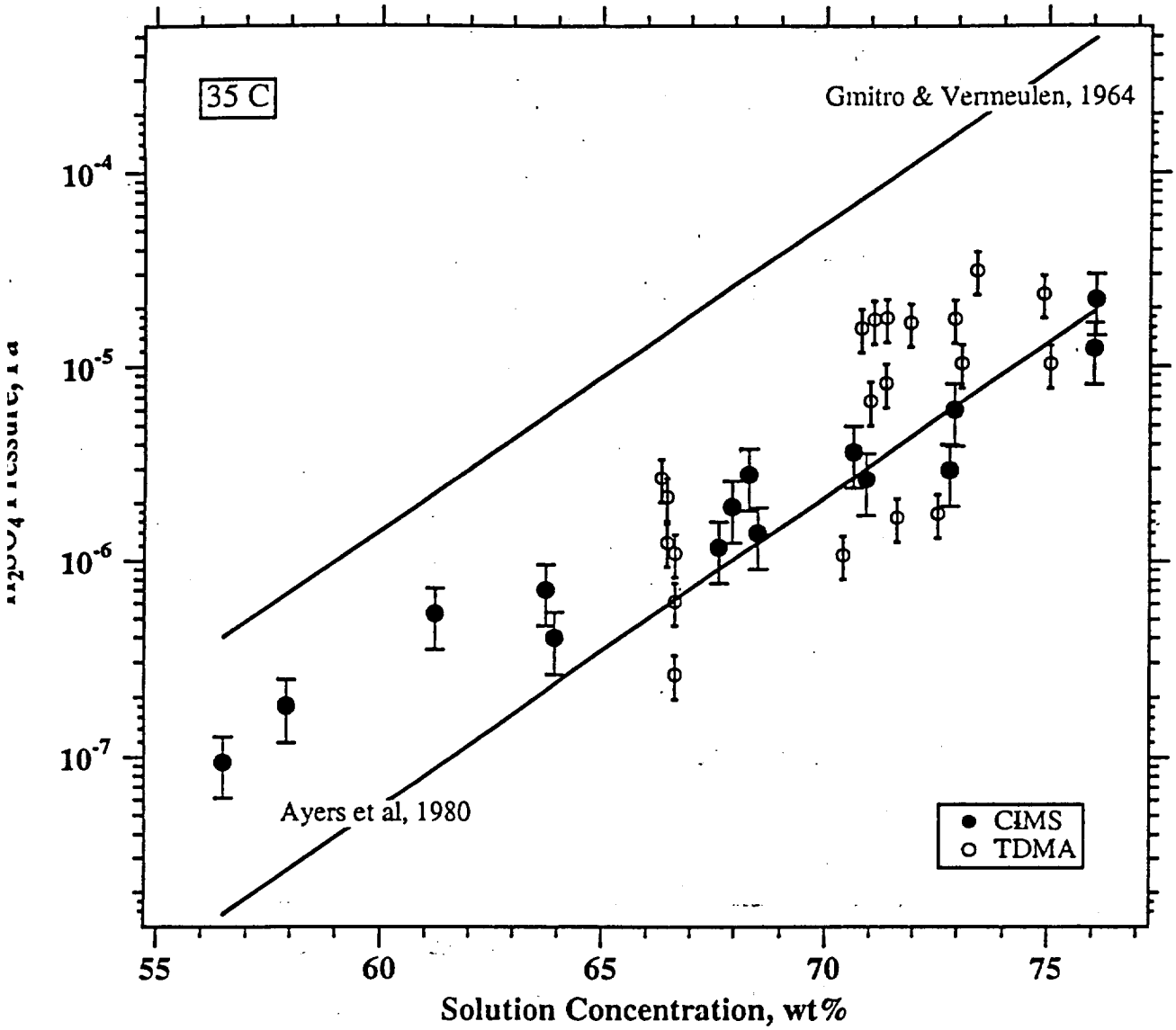
35 C
Gmitro & Vermeulen, 1964
Ayers et al, 1980
CIMS
TDMA
10^{-4}
10^{-5}
10^{-6}
10^{-7}
55
60
65
70
75
Solution Concentration, wt%

FIGURE 3c.

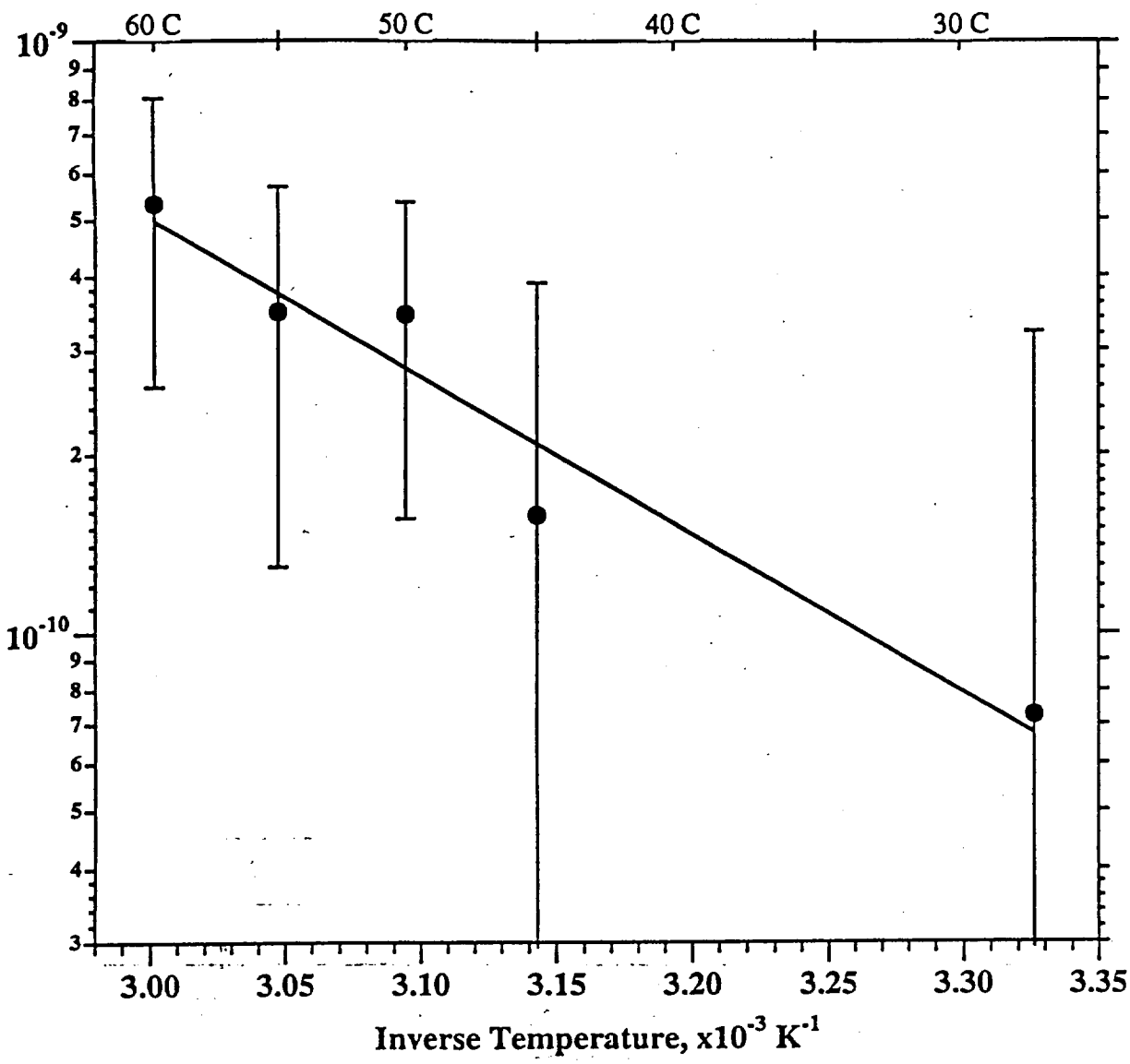
60 C
50 C
40 C
30 C
10^-9
9
8
7
6
5
4
3
2
10^-10
9
8
7
6
5
4
3
3.00
3.05
3.10
3.15
3.20
3.25
3.30
3.35
Inverse Temperature, x10^-3 K^-1

FIGURE 4

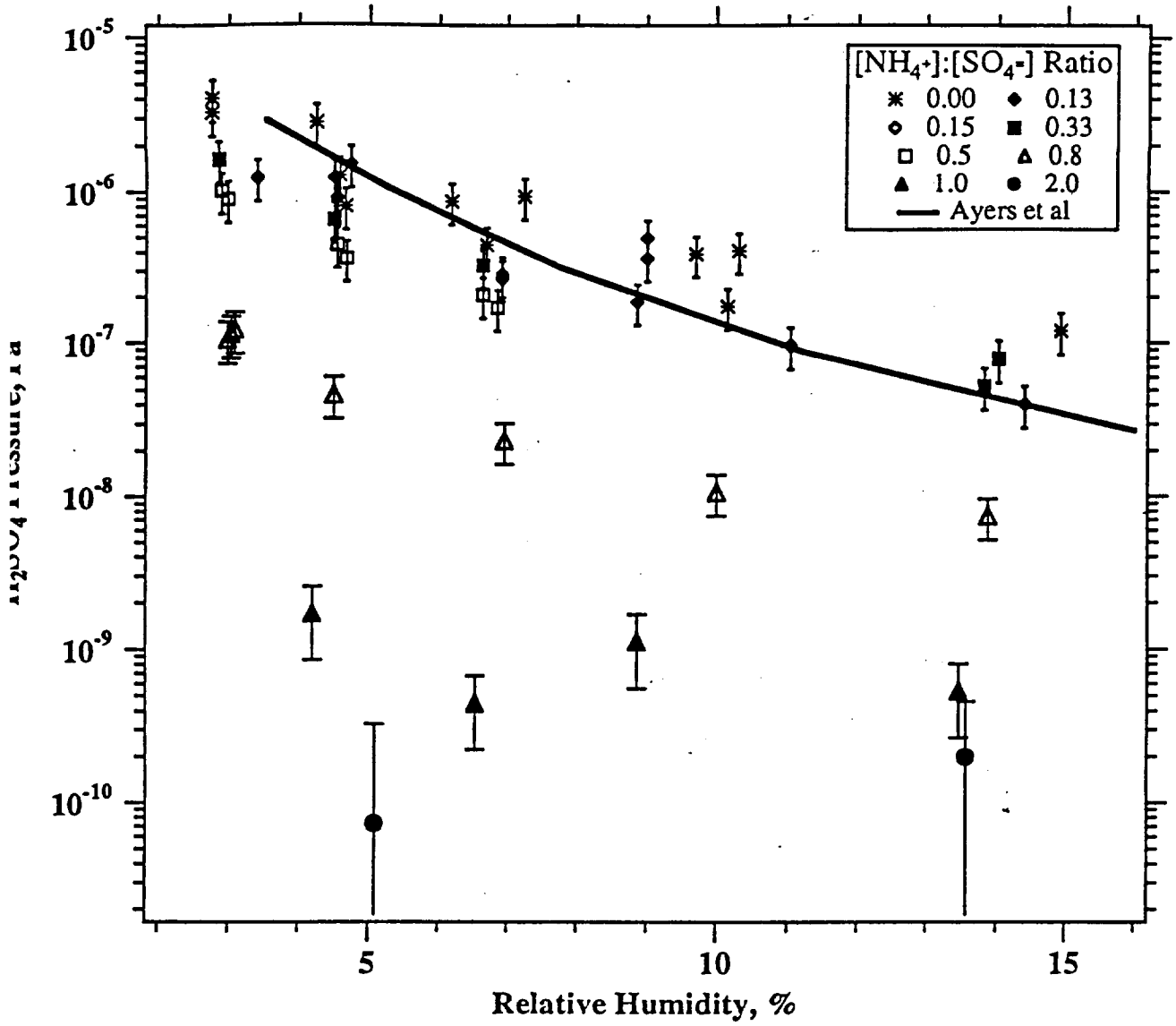
[NH4+]:[SO4-] Ratio
0.00
0.13
0.15
0.33
0.5
0.8
1.0
2.0
Ayers et al
10-5
10-6
10-7
10-8
10-9
10-10
5
10
15
Relative Humidity, %

FIGURE 5.